The Application of Nonlinear Control Theory to Robust Helicopter Flight Control

by

Davendra Yukteshwar Maharaj

December 1994

Department of Aeronautics

Imperial College of Science, Technology and Medicine

Thesis submitted for the degree of Doctor of Philosophy

of the University of London

and for the Diploma of Imperial College

So long as man imagines that he cannot do this or that, so long is he determined not to do it; and consequently so long is it impossible to him that he should do it.

- Benedict Spinoza (1632-1677) Ethics

Abstract

The design of robust nonlinear automatic flight control systems for a helicopter along with a set of simulation results are presented in this thesis. The controllers are synthesized by first applying the theory of Feedback Linearization and then enhancing their robustness properties by additionally applying techniques from Sliding mode and Lyapunov based control. The thesis begins with an introduction to the helicopter control problem, the difficulties associated with current control practices and the potential improvements achievable by using nonlinear control. This is followed by a review of the literature in which the theoretical tools of differential geometric control have been developed. The survey further includes progress made in the area of robust nonlinear control and appropriate applications studies. Next a comprehensive mathematical model of a single rotor helicopter is presented in a form amenable to the manipulations required by nonlinear system theory. A brief overview of the physical interpretation of the dynamic equations, which is important to the control system designer's understanding of the system, is given. At this point Input-Output Linearization is fully developed since it is this aspect of Feedback Linearization that is later applied. This is followed by further mathematical descriptions of the robust techniques used to augment the basic control law. As a mathematical theory Feedback Linearization necessarily restricts the class of systems to which the technique can be applied. In engineering, however, it is found that a knowledge of a particular system dynamics and its performance requirements can be used to weaken some of the stringent conditions imposed by the global *system independent* theory. Bearing this in mind, the helicopter control system is constructed and an iterative scheme is presented for dealing with the peculiar input multiplicities that appear in the helicopter equations. The robust schemes, Lyapunov based control and Sliding mode control, are then applied and this results in two robust control laws. Finally simulation studies are presented along with a discussion of the helicopter handling quality requirements and the performance of the control laws in satisfying these specifications.

Acknowledgements

I wish to express my sincere appreciation to my supervisor Dr. K. G. Woodgate whose guidance and encouragement has been of immeasurable assistance to me in many ways. I thank him also for the valuable comments on the contents and organisation of this thesis.

Thanks are also due to Dr. G. D. Padfield and Mr. A. T. McCallum of the DRA Bedford, for their help and advice with regard to the mathematical helicopter model. In addition, I thank Dr. R. Cipolla for providing me with the LaTeX style files used in this thesis.

This research undertaking was funded by the Science and Engineering Research Council and I gratefully acknowledge their support.

I also wish to thank the departmental administrative and computing services staff for always being friendly and helpful.

Thanks to all my friends and colleagues, past and present, in the Aeronautics Department who have sympathised through the lows and delighted in the highs, helping to make the whole experience memorable for the right reasons.

Finally I thank my parents and family for their continuous support and for their belief in me.

Contents

Chapter 1

Introduction

The research objective is to investigate and extend nonlinear geometric control theory to the design of robust controllers for helicopters. Robustness properties, which are not directly addressed by geometric control theory, are enhanced by augmenting the basic control law with additional techniques based on Lyapunov control and Sliding mode control. Developing these ideas to facilitate the ease of their application is desirable because of the potential improvement that may be achieved over existing design techniques employing linear analyses. The general manner in which the investigation is carried out ensures that the ideas may be easily applied to more general systems. For the helicopter control problem the objective is essentially to construct stabilizing and tracking controllers for the outputs whereof pilots normally desire good decoupled tracking performance in order to fly the vehicle with relative ease.

Given a time varying nonlinear system of the following form:

$$\dot{x}(t) = f(t, x(t)) + g(t, x(t), u(t)) \tag{1.1}$$

where $x(t) \in \Re^n$ is the state vector, $u(t) \in \Re^m$ is the input vector and f, $g \in \Re^n$ are vectors, the basic task for control system designers is that of choosing the control vector u to ensure that the system's state vector x meets some pre-specified requirements. The solution to this problem is usually approached in one of two ways.

The first is to approximate the nonlinear system by a small perturbation linearized model and then to design a locally valid controller using existing linear techniques. This approach suffers from from the fact that the controller designed is only valid in a small region around the design point, i.e. the region in which the linearity assumptions hold. This means that to ensure adequate performance over the entire operating range, it is generally necessary to use some form of *Gain Scheduling* to interpolate the control

law parameters between design points. Although this approach does not form part of the work presented here, this scheme and its associated problems are described in more detail later.

The second approach, followed in this thesis, uses the nonlinear model to find a nonlinear control law that achieves the design objectives. Generally this is not an easy task and in the past designs tended to be unique and system dependent. However great advances in the differential geometric approach to nonlinear control in the 1980's led to *Feedback Linearization*, a method that provides a systematic approach to the design of control systems for fairly general nonlinear systems.

Feedback Linearization is essentially based on two concepts, Input-State Linearization and Input-Output Linearization both of which will be introduced later on. Most of the nonlinear helicopter controllers described in the literature were derived using the Input-State Linearization technique. The first problem in using this technique is the need to make extensive simplifying assumptions to the model in order to satisfy the restrictive conditions necessary for Input-State Linearization. The second deficiency lies in the fact that Input-State Linearization is more conducive to state regulation problems and thus necessarily restricts the designer to producing a tracking controller for the somewhat arbitrary *output* functions automatically determined by the method. Therefore there is no freedom to choose outputs for tracking.

As will be shown later Input-State Linearization of the simplified helicopter equations leads to a flight path trajectory controller since the outputs, automatically generated by the method which may be used for tracking, are the displacements in the x, y and z directions as well as the yaw angle. However as Smith [71] and Garrard-Low-Prouty [21] point out, pilots prefer to have the flight control system track pitch angle, bank angle, altitude rate and heading rate. Since this is not achievable using Input-State Linearization this thesis will focus on the use of Input Output Linearization which constitutes an advance on what is already available in the literature. This procedure is less restrictive than Input-State Linearization and the unsimplified comprehensive nonlinear model is used in the control system design, thus potentially increasing its range of validity over previous designs.

This chapter commences with a brief introduction to some of the concepts that will be developed in detail in the later chapters. This is then followed by a survey of pub-

lished studies related to this research undertaking. Chapter 2 provides an introduction to the dynamics of helicopters illustrating the highly nonlinear nature of the system. It is the severely coupled nonlinear aerodynamic contributions to the helicopter dynamics that vindicates the design of nonlinear controllers. The nonlinear control theory is then described in detail in Chapter 3. The procedure involved in the decomposition of a nonlinear system into a linear subsystem with its accompanying reduced order nonlinear subsystem is given. The methods employed in ensuring that the basic nonlinear control law is robust to model uncertainty and other disturbances are detailed next in Chapter 4. The robust theory outlined is that of Sliding mode control and a Lyapunov based technique. Chapter 5 describes the application of the nonlinear control theory to helicopter control system design. This is followed by the necessary control law augmentation by certain *robustifying components* derived using Sliding mode and Lyapunov analyses. To illustrate the validity of the designs, several simulation studies are presented in Chapter 6. The performance of each controller is evaluated in terms of the *Pilot Handling Quality Requirements* documented in the Aeronautical Design Standard (**ADS-33C**) [1]. By satisfying these specifications it is expected that there will be no limitations on flight safety or on the capability to perform intended missions. Finally, conclusions regarding the research are made in Chapter 7 and are followed by potential areas for further development.

1.1 Gain Scheduling

Even the most sophisticated linear control method can suffer from limitations to its range of operation when applied to the actual nonlinear system. To remedy this degradation of performance, gain scheduling is employed when the controller is outside its region of validity. Typically an entire operational range controller is constructed in two parts. Linear design methods are applied to the linearized models at various operating points in order to arrive at a set of linear feedback control laws, parametrized by some gain(s), that perform satisfactorily when the closed loop system is operated near the respective operating points. The next step is the gain scheduling which is intended to handle the nonlinear aspects of the design problem. The idea is to interpolate the linear control law at intermediate operating conditions. In fact a scheme is devised for changing the parameters in the linear control law structure based on some monitored operating condition. Figure 1.1 overleaf illustrates the gain scheduling requirement.

Even with certain practical guidelines, gain scheduling still remains far from a trivial task. Some of the problems associated with its implementation are as follows:

- The scheduling variable i.e. the monitored variable should *capture* the system's nonlinearities. Such a variable is inferred from an in-depth understanding of the *physics* of the problem.
- The scheduling variable should vary slowly. Rapid changes in the dynamic response of high performance systems will be severely restricted by such a constraint.
- The scheduling procedure, i.e. a program by which the control law gains can be changed as a function of the scheduling variable must be devised. At present linear interpolation seems to be the standard practice however, as Figure 1.1 indicates, this will not always yield satisfactory results. The introduction of more powerful techniques for robust multivariable linear design will result in increased difficulty associated with the satisfactory scheduling of such complex control laws.
- At present important system properties such as performance or even nominal stability are not addressed explicitly in this rather ad hoc design process. In fact such properties must be inferred from extensive simulations.

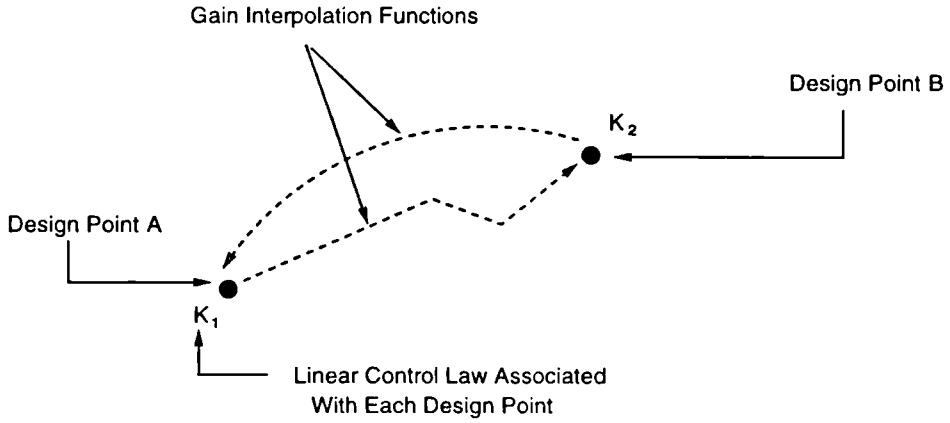

Figure 1.1: Gain Interpolation

Due to these problems with current gain scheduling practices, recent research has aimed at providing an analytical framework for gain scheduling and overcoming the

limitations highlighted. Shamma [64] provides rigorous mathematical justification for the gain scheduling guidelines such as scheduling on a slow variable. He showed how these *rules of thumb* can be transformed into quantitative statements. This work goes on to identify the fundamental limitations on the achievable performance by such rules of thumb. Shamma and Athans [65] point out that gain scheduling needs to address the possibility of fast parameter variations otherwise guaranteed properties cannot be established. They further suggest that a theory for fast parameter varying systems would involve modification of robust control design methodologies such as H_∞ and μ-synthesis in order to explicitly address the variations. Research in this area is still very much in its infancy.

Rugh [61] introduces an independent study of an analytical framework for gain scheduling. At this early stage difficulties still remain and any comprehensive analysis has yet to appear.

In view of these remaining difficulties the gain scheduling problem is far from being resolved and research into explicit nonlinear systems analysis will of course continue and justifiably so. One of the key motivations for the work of this thesis is the deficiencies of current practice outlined above.

1.2 Helicopter Control

The open loop dynamics of un-augmented, high-performance, single-rotor helicopters exhibit unacceptable responses. Consequently pilot workload is high and precise control is difficult. The deficiencies due to the highly nonlinear dynamics are as follows:

- Both the lateral and the longitudinal responses are unstable
- There is substantial coupling between the lateral and the longitudinal modes
- The bandwidths in the pitch, yaw and heave axes are too low to satisfy level 1 handling qualities criteria. This essentially implies that the pilot's workload in controlling the helicopter in these axes is likely to be unacceptably high. Chapter 6 provides a more precise insight into the numerical levels associated with the handling qualities criteria.

Flight control systems for helicopters are currently designed by using linear control theory. A review of recent linear helicopter control follows in Section 1.5.5 of the literature survey. The deficiencies associated with gain scheduling, often cause the flight control system performance to degrade as the helicopter moves away from the design conditions. The use of nonlinear control theory in the design of flight control systems allows for the possibility of achieving global control, that is around the entire flight envelope, by means of a single control law. This is because the design is based on the explicit nonlinear equations of motion and not linearized dynamics that are only valid locally. In addition, improved performance and safety over current linear designs may be achieved in regions where severe nonlinearities inevitably limit linear designs.

The helicopter flight control systems reported here are based on nonlinear system theory that employs mathematical tools from differential geometry. A few slightly differing nonlinear geometric control designs have been implemented in various aerospace applications in the past. The success and scope of these applications is documented in the Literature Survey, Section 1.5.2.

1.2.1 Helicopter Model

The model includes the main rotor rigid body effects, coning and quasi-steady flapping all of which are described in more detail in Chapter 2. The tail rotor is based on a similar analysis except that here the flapping is neglected. Due to the complexity of the flow field around the helicopter fuselage no analytical framework is used to express their effects; instead wind tunnel results are used to model these aerodynamic contributions. Although this model, due to Padfield [55], contains certain simplifying assumptions, its performance in stability and control studies is fairly well validated. This model has been used extensively in helicopter flight control system studies in the U.K.

The helicopter model was set up in *Simulink*[1] the nonlinear systems simulation package that operates in conjunction with *Matlab*[1]. Due to the immensity and complexity of the equations, implementation was expedited by programming the equations into *C*-Language *Mex* files that are readily accessed through Simulink.

[1]Simulink and Matlab are registered trademarks of The Maths Works Inc.

1.3 Feedback Linearization

Conceptually, Feedback Linearization is a means of transforming a nonlinear system into an equivalent linear system by means of coordinate changes and state feedback. Based on this linear equivalent system, a linear control law can then be formulated and then inverse-transformed to meet the design requirements.

To illustrate the concept of Feedback Linearization, consider the simple academic example:

$$\begin{aligned} \dot{x}_1 &= a \sin(x_2) \\ \dot{x}_2 &= -{x_1}^2 + u \end{aligned} \tag{1.2}$$

where a is a positive constant.

Consider the following state space coordinates change:

$$z_1 = x_1 \tag{1.3}$$

$$z_2 = a \sin(x_2) \tag{1.4}$$

and the coordinate change in the input space given by:

$$u = \frac{1}{a \cos(x_2)} v + {x_1}^2 \tag{1.5}$$

which can be viewed as a state feedback.

Applying the above mappings to the nonlinear dynamic system (1.2) yields:

$$\begin{aligned} \dot{x}_1 &= z_2 \\ \dot{x}_2 &= -{z_1}^2 + \frac{1}{a \cos(x_2)} v + {x_1}^2 \end{aligned} \tag{1.6}$$

Differentiating z_1 and z_2 and rearranging gives:

$$\begin{aligned} \dot{x}_1 &= \dot{z}_1 \\ \dot{x}_2 &= \frac{\dot{z}_2}{a \cos(x_2)} \end{aligned} \tag{1.7}$$

Replacing $\dot{x}_1$ and $\dot{x}_2$ of system (1.6) by the functions in (1.7) and rearranging:

$$\begin{aligned} \dot{z}_1 &= z_2 \\ \dot{z}_2 &= -{z_1}^2 a \cos(x_2) + v + {x_1}^2 a \cos(x_2) \end{aligned} \tag{1.8}$$

but since $x_1 = z_1$, system (1.8) becomes the following linear equivalent system

$$\begin{aligned} \dot{z}_1 &= z_2 \\ \dot{z}_2 &= v \end{aligned} \tag{1.9}$$

It is now possible to compute v using linear techniques, for example feedback of z, to achieve the necessary design requirements

Figure 1.2 and the worked example serve to simply illustrate the concept of Feedback Linearization. This example highlights two important consequences of the methodology.

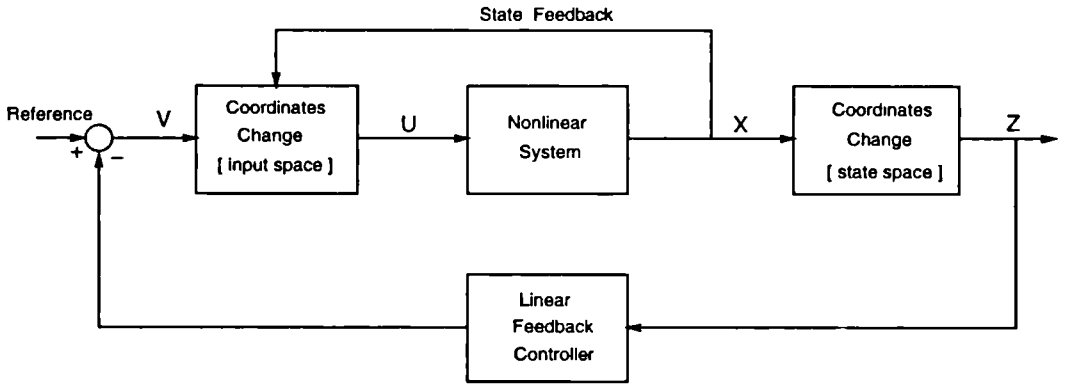

Figure 1.2: Feedback Linearization

The first is that regions exist in which the input space coordinates change is invalid. This is because the denominator contains the term $\cos(x_2)$ causing the transformation to be valid only when $\cos(x_2) \neq 0$, that is, for example, when $-\frac{\pi}{2} < x_2 < \frac{\pi}{2}$. This implies that the transformation is only local, if however no such restrictions apply then the transformation is globally applicable. For an appreciation of what the *local* restriction means for the control law, consider a small perturbation linearization of system 1.2 around the equilibrium point $x_1 = x_2 = 0$:

$$\begin{aligned} \dot{x}_1 &= a\, x_2 \\ \dot{x}_2 &= u \end{aligned} \tag{1.10}$$

By inspection, any control law based on this system may be applied at best when, say, $-\frac{\pi}{6} < x_2 < \frac{\pi}{6}$ and $-0.1 < x_1 < 0.1$. Clearly even the local feedback linearized control

law which has a region of validity $-\frac{\pi}{2} < x_2 < \frac{\pi}{2}$ and $-\infty \leq x_1 \leq \infty$, is far better, in this sense, than any linear design.

The second point that is worth noting is that the parameter a appears explicitly in the nonlinear control law. The method assumes that a is completely known, this however is often not so in practice and it is usually necessary to augment the basic feedback linearized control law with *certain robust terms* to ensure that performance is maintained despite such model uncertainty.

The above analysis is in fact an example of Input-State Linearization in which the *entire* nonlinear system is transformed into a linear equivalent system. This required coordinate changes in the state space and the input space and also the nonlinear feedback of state variables. More generally, under certain conditions, the nonlinear system of the form:

$$\dot{x} = f(x) + \sum_{i=1}^{m} g_i u_i \tag{1.11}$$

can be transformed to the following linear form:

$$\dot{z} = Az + \sum_{i=1}^{m} b_i v_i \tag{1.12}$$

where A is a constant real matrix, b_i are constant real vectors, z is the new state and v is the new input.

Using the linear equivalent system, linear control techniques such as pole placement may be used to design a controller for the system that ensures that the closed loop response is stable and satisfies other design specifications achievable with linear feedback control.

Feedback Linearization is based on nonlinear systems such as (1.11) which are *affine* in the control (i.e. the control variable enters linearly into the system). Since most practical systems are of this kind, this assumption is not generally a problem. The helicopter model unfortunately is not affine and in order to apply the theory directly an *iterative* scheme is introduced into the computations. This iterative scheme is independent of the helicopter model and may be used with other similar systems not satisfying the affine condition.

The method above is concerned with finding a linear equivalent to the entire nonlinear system and in doing so ignores the outputs and the input-output functional aspect

of the system. When faced with control objectives such as output command tracking and output decoupling the concept of Input-Output Linearization is more useful.

Input-Output Linearization is based on finding a nonlinear control law which achieves some degree of decoupling of the system outputs. By decoupling it is meant that certain outputs are independent of the other outputs. Input-Output Linearization of the following nonlinear system:

$$\begin{aligned} \dot{x} &= f(x) + \sum_{i=1}^{m} g_i u_i \\ y_i &= h_i(x) \end{aligned} \tag{1.13}$$

where y_i is some output, is achieved by finding an explicit relationship between the inputs to the system and its outputs. This *input-output map* gives rise to the decoupling control law and a corresponding state space coordinates transformation. Applying the control law and the coordinate change to the nonlinear system results in a system having a decoupled linear part as well as a reduced order nonlinear part. Again standard linear techniques may be applied to the linear part in designing a tracking controller for the system outputs. However it is also necessary to ensure that the remaining nonlinear subsystem ,which is called the *internal dynamics*, remains well behaved as a result of the Input-Output Linearization and the subsequent linear control design. The *zero dynamics*, which is a simplification of the internal dynamics, is used in the determination of the stability characteristics of the internal dynamics. The concept of zero dynamics is expounded in Chapter 3.

A variation of Input-Output Linearization is based on the concept of *Dynamic Inversion*. This may be described by considering the input-output map which takes the form:

$$y_i^{(r_i)} = M(x)u_i \tag{1.14}$$

where $y_i^{(r_i)}$ is the r_i th time derivative of y_i

If this mapping can be inverted then:

$$u_i = M^{-1}(x)y_i^{(r_i)} \tag{1.15}$$

Since it is desirable to have the output y track certain reference trajectories, y_{ref}, it is then possible to substitute y_{ref} into the inverse mapping in order to find the corresponding input u. In system analysis it is usual for the outputs to be computed based

on a knowledge of the inputs. However, in this case the *inverse* is done, that is the inputs required are calculated from a knowledge of the reference outputs.

1.4 Nonlinear Robust Control

For many physical systems, the development of accurate mathematical descriptions is still rather difficult and, as a result, uncertainties inevitably arise in these models. These uncertainties may be due to imperfectly known or even entirely unknown parameter values of the systems and their changing environment, as well as to the unpredicted disturbances, such as measurement noise. Consequently control laws that are resistant to the performance degradation effects of these uncertainties are important in the design of good and efficient control systems.

In recent years, essentially three control methodologies have been proposed to compensate for the effects of system uncertainties in nonlinear systems.

- Adaptive Control
- Sliding Mode Control
- Lyapunov-Based Control

In self-tuning and other stochastic adaptive control systems, on-line identification algorithms constantly monitor parameter values and disturbances to provide information to appropriate adaptive controllers. These schemes tend to be expensive and result in additional control system complexity.

In contrast to adaptive schemes, deterministic control methods use fixed nonlinear feedback control functions, which operate effectively over a range of system uncertainties of specified bounded magnitude, without using on-line identification. For such methods the uncertain quantities are described only in terms of bounds on their possible sizes, that is, no statistical description is assumed. Within this framework, the controllers guarantee stable operation for all possible variations of the uncertainties. The two principal approaches to deterministic control are Sliding Mode Control and Lyapunov Based Control.

Sliding mode control was originally developed from the variable structure control concept of Utkin [76]. It is based on a notational simplification allowing an n^{th} order tracking problem to be replaced by an equivalent first order stabilization problem. Sliding mode control first defines the sliding surface in the error state space which achieves the desired tracking objective in that tracking is achieved by remaining on this surface. Secondly a switching state feedback control that incorporates the bounds of the uncertainty is derived. This forces the error state to slide along the surface until it converges and tracking is attained. The undesirable *chattering* inevitable using the switching control law may be eliminated by using a saturation control. This however causes a steady state error to persist. The control system bandwidth can be tuned by adjustable parameters in the control law. Unfortunately the tuning capability is limited so there exists a trade-off between tracking accuracy and robustness to the uncertainties.

The Lyapunov approach uses a Lyapunov function and specified magnitude bounds on the uncertainties. A nonlinear control is then constructed to ensure uniform ultimate boundedness of the closed loop feedback trajectory to within a certain desirable accuracy. The controller is a discontinuous control function, with continuous control in a boundary layer in the neighbourhood of the switching surface. The boundary layer control prevents the excitation of high frequency un-modelled parasitic dynamics.

To date results fall into two categories. There are those that can be termed *structural* in nature. This means that the uncertainty cannot enter arbitrarily into the state equations, certain conditions must be met regarding the locations of the uncertainty within the system description; such requirements are referred to as *matching conditions.* In this situation uncertainties with an arbitrarily large prescribed bound can be tolerated . The second body of results is termed *non-structural* in nature. Instead of imposing matching conditions on the system, more general uncertainties are permitted at the expense of *sufficient smallness* assumptions on the allowable sizes of the uncertainties.

When considering uncertain nonlinear systems, Feedback Linearization provides a unified approach for the design of tracking or stabilization controllers. This approach does not however, guarantee robustness of the controller. To compensate for this deficiency , the above techniques have been used in conjunction with Feedback Linearization. The control system resulting from the incorporation of the robust methodologies

into the geometric control framework is described in Chapter 4.

1.5 Literature Survey

A general review of past investigations related to robust nonlinear control and helicopter control system design is presented below.

1.5.1 Nonlinear Geometric Control

This section outlines studies in the theoretical development of nonlinear geometric control theory.

In the area of Input-State Linearization, Krener [40] studied the question of finding a diffeomorphism that is, a local (or global) and smooth change of coordinates in the state space, that changes a nonlinear system into a linear one. Brockett [7] enlarged the class of transformations by also allowing for the use of a certain form of feedback. Following Brockett's paper, Jakubczyk and Respondek [37] found necessary and sufficient conditions for the existence of linearizing transformations for multi-input systems. Independently Su [73] used a slightly different formulation in providing a local solution for the single-input feedback equivalence problem. This was later improved by Hunt-Su-Meyer [31] in which a global solution was presented. Hunt-Su-Meyer [30] then found necessary and sufficient conditions for the existence of local linear transformations in the multivariable case. These conditions, not surprisingly, impose stringent requirements on the structure of the system. The transformations are generally difficult to find for all but fairly simple models.

The other trend in nonlinear differential geometric control, that is, the linearization of the input-output response of a nonlinear system has also received much attention in the recent past. Isidori [34] and Nijmeijer and van der Schaft [54] provide a comprehensive treatment of nonlinear control studied from this viewpoint. The immense potential offered to nonlinear control by the Input-Output Linearization approach, causes research to continue undaunted by certain obstacles identified during early work. The difficulties are generally associated with the dynamics rendered unobservable by the method. Some fairly recent advances that try to resolve the problems of the basic theory are presented below. These recent developments, although not essential to this

study, constitute significant advances in nonlinear geometric control.

For example, it can be shown that the Input-Output Linearization method may hide part of the nonlinear system that is linearizable. Therefore the control designers may unwittingly be ignoring dynamics that can readily be incorporated into the design procedure. Hunt and Verma [32] proved a sufficient condition for uncovering hidden modes for an n-th order single input single output system. By appropriate coordinate changes and state feedback a linear system of dimension k, where $n \geq k \geq r$, is produced. Note that r is the order of the linear subsystem obtained by Input-Output Linearization.

The problem of controlling a fixed nonlinear plant, in order to have its output track a reference signal and for stability of the entire closed loop system, is solvable by *standard* Input-Output Linearization if and only if the zero dynamics are asymptotically stable, i.e. if the system is *minimum phase*. However, in the non-minimum phase case, Isidori and Byrnes [35] showed that a solution may be achieved if the zero dynamics of the plant have a hyperbolic equilibrium. This means that the zero dynamics are either unstable or asymptotically stable so that a small perturbation linearization of the zero dynamics has no eigenvalues with real part equal to zero.

Isidori and Grizzle [36] showed how the achievement of noninteracting control with internal stability is possible for a system exhibiting unstable zero dynamics. They showed that the zero dynamics, based on any regular static feedback that achieves noninteracting control possesses an invariant manifold whose dynamics is independent of the particular decoupling control law used. These invariant P^* dynamics are called the fixed modes. Further they found that noninteracting control with internal stability can be achieved by regular static state-feedback only if the induced fixed dynamics is asymptotically stable.

For square nonlinear systems, Wagner [78] considered the use of dynamic feedback for the above problem. He found that the P^* dynamics contains another generally lower-dimensional sub-dynamics called the Δ_{mix} dynamics which is invariant even under dynamic feedback. If these dynamics are unstable, noninteraction with stability cannot be achieved. It is further shown that a system with unstable P^* dynamics that is not solvable via static feedback laws, can still be rendered non interactive and stable by way of a suitable dynamic feedback, provided the smaller Δ_{mix} dynamics is stable.

Battilotti [4] extended Wagner's work and found a sufficient condition for nonlinear noninteracting control with stability via dynamic state feedback for square systems. He proved that Δ_{mix} dynamics must be locally asymptotically stable along with the fulfilment of some rank conditions. Battilotti [5] generalised the above sufficient condition to systems having block partitioned outputs i.e. a nonlinear system with n inputs, p outputs grouped into μ blocks.

1.5.2 Aerospace Applications of Nonlinear Geometric Control

Most of the studies in this section do not attend to the most important property of any control law, that is, robustness to uncertainties. Instead they assume that the model corresponds exactly to the plant. However, these early studies are still important since they have exposed varying degrees of success in applying nonlinear geometric control to real systems. Importantly too, difficulty in applying such theories have been uncovered and areas for future research identified.

Meyer-Su-Hunt [52, 51] applied the equivalence theory to a somewhat simplified helicopter model. A regulator was designed for the transformed system, forcing it to track the output of a flight path reference model. Several simplifying assumptions were made in order to apply the equivalence theory; in spite of this, the robustness aspect of the control to uncertain dynamics was not investigated. The tracking outputs for the flight path trajectory, i.e. the three translation displacements, are not really consistent with guidelines given in (ADS-33C) where bank angle, pitch angle, yaw rate and altitude rate are the preferred tracking outputs for low speed and hovering flight.

Smith and Meyer [70] designed a full flight envelope controller using the inverse of the complete helicopter model in the feedforward control path. Continuous real time inversion of the helicopter model was achieved using a Newton-Raphson trim algorithm. Successful flight tests were carried out on a UH-1H helicopter.

Menon-Badgett-Walker-Duke [50] designed a flight trajectory controller for an aircraft using linearizing transformations and singular perturbation theory. They showed that by exploiting the time scale separation between the fast and the slow dynamics, the nonlinear control law can be simplified. For this type of system it is important to ensure that the assumed time scale separation is valid for the manœuvres considered.

Lane and Stengel [42] used the nonlinear inverse dynamics technique to design a controller for an aircraft at high angle of attack. Specific state variables that are of particular interest to the pilot were decoupled and arranged in sets that are varied as functions of the flight phase. This is a particularly interesting study since it identifies key points in the application of inverse dynamics such as the decoupling of outputs and the range of validity of the control law which depends directly on the range over which the input-output map is nonsingular. Unfortunately only the decoupled dynamics was addressed, the unobservable internal dynamics were not mentioned.

The application of the Input-State Linearization technique to the design of a helicopter trajectory following control system was carried out by Licéaga and Bradley [46]. In order to apply the method certain simplifications were made to the system, the first being to design a compensator to perform a partial linearization and decoupling of the system's angular rates and its normal velocity. This was carried out under the assumption that angular velocities evolve much faster than translational ones and that pilots therefore control flight trajectories by controlling the vehicle's attitude. Neglecting certain parameters by assuming *smallness* values, an equivalent system was then found using linearizing transformations on the partially linearized simplified system. A regulator was then designed to ensure tracking of the x, y, z displacements and the yaw angle trajectories. The control law here was derived analytically unlike Meyer et al [52] whose control system depended on a numerical method for calculation of the inverse solution.

Chartlet-Levine-Marino [9] present, without proof, necessary and sufficient conditions for full dynamic Feedback Linearization. These conditions are generalizations of those given for static Feedback Linearization by Hunt et al [30]. These transformations are applied to a simple *academic* aircraft model in which the inputs are assumed to be thrust and the three angular rates.

In problems in which the input-output map $M(x)$ in (1.14) is nearly singular, large control, which may not be permissible, is usually required. In aircraft control problems the input-output maps are often nearly singular if the small forces generated by the moment producing control devices are included in the design. Singh [66] incorporated these small forces into the aircraft model and managed to derive a decoupling control law that required only small control input. The decoupling scheme used gives rise to singularly perturbed systems. The quasi-steady state solution produces a control law

that decouples the system in an approximate manner.

Pantalos [56] showed how to Input-Output Linearize a somewhat academic helicopter model to ensure that no internal dynamics is produced. By assuming that each force, (drag, lift and side-force), and each moment, (rolling, pitching and yawing), are inputs to the system, an appropriate selection of six output variables enables full Input-Output Linearization to be performed. Additionally digital implementation of the continuous control law as well as inclusion of an adaptive scheme to overcome helicopter mass uncertainty was detailed.

The nonlinear inversion technique was used by Romano and Singh [60] to design a trajectory tracking control law for an aircraft carrying out large manœuvres. Robustness to parameter uncertainty was enhanced by use of integral feedback. Stability of the zero dynamics was also demonstrated.

Heiges-Menon-Schrage [29] used a similar approach to Menon et al [50], in that singular perturbation theory was used to simplify the linearizing transformations for a helicopter full authority trajectory controller. The important assumption made is that the cyclic stick and the pedals are moment generating devices with very little contribution to the body forces. Only the collective is used as a direct force control. This assumption aids the fast and slow time-scale controller approach. This leads to the development of a control law for the collective, (in the fast time scale), in conjunction with an analytical solution to the inverse mapping for the attitude dynamics, (in the slow time scale). This approach is good for tracking of the displacements x_e, y_e, z_e and yaw attitude, however this is not consistent with the requirements of ADS-33C.

Most of the fixed wing aircraft applications of nonlinear geometric control theory assume, without satisfactory proof, that the moment-to-force coupling is small and can therefore be neglected. Hauser-Sastry-Meyer [28] provided rigorous justification for the neglect of this small moment-to-force coupling. They also derived an approximate Input-Output Linearizing control law to achieve desirable closed loop properties for a simplified aircraft model. Finally they developed a theory for approximate Input-Output Linearization for a class of nonlinear systems called slightly non-minimum phase to which highly manœuvrable aircraft such as the V/STOL belong.

Gopalswamy and Hedrick [22, 23] showed how standard Input-Output Linearization

may fail to produce an adequate controller due to the instability of the unobservable modes when applied to a simplified high performance aircraft model. By identifying *ideal internal dynamics* and then redefining the outputs, they designed a control law such that asymptotic tracking of the real outputs is achieved while ensuring that the internal dynamics remains acceptable. The later paper also presents Sliding mode control used in conjunction with Input-Output Linearization for the design of a pitch-axis control system for an aircraft. The uncertainties considered are norm bounded and satisfy matching assumptions.

The studies concerning non-minimum phase nonlinear systems, or in this case input-output linearized systems whose internal dynamics are unstable, are important to this thesis since helicopters are non-minimum phase. The method employed in this thesis for treating the internal dynamics exploits the important fact that pilots control translational velocities by controlling body attitudes. Due to this, control of the internal dynamics can be achieved by using a secondary outer loop as shown in Chapter 5. Furthermore the similarity that exists between the outer loop method of this thesis and the formal output redefinition approach of Gopalswamy and Hedrick is indicated there.

1.5.3 Lyapunov Based Control

This section contains studies of early pioneering work in the area of control for uncertain systems. In addition, recent progress in enhancing the robustness properties of Feedback Linearization using a Lyapunov based control technique is included.

Gutman [24] presented the Lyapunov Min-Max approach to treat general nonlinear systems with uncertainties satisfying matching assumptions. The technique uses a discontinuous control law to ensure that every system trajectory is asymptotically stable. This approach motivated Leitmann [43] to find nonlinear control laws that stabilized linear dynamical systems containing uncertain elements which again satisfy the matching assumptions. In this case, however, the control discontinuity was smoothed by using a saturation controller which is only able to guarantee that every system response is ultimately bounded within a certain neighbourhood of the zero state. Corless and Leitmann [14] also used the Min-Max approach with the saturation control on nonlinear dynamical systems containing uncertainties. Unfortunately there is no general

rule for finding the Lyapunov function needed in this approach. Chapter 4 describes these studies further since they are central to the development of the Lyapunov-based control law analysis presented in Chapter 4.

Dispensing with the matching assumptions, Barmish and Leitmann [3] decomposed the system into two parts: a matched portion and a mismatched portion. A measure of mismatch M is defined for the unmatched part. Effective control is shown to be possible as long as the measure of mismatch M does not exceed some critical mismatch threshold M^*. Essentially the feedback control is based on the matched uncertainty and the resulting robustness margin will accommodate mismatched uncertainty, provided it remains small. This work carried out for linear systems was extended by Chen and Leitmann [12] to general nonlinear uncertain dynamical systems.

The following studies form the basis of recent work where Lyapunov based robustness theory is introduced into the Feedback Linearization structure.

Feedback Linearization was shown to be a robust method by Su-Meyer-Hunt [74]. It is robust in the sense that all systems close to the mathematical model are asymptotically stabilized about corresponding equilibrium points and that stability holds for any trajectory starting in some fixed compact set in the state space. By way of proof a method of constructing Lyapunov functions using the transformation method is presented.

The multivariable robust tracking of a Feedback Linearizable nonlinear system was studied by Ha and Gilbert [25]. To be fully linearizable the model exhibited special structural characteristics, further the uncertainties considered were only of the matched kind. The controller was designed by way of Lyapunov functions and ensured that the tracking error was ultimately bounded in the presence of modelling errors.

Kravaris and Palanki [39] used a similar approach on a single input single output system. Input-Output Linearization of the nominal model, i.e. without uncertainty, decomposed the system into a linear part and a reduced order nonlinear part, the *internal dynamics*. The uncertainties considered were matched, however a further restriction was the requirement for the internal dynamics to be stable, independent of the control variable and not subject to any uncertainty.

Robust stabilization of uncertain single input single output nonlinear systems was

considered by Korasani [38]. A singular perturbation analysis was used to reduce the system into two decoupled subsystems representing the slow and the fast dynamics. Coordinate transformations and static state space control laws were found such that the certain parts of both subsystems were both transformed to linear controllable and observable systems. The control laws were then modified to ensure boundedness of the solutions to the inclusion of uncertainty.

Singh [68] applied a Lyapunov type robust controller to an aircraft. The controller design required that the uncertainty be bounded and that the uncertainty appears at the same order of differentiation as the control input, i.e. the matching condition is satisfied. To improve tracking performance an integral term was included in the design. Unfortunately the effect of the robust control law on the internal dynamics, which were input variable dependent, was not mentioned.

Using Feedback Linearization, the robust stabilization of nonlinear uncertain systems was investigated by Chen and Chen [10]. Both matched and mismatched uncertainties are considered. Adopting saturation type controllers, arbitrarily large matched uncertainties were compensated while a certain *smallness* was necessary in the mismatched case. The nominal systems considered were fully feedback linearizable. This approach is followed in Chapter 4 where the Lyapunov Control is introduced into the Input-Output Linearization framework.

Liao-Fu-Hsu [45] employ matrix norm techniques in Lyapunov theory along with Input-Output Linearization to design a robust control law for a single input single output system. The mismatched uncertainties tolerated are assumed to lie within a *small* set. The analysis presented for the mismatched uncertainties provided the basis for the analysis presented in Chapter 4 for ensuring the boundedness of the internal dynamics.

1.5.4 Sliding Mode Control

A good introduction to the basics of Sliding mode control theory is given in Slotine and Li [69] and DeCarlo et al [15]. Further insight into the theory and current applications can also be found in Zinober [82, 83]. This section concentrates on studies that have incorporated Sliding mode ideas into the Feedback Linearization framework.

An early example of merging Sliding mode control techniques with multivariable Input-Output Linearization was presented by Fernández and Hedrick [18]. The feasibility of using the technique is demonstrated by application to a continuously stirred tank reactor problem. The issues pertaining to potential problems concerning internal dynamics and robustness to uncertainties, though mentioned, are not really developed.

Singh [67] used Sliding mode control (SMC) to design a discontinuous control law for an uncertain nonlinear aircraft model. The nominal system was decoupled by Input-Output Linearization and the uncertainties considered satisfied the structural matching conditions. The control law accomplished asymptotic decoupled output trajectory following. The stability or otherwise of the internal dynamics were not discussed.

For general single input single output (SISO) systems Behtash [6] combined SMC with Input-Output Linearization. The uncertainties satisfied a generalized matching assumption. The internal dynamics were assumed to be stable and independent of the control input. Therefore there was no need to assess the effect of the SMC law on the internal dynamics. The switching control law, while providing zero steady state tracking error, is somewhat imperfect due to the associated chattering as seen in Chapter 4.

Combining SMC with Input-Output Linearization, Fu and Liao [20] considered uncertain MIMO systems. As above, the uncertainty was matched and the internal dynamics were stable and unaffected by the control variable. Using matrix norm techniques, a discontinuous control law was derived. The controller design was finally applied to a two degree of freedom robotic manipulator with variable payload representing the uncertainty. This study forms the basis for the Sliding mode control law analysis detailed in Chapter 4.

Following the above study Liao-Fu-Hsu [44] used a similar system and conditions to derive a robust adaptive tracking control law having no knowledge of bounds on the uncertainty. Essentially, the uncertainty bound $\|\Delta\|$ is parametrized by an unknown parameter ψ and is given by:

$$\|\Delta\| \leq P\psi \tag{1.16}$$

where P is a known function.

In the Input-Output Linearization framework Elmali and Olgac [16] derived a second order SMC law for uncertain MIMO systems. To minimise on complications the

uncertainty was assumed to satisfy the matching conditions and the internal dynamics were considered stable and input variable independent. This latter assumption implies that the stable internal dynamics of the nominal system remains the same even when uncertainties are introduced. This work emphasised the difficulty incurred in choosing the tuning parameters, a procedure which still remains rather ad hoc.

1.5.5 Linear Helicopter Control

This section investigates recent advances in the use of linear control for the design of helicopter control systems. These studies are important since they provide useful insight into the specific problems that helicopter control designers should aim to resolve. Further they serve to expose areas of deficiency in current control laws. The results and performance analyses presented in these studies provide a qualitative measure against which the nonlinear control laws designed here may be compared.

Manness and Murray-Smith [49] presented a design for an Eigenstructure Assignment helicopter control system. The outputs $\dot{h}$, r, θ, ϕ were chosen to provide an attitude command attitude hold system. The performance of the controller was evaluated with respect to the requirements of ADS-33C. This study provides a clear insight into the vehicle dynamics and specific problems associated with it. The authors found that the explicit inclusion of the high frequency rotor dynamics in the model resulted in a certain deterioration in the control law, in particular a decrease in the achievable bandwidth and an increase in phase delay compared to the model involving only quasi-steady flapping.

Takahashi [75] designed an H_2 control law for a helicopter in a near hover flight condition. The control law consisted of a rate command system to decouple the three angular rates and the vertical velocity. Even though the control system bandwidths were consistent with the specifications of (ADS-33C) [1], the controller when tested in a vertical motion simulator was found to satisfy only level 2 handling quality requirements due to certain tendencies of the controller to cause pilot induced oscillation in the roll axis. This controller is restricted to operate only in the neighbourhood of the hover design condition.

Low and Garrard [47] present a design based on eigenstructure assignment for the improvement of helicopter handling qualities. The inner loop control law was designed

to decouple roll, pitch and yaw rates along with vertical velocity. Stability robustness was investigated by unstructured singular value techniques. The results presented for the nominal design were quite good, however the authors acknowledge that the control law needs to be tested on more realistic mathematical models. Gain scheduling of such a controller to provide full envelope control was not discussed.

Yue and Postlethwaite [80] outlined the application of H_∞ optimisation to a helicopter problem. The control law was designed for the hover flight condition and the nonlinear simulation results presented indicated the value of the approach to that flight condition. This was followed later by Yue and Postlethwaite [81] in which a handling qualities assessment and piloted simulation results, using a large motion system simulator, were presented. Certain deficiencies in the yaw axes were uncovered. Research in this area has continued over recent years with the following publications: Postlethwaite and Walker [58], Walker et al [79] and Postlethwaite and Skogestad [57]. At the time of the last publication further piloted simulation trials had been carried out but now for a full envelope controller. The scheduled controller was based on five fixed point designs at 0, 20, 40, 60 and 80 knots. Forward speed was chosen as the scheduling variable while linear interpolation was the scheduling algorithm. For the trajectories chosen the results were fairly good, however the problem that still remains is the operation of the controller in a more highly nonlinear phase of the flight envelope. As Shamma et al [65] point out, if gain scheduling is not developed further, then sophisticated linear control techniques are likely to be limited by somewhat inferior gain interpolation practices.

1.6 Contribution of the Thesis

Nonlinear control systems using Input-Output Linearization have been designed in Chapter 5 for a nonlinear helicopter model. These control laws are valid over the entire flight envelope therefore precluding any gain scheduling requirement.

Robustness to uncertainties such as disturbances or unmodelled dynamics has been addressed by augmenting the nominal Input-Output Linearization control law with Sliding mode and Lyapunov based methodologies as shown in Chapter 5. In addition, comparisons of the performance of these two robust techniques when applied to a real system are readily available from the simulation studies of Chapter 6.

The entire closed loop system was tested by computer simulation paying particu-

lar attention to the requirements of ADS-33C [1]. It was found, Chapter 6, that in general that the control laws enabled the helicopter to satisfy Level 1 handling quality specifications during hovering and low speed flight.

The Input-Output Linearization theory generally requires systems to be affine, i.e. to be linear in the control variable, if immense complexity is to be avoided in applying the theory. Although the helicopter system is non-affine the theory was still applied while avoiding additional computation and analysis by introducing an iterative scheme the details of which appear in Chapter 5.

Helicopter systems are non-minimum phase which in the context of nonlinear geometric control implies that the internal dynamics are unstable. Systems of this kind are generally not thought amenable to the application of Input-Output Linearization. However it is shown here, Chapter 5, how this problem may be resolved in the helicopter case by exploiting physical characteristics of the dynamic system.

The subsection entitled Internal Dynamics in Section 4.2.2 addresses the behaviour of the internal dynamics of an uncertain system when an Input-Output Linearization control law augmented with a robust Lyapunov scheme is applied. The analysis presented has been developed from ideas presented in Liao-Fu-Hsu [45]. While this section is not entirely original it contains elements of novelty.

Finally the *UK-Standard* helicopter model due to Padfield [55] was implemented in Simulink and provides a complete control system design and performance testing environment by allowing usage of Matlab's control system analysis features. Particular model details appear in Chapters 2, 5 and 6 as deemed appropriate.

In summary two nonlinear control laws for a single rotor helicopter were constructed using Input-Output Linearization as a basis for the designs. Robustness to uncertain dynamics was enhanced by incorporating either Lyapunov-based or Sliding mode control techniques. The existence of nonlinear control terms in the helicopter model was effectively dealt with by means of an iterative scheme which eliminates the need for a more complex analysis when such non-affine systems are encountered. The internal dynamics has been examined and it was shown that in spite of the non-minimum phase nature of the system, effective control is maintained by exploiting physical characteristics of the system. Finally compliance with Level 1 handling qualities requirements has been demonstrated though computer simulation.

Chapter 2

The Helicopter System

The main components of the helicopter considered in this study are shown below in Figure 2.1. The lift required to balance the weight or to produce vertical translational motion is generated by the single main rotor. By tilting this lift vector pitching and rolling moments can be produced which, as seen later, allows the vehicle to be accelerated in the fore and aft as well as the lateral directions respectively. The tail rotor thrust is varied to balance the torque developed by the main rotor and also enables the helicopter to be controlled in yaw. The fin and the tailplane, although not control surfaces, facilitate lateral and longitudinal open loop stability in forward flight. The main rotor generates both forces and moments which cause severe coupling between axes and therefore helicopters are substantially more difficult to control than fixed wing aircraft.

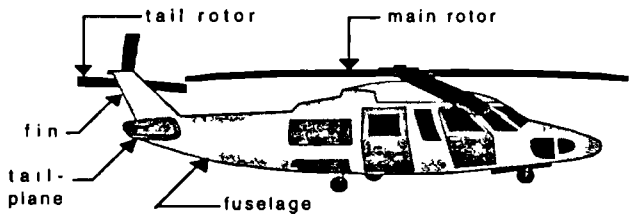

Figure 2.1: Helicopter System

This chapter discusses the dynamics of the helicopter, highlighting the unique problems associated with helicopter control. To do this a brief introduction to rotor behaviour is presented in Section 2.1. This is followed in Section 2.2 by comments regarding the severe cross coupling present in the dynamic behaviour of the helicopter.

Finally, in Section 2.3, the equations of motion for the helicopter model are presented in a form amenable to Input-Output Linearization.

2.1 Main Rotor Dynamics

As an introduction to the rotor blade motion, consider a typical rotor hub configuration shown in Figure 2.2.

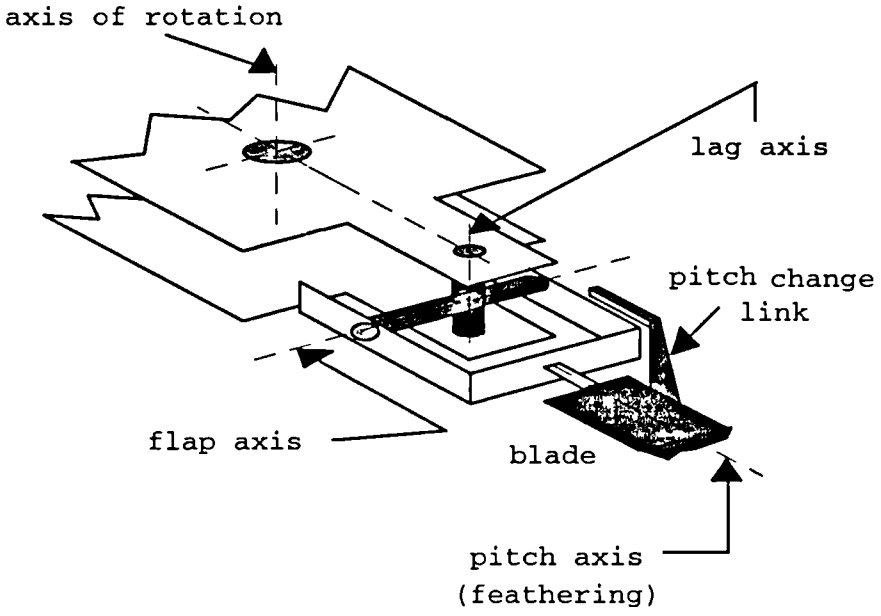

Figure 2.2: Rotor Hub Configuration

The hinges in this arrangement are fully *articulated* and as such each rotor blade is individually attached to the hub through two virtually perpendicular hinges. This allows rigid motion of the blade in two directions: out-of-plane rotation (flapping motion) and in-plane rotation (lag motion).

Smith [71] provides a simple treatment of the rotor dynamics. As the blades rotate they will take up a *coning* angle β as shown Figure 2.3. This arises due to the force balance between the weight of the blades, lift and the centrifugal forces acting on them.

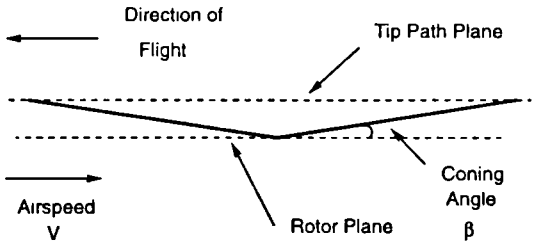

Figure 2.3: Coning Angle

When the helicopter is in forward flight, the increase in lift on the advancing blade due to the increased relative velocity causes it to flap up through an angular displacement called the flapping angle as shown in Figure 2.4. This motion reduces the effective blade incidence and hence lift on the blade and ultimately allows the blade to flap down again. The reverse process occurs on the retreating blade. This combined effect tends to equalise lift across the entire rotor. This phenomenum is called *flapping.*

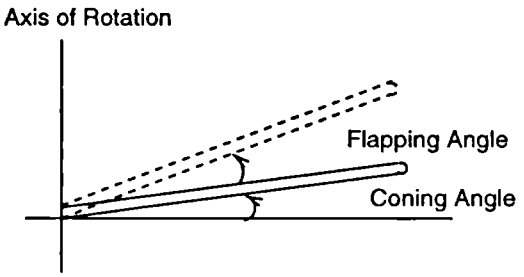

Figure 2.4: Flapping Angle

The flapping motion sets up Coriolis moments in the plane of the disc which subsequently gives rise to an in-plane motion called *lagging.* Note however that this lead-lag motion, with its accompanying lag angle Figure 2.5 , tends to make only a minor contribution to the rotor's performance, Seddon [63].

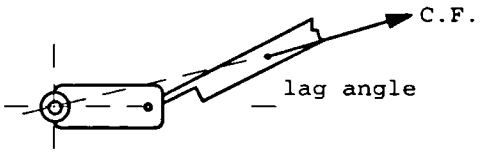

Figure 2.5: Lag Angle

2.1.1 Rotor Control

To control a rotor, the pitch angles of its blades can be altered to produce a change in the blades' angle of attack, thereby controlling the corresponding aerodynamic forces. During rotation there will be an azimuthal variation of lift as indicated by the velocity distribution of Figure 2.6.

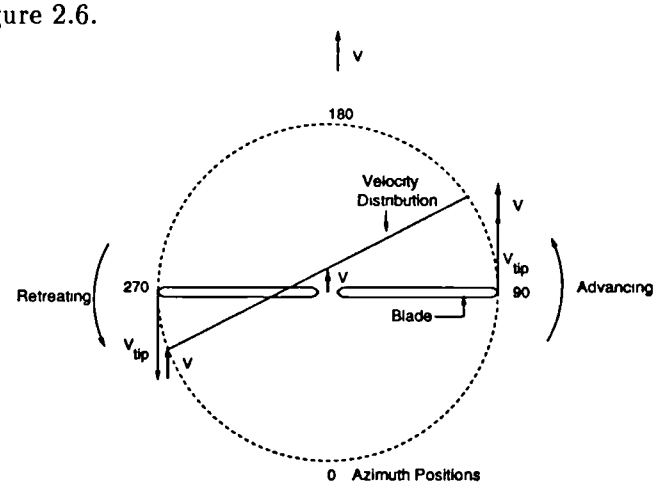

Figure 2.6: Velocity Distribution

This variation affects the degree of flapping motion, as shown Figure 2.7, and consequently the direction of the average thrust vector.

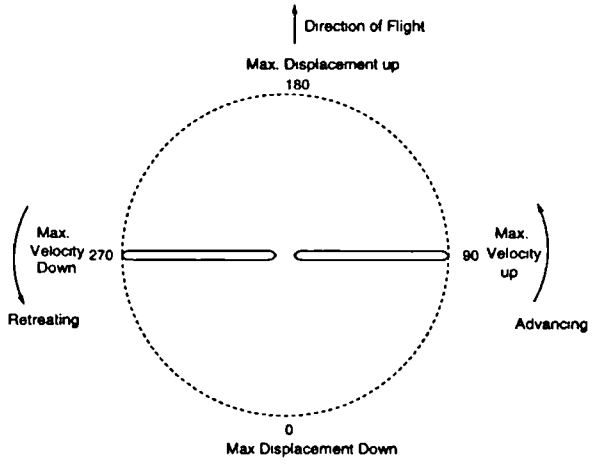

Figure 2.7: Flapping Behaviour

Essentially, with the advancing blades producing lift more efficiently than the re-

treating ones, a large lift asymmetry is created between the advancing and the retreating blades. Reducing the pitch of each blade as it traverses the advancing side while increasing it on the retreating side will compensate for the lift asymmetry. In other words a cyclic variation of lift can be effected by changing the pitch of the blades as they rotate; this is known as cyclic pitch control. When the result of the cyclic pitch is a pitching moment applied to the helicopter, then it is called the longitudinal cyclic θ_{ls}. If the result is a rolling moment then the control is termed the lateral cyclic θ_{lc}.

Yaw is controlled by changing, by the same amount, the pitch angle of all the blades of the tail rotor. This collective pitch deflection of these blades is called the tail rotor collective θ_{ot}. When a collective pitch deflection is made to the all blades of the main rotor θ_o, a change in lift occurs. Collective pitch changes cause subsequent changes in lift thereby allowing for direct control of the helicopter's vertical motion.

2.2 Helicopter Dynamics

The forces and moments acting on a helicopter arise from two sources, aerodynamic and inertial. All surfaces exposed to the airstream produce aerodynamic forces, due to the lack of lateral symmetry these give rise to considerable coupling between the lateral and the longitudinal motions.

An example of the kind of coupling that occurs is that between rolling and yawing; a roll acceleration is experienced when the pedals are moved to effect a yaw change. This occurs because the tail-rotor is generally above the roll axis and therefore the tail-rotor thrust acting through the moment arm produces a rolling moment.

The inertial forces are extremely important to the helicopter since they play the dominant role in many helicopter motions. The gyroscopic moments from the main rotor are of principal importance. As presented in Saunders [62] the inter-axis coupling that arises from these gyroscopic moments may be illustrated as follows. Assuming counterclockwise blade rotation as viewed from above, then following an applied moment the gyroscopic action of the rotor produces a rate (or precession) as given below:

Applied Moment	Gyroscopic Precession
Pitch up	Rolling left
Pitch down	Rolling right
Roll right	Pitching down
Roll left	Pitching up

The gyroscopic action of the rotor does not end here; due to the reversibility of the torque-rate equation, Cochin [13], an established rotational rate, from whatever source, will in turn produce a gyroscopic moment as follows:

Established Motion	Gyroscopic Moment
Pitching up	Roll right
Pitching down	Roll left
Rolling right	Pitch up
Rolling left	Pitch down

This gyroscopic cross-coupling behaviour makes a helicopter's dynamics fundamentally different from those of a fixed wing aircraft.

Since the main rotor is used for direct lift control as well as for generating pitching and rolling moments, normal, longitudinal and lateral motions are all coupled together. To illustrate this consider the mechanisms involved in a *slowing down* procedure.

- It is first necessary to pitch the helicopter nose up using the longitudinal cyclic. This effectively tilts the rotor disc backwards giving rise to a rearward component of thrust, hence achieving deceleration by a pitch attitude change.
- The normal component of thrust is now insufficient to balance the helicopter weight; in order to avoid loss of height an increase in main rotor collective is necessary to effectively increase the thrust.
- The increased rotor thrust gives rise to greater torque, therefore a change in tail rotor collective must follow to balance this torque and so avoid the development of significant sideslip.
- The change in tail-rotor collective then induces a rolling moment which must be countered by an input through the lateral cyclic.

These coupled motions, if not dealt with quickly and effectively, will result in the helicopter pitching and rolling and certain deviation from the desired flight path on

approach.

This sort of complex interplay between balancing forces and moments makes flying a helicopter more complicated and therefore more difficult than flying a fixed wing aircraft. The excessive pilot workload that occurs under most conditions makes the use of an automatic flight control system mandatory. In fact, the nonlinear control theory presented in this thesis offers the possibility of decoupling these motions which would then greatly enhance the pilot's effectiveness in highly complex manœuvres. In fact this decoupling control system allows for the expansion of the flight envelope into regions where previously pilots were unsuccessful in achieving adequate control over the vehicle.

2.3 Helicopter Model

In helicopters six *rigid body* degrees of freedom for the fuselage are considered. These are:

	Translation along the three body axes:	Rotation about these three axes:
z-axis	up-down motion	yawing
y-axis	right-left motion	pitching
x-axis	fore-aft motion	rolling

In addition, the main rotor itself has some independent degrees of freedom including collective coning, flapping, lagging and rotational speed. The pilot judges the flying qualities in terms of the first six and is only indirectly concerned with the blade motions themselves. Ironically it is the blade motions that determine the major forces and moments on the fuselage.

The model used in this thesis is due to Padfield [55] and includes the main rotor rigid body effects, coning and *quasi-steady* flapping. According to Prouty [59] the time constant for the flapping of conventional rotor blades corresponds to $\frac{1}{4}$ to $\frac{1}{2}$ of a rotor revolution and it is this rapid response that justifies the use of the quasi-steady assumption. The approximation effectively eliminates blade motion as separate degrees of freedom and simulates replacing the rotor with a *black box* at the top of the mast, which essentially produces forces and moments instantaneously in response to changes

in flight condition or control inputs.

In addition the main rotor lag degree of freedom is also omitted which as noted earlier contributes relatively little to the blade dynamics. The tail rotor is based on a similar analysis to the main rotor except here flapping is neglected. The rotational speed of each rotor is assumed to be constant for these studies. Due to the complexity of the flow field around the helicopter fuselage no analytical framework is used to express their effects; instead wind tunnel results are used to model these aerodynamic contributions.

Although this model contains certain simplifying assumptions, its performance in stability and control studies is fairly well validated and has been used widely in helicopter flight control system studies in the U.K. One should note however that increasingly challenging control tasks will only be solved by high gain, high bandwidth control laws. Under these circumstances quasi-steady rotor modelling may not be sufficient and the interaction of the high frequency flapping modes with the control system modes must be assessed at the design stage.

2.3.1 Reference Frames

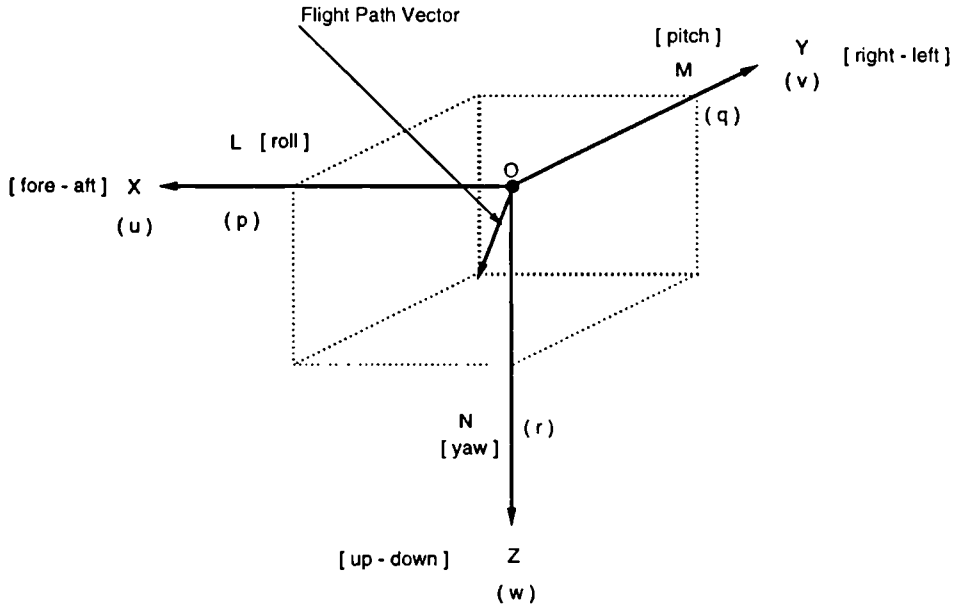

Figure 2.8: Axis System

OX is the longitudinal axis. positive forward

OY is the lateral axis. positive starboard

OZ is the normal axis. positive towards undercarriage

In the analysis of helicopter dynamics, the equations of motion are usually given in terms of the body axes system. The body reference frame is shown in Figure 2.8, where the origin O lies at the centre of gravity of the helicopter.

The attitude of the body with respect to the inertial reference frame is defined by the Euler angles : θ, ϕ, ψ. These angles, as shown in Figure 2.9, are the angles between the body axes and the earth fixed inertial frame.

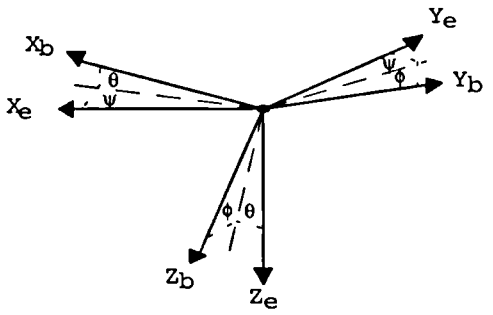

Figure 2.9: Euler Angles

The helicopter, which is assumed to be rigid, has six degrees of freedom: three of these define the location of a reference point in the body (translational) and three define the orientation of the body (rotational).

Now each of the six degrees of freedom requires two state variables (one position and one velocity) giving a total of twelve states that completely describe the motion of the helicopter. However, in general not all of these twelve state variables are of interest and some of the corresponding differential equations may be neglected.

The six states associated with the three translational degrees of freedom are:

x, y, z	u, v, w	Displacements and velocities in the ox,
position	velocity	oy and oz directions respectively.

The six states associated with the three rotational degrees of freedom are:

θ, ϕ, ψ	p, q, r	Orientation angles with respect to the earth
attitude	rate	and angular velocities about the ox, oy, oz
		directions respectively.

2.3.2 The General Equations of Motion

The following equations were taken from Padfield [55], which are essentially the same dynamic equations given by standard texts such as Etkin [17].

$$\dot{u} = vr - wq - g\sin\theta + \frac{X}{m} \tag{2.1}$$

$$\dot{v} = wp - ur + g\cos\theta\sin\phi + \frac{Y}{m} \tag{2.2}$$

$$\dot{w} = uq - vp + g\cos\theta\cos\phi + \frac{Z}{m} \tag{2.3}$$

$$\dot{p} = \frac{(I_{yy} - I_{zz})qr + I_{xz}(\dot{r} + pq) + L}{I_{xx}} \tag{2.4}$$

$$\dot{q} = \frac{(I_{zz} - I_{xx})rp + I_{xz}(r^2 - p^2) + M}{I_{yy}} \tag{2.5}$$

$$\dot{r} = \frac{(I_{xx} - I_{yy})pq + I_{xz}(\dot{p} - qr) + N}{I_{zz}} \tag{2.6}$$

$$\dot{\theta} = q\cos\phi - r\sin\phi \tag{2.7}$$

$$\dot{\phi} = p + [q\sin\phi + r\cos\phi]\tan\theta \tag{2.8}$$

$$\dot{\psi} = [q\sin\phi + r\cos\phi]\sec\theta \tag{2.9}$$

$$\begin{aligned}\dot{x}_e = {} & u[\cos\theta\cos\psi] + v[\sin\phi\sin\theta\cos\psi - \cos\phi\sin\psi] \\ & + w[\cos\phi\sin\theta\cos\psi + \sin\phi\sin\psi]\end{aligned} \tag{2.10}$$

$$\begin{aligned}\dot{y}_e = {} & u[\cos\theta\sin\psi] + v[\sin\phi\sin\theta\sin\psi + \cos\phi\cos\psi] \\ & + w[\cos\phi\sin\theta\sin\psi - \sin\phi\cos\psi]\end{aligned} \tag{2.11}$$

$$\dot{z}_e = u[-\sin\theta] + v[\sin\phi\cos\theta] + w[\cos\phi\cos\theta] \tag{2.12}$$

The above equations were derived subject to the following assumptions:

- The earth is a sphere rotating on an axis fixed in inertial space and g is a constant acting normal to the surface.
- The centripetal acceleration associated with the earth's rotation is neglected.
- The atmosphere is at rest relative to the rest of the earth.
- The vehicle is a rigid body.
- xz is a plane of symmetry.

Note that x_e, y_e and z_e instead of x, y, z are used in these equations, this is because in practice the position of the vehicle relative to the Earth and not the vehicle's body fixed reference frame is of interest.

The total forces X, Y, Z and the total moments L, M, N are the sum of the contributions from each of the helicopter's five main components : the main rotor, the tail rotor, the tail plane, the fin and the fuselage. If the vertical plane of the helicopter is considered to be a plane of symmetry then the force and moment equations have the following contributions

$$X = X_r + X_f \tag{2.13}$$

$$Y = Y_r + Y_t + Y_{fn} + Y_f \tag{2.14}$$

$$Z = Z_r + Z_{tp} + Z_f \tag{2.15}$$

$$L = L_r + L_t + L_{fn} \tag{2.16}$$

$$M = M_r + M_{tp} + M_f \tag{2.17}$$

$$N = N_r + N_t + N_{fn} + N_f \tag{2.18}$$

The subscripts relate to the contribution from each of the helicopter's main components:

r : [main rotor] fn : [fin] tp : [tailplane] f : [fuselage] t : [tail rotor]

The main rotor forces and moments are functions of the aerodynamic parameters, the state variables and the main rotor pilot inputs. Similarly the tail rotor forces and moments are functions of the states and the pilot input controlling the tail rotor. The fuselage forces and moments which are calculated from semi-empirical wind tunnel data given in Padfield [55] do not however depend directly on the helicopter commands. The fin and the tailplane contributions are functions of the state variables but again they are independent of the pilot inputs.

As mentioned earlier, the four control inputs available to the pilot are :

Collective	θ_o	
Longitudinal Cyclic	θ_{ls}	MAIN ROTOR
Lateral Cyclic	θ_{lc}	
Tail-Rotor Collective	θ_{ot}	TAIL ROTOR

Of the twelve state equations presented earlier only the first eight are critical to a mathematical model of the helicopter's dynamic behaviour. This is because these eight equations are each dependent on all of these eight state variables, $\{u,\ v,\ w,\ p,\ q,\ r,\ \theta,\ \phi\}$, but independent of the remaining four states, $\{\psi,\ x_e,\ y_e,\ z_e\}$. The remaining four states, though providing information about the helicopter's motion, do not contribute to the basic model. The eight state model may then be rewritten as:

$$\dot{u} = vr - wq - g\sin\theta + \frac{X_f(\mathbf{x})}{m} + \frac{X_r(\mathbf{x},\mathbf{u})}{m} \tag{2.19}$$

$$\dot{v} = wp - ur + g\cos\theta\sin\phi + \frac{Y_f(\mathbf{x})}{m} + \frac{Y_{fn}(\mathbf{x})}{m} + \frac{Y_r(\mathbf{x},\mathbf{u})}{m} + \frac{Y_t(\mathbf{x},\mathbf{u})}{m} \tag{2.20}$$

$$\dot{w} = uq - vp + g\cos\theta\cos\phi + \frac{Z_f(\mathbf{x})}{m} + \frac{Z_{tp}(\mathbf{x})}{m} + \frac{Z_r(\mathbf{x},\mathbf{u})}{m} \tag{2.21}$$

$$\dot{p} = \frac{(I_{yy} - I_{zz})qr + I_{xz}(\dot{r} + pq) + L_{fn}(\mathbf{x}) + L_r(\mathbf{x},\mathbf{u}) + L_t(\mathbf{x},\mathbf{u})}{I_{xx}} \tag{2.22}$$

$$\dot{q} = \frac{(I_{zz} - I_{xx})rp + I_{xz}(r^2 - p^2) + M_f(\mathbf{x}) + M_{tp}(\mathbf{x}) + M_r(\mathbf{x},\mathbf{u})}{I_{yy}} \tag{2.23}$$

$$\dot{r} = \frac{(I_{xx} - I_{yy})pq + I_{xz}(\dot{p} - qr) + N_f(\mathbf{x}) + N_{fn}(\mathbf{x}) + N_r(\mathbf{x},\mathbf{u}) + N_t(\mathbf{x},\mathbf{u})}{I_{zz}} \tag{2.24}$$

$$\dot{\theta} = q\cos\phi - r\sin\phi \tag{2.25}$$

$$\dot{\phi} = p + [q\sin\phi + r\cos\phi]\tan\theta \tag{2.26}$$

where x is the state vector and u is the input vector.

As seen in chapter 1, in order to carry out Feedback Linearization, the nonlinear system must be presented in the following form:

$$\dot{\mathbf{x}} = f(\mathbf{x}) + g_1(\mathbf{x})\,\mathbf{u}_1 + \ldots + g_m(\mathbf{x})\,\mathbf{u}_m \tag{2.27}$$

The first change must then be to rewrite the $\dot{p}$ and $\dot{r}$ equations such that the state derivatives $\dot{p}$ and $\dot{r}$ appear only on the left hand side of the equations.

$$\begin{aligned}\dot{p} = {} & I_1\,q\,r + I_2\,p\,q + I_3\,\{L_{fn}(\mathbf{x}) + L_r(\mathbf{x},\mathbf{u}) + L_t(\mathbf{x},\mathbf{u})\} + \\ & I_4\,\{N_f(\mathbf{x}) + N_{fn}(\mathbf{x}) + N_r(\mathbf{x},\mathbf{u}) + N_t(\mathbf{x},\mathbf{u})\}\end{aligned} \tag{2.28}$$

$$\dot{q} = I_5\, r\, p + I_6\,(r^2 - p^2) + I_7\,\{M_f(\mathbf{x}) + M_{tp}(\mathbf{x}) + M_r(\mathbf{x},\mathbf{u})\} \tag{2.29}$$

$$\dot{r} = I_8\, p\, q + I_9\, q\, r + I_{10}\,\{L_{fn}(\mathbf{x}) + L_r(\mathbf{x},\mathbf{u}) + L_t(\mathbf{x},\mathbf{u})\} + I_{11}\,\{N_f(\mathbf{x}) + N_{fn}(\mathbf{x}) + N_r(\mathbf{x},\mathbf{u}) + N_t(\mathbf{x},\mathbf{u})\} \tag{2.30}$$

Note that $\dot{q}$ is included so as to maintain consistency. The constants I_1 to I_{11} are listed in appendix A.

The forces and moments due to the main rotor are highly nonlinear functions of the state (x) and the inputs (u). Extensive manipulation of these expressions using the *Symbolic Algebra* capability of the program *Mathematica*[1], reduces these expressions to nonlinear functions of the state explicitly multiplied by the inputs. The general form that is then achieved for the main rotor contributions is as follows:

$$\begin{aligned} X_r(\mathbf{x},\mathbf{u}) = {} & X_{r_0}(\mathbf{x}) + X_{r_1}(\mathbf{x})\,\theta_o + X_{r_2}(\mathbf{x})\,\theta_{ls} + X_{r_3}(\mathbf{x})\,\theta_{lc} + X_{r_4}(\mathbf{x})\,\theta_o\,\theta_{ls} + \\ & X_{r_5}(\mathbf{x})\,\theta_o\,\theta_{lc} + X_{r_6}(\mathbf{x})\,\theta_o^2 + X_{r_7}(\mathbf{x})\,\theta_{ls}\,\theta_{lc} + X_{r_8}(\mathbf{x})\,\theta_{ls}^2 + \\ & X_{r_9}(\mathbf{x})\,\theta_{lc}^2 \end{aligned} \tag{2.31}$$

The other terms Y_r, L_r, M_r, N_r are similarly expressed. However Z_r alone has the unique form.

$$Z_r(\mathbf{x},\mathbf{u}) = Z_{r_0}(\mathbf{x}) + Z_{r_1}(\mathbf{x})\,\theta_o + Z_{r_2}(\mathbf{x})\,\theta_{ls} + Z_{r_3}(\mathbf{x})\,\theta_{lc} \tag{2.32}$$

Likewise the tail rotor contribution to the forces and the moments are rewritten as:

$$Y_t(\mathbf{x},\mathbf{u}) = Y_{t_0}(\mathbf{x}) + Y_{t_1}(\mathbf{x})\,\theta_{ot} \tag{2.33}$$

and L_t, N_t have the same structure.

To summarize, the helicopter dynamics have been presented paying special attention the coupling effects which mainly arise as a result of the dual-role of the main rotor in producing forces as well as moments. The equations of motion of the system are also presented in a form that can be used directly with the Input-Output Linearization theory to design nonlinear helicopter control laws as shown in Chapter 5.

[1]Mathematica is a registered trademark of Wolfram Research, Inc.

Chapter 3

Nonlinear Geometric Control

Linear control is a well-developed subject with a long history of successful applications. Unfortunately designs based on linear theory often deteriorate rapidly due to their restricted regions of operation. Modern technology such as high-speed, high-accuracy robots or high performance aircraft, is demanding increasingly sophisticated control systems which will operate over wide regions. The limitations of linear control are now significantly restricting the achievable performance of such systems.

Faced with the problem of a nonlinear reality that is difficult to treat, together with the availability of a good understanding of linear systems, a natural development was the concept of the linear equivalence of a nonlinear system. By applying the usual automatic control transformations, that is, a change of coordinates and feedback, an attempt is made at making the nonlinear system behave the same, at least locally, as a linear system. Achieving this globally is unlikely in practice, however examples have shown that even the local equivalence approach is far superior to that of the small perturbation linearization methods.

This chapter details Input-Output Linearization along with the necessary tools from differential geometry that are necessary for the theoretical description. As mentioned in Chapter 1, Input-Output Linearization is concerned with explicitly linearizing the input-output response of a system by means of coordinate transformations and feedback. This often results in a decomposition of the original system into a linear observable part and a reduced order unobservable nonlinear part. Before embarking on the theoretical analysis a brief outline, is given next, of the mathematical tools that will be of use later.

3.1 Mathematical Background

The following definitions can be found in Isidori [34] and Slotine and Li [69]. An n-dimensional space with its ordinary topology is denoted by $\Re^n$. A *vector field* $f : \Re^n \to \Re^n$ is *smooth* (C^∞), if the partial derivatives of $f(x)$ of any order with respect to $x_1, \ldots, x_n$ exist and are continuous.

Given a scalar function $h(x)$ and vector fields $f(x)$ and $g(x)$, note the following definitions:

Definition Let $h : \Re^n \to \Re$ be a smooth scalar function and $f : \Re^n \to \Re^n$ be a smooth vector field on $\Re^n$, then the *Lie Derivative* of h with respect to f is a scalar function defined by:

$$L_f h = \frac{\partial h}{\partial x} f$$

Repeated Lie derivatives are defined recursively as follows

$$\begin{aligned} L_f^0 h &= h \\ L_f^i h &= L_f(L_f^{i-1} h) = \frac{\partial (L_f^{i-1} h)}{\partial x} f \end{aligned}$$

Definition Let f and g be two smooth vector fields on $\Re^n$. The *Lie Bracket* of f and g is a third vector field defined by:

$$[f, g] = \frac{\partial g}{\partial x} f - \frac{\partial f}{\partial x} g$$

The Lie bracket $[f, g]$ may also be written as $ad_f g$ and repeated Lie brackets are defined as follows:

$$\begin{aligned} ad_f^0 g &= g \\ ad_f^i g &= [f, ad_f^{i-1} g] \end{aligned}$$

A *Diffeomorphism* can be viewed as a generalization of the coordinate transformation, the formal definition however is given below:

Definition A function $\Phi : \Re^n \to \Re^n$, defined in a region Ω, is called a diffeomorphism if it is smooth and if its inverse Φ^{-1} exists and is smooth.

Note that if the region Ω is the whole space $\Re^n$, then the diffeormorphism $\Phi(x)$ is global.

The following lemma given by Slotine and Li [69], is a direct consequence of the well known Implicit Function Theorem, and may be used to determine whether a function $\Phi(x)$ is a diffeomorphism.

Lemma Let $\Phi(x)$ be a smooth function defined in a region Ω in $\Re^n$. If the Jacobian matrix $\frac{\partial \Phi}{\partial x}$ is non-singular at a point $x = x_o$ of Ω, then $\Phi(x)$ defines a local diffeomorphism in a subregion of Ω.

To illustrate the use of a diffeomorphism, consider the system below:

$$\dot{x} = f(x) + g(x)\, u \tag{3.1}$$

The diffeomorphism $\Phi(x)$ is used to transform the system into another nonlinear system in terms of a new set of states. Let the new set of states be defined by $z = \Phi(x)$. Differentiation of z and use of the original dynamic equation yields:

$$\dot{z} = \frac{\partial \Phi}{\partial x}\,\dot{x} = \frac{\partial \Phi}{\partial x}\,(f(x) + g(x)\, u) \tag{3.2}$$

Therefore the new state space representation is

$$\dot{z} = \bar{f}(z) + g(z)\, u \tag{3.3}$$

where $x = \Phi^{-1}(z)$ has been used and $\bar{f}$ and g are defined obviously.

Essentially the above lemma and example illustrate that a set of functions

$$\Phi(x) \;=\; \begin{bmatrix} \phi_1(x) \\ \vdots \\ \phi_n(x) \end{bmatrix} = \begin{bmatrix} z_1 \\ \vdots \\ z_n \end{bmatrix} \tag{3.4}$$

can be used as new coordinates if their gradients:

$$\left\{ \frac{\partial \phi_1}{\partial x} \;\cdots\; \frac{\partial \phi_n}{\partial x} \right\}^T \tag{3.5}$$

are linearly independent.

3.2 Input-Output Linearization

The discussion here is confined to square multi-input multi-output (MIMO) nonlinear systems, that is, systems where the number of outputs is equal to the number of inputs.

This does not constitute a restriction however since it is only possible to independently control at most the same number of outputs as there are inputs.

Consider

$$\begin{aligned} \dot{x} &= f(x) + \sum_{i=1}^{m} g_i(x)\, u_i \\ y_1 &= h_1(x) \\ &\vdots \\ y_m &= h_m(x) \end{aligned} \tag{3.6}$$

where x is the state vector, $u_1, \ldots, u_m$ are control inputs, $y_1, \ldots, y_m$ are outputs, $f, g_1, \ldots, g_m$ are smooth vector fields and $h_1, \ldots, h_m$ are smooth scalar functions defined on an open set of $\Re^n$.

Slotine and Li [69] provide a good reference for the basic Input-Output Linearization procedure which begins with finding a relationship between the inputs and the outputs. This is done by differentiating the outputs y_j so that they are explicitly related to the inputs, as follows:

$$y_j = h_j(x) \tag{3.7}$$

$$\dot{y}_j = \frac{\partial h_j}{\partial x}\,\dot{x} = \frac{\partial h_j}{\partial x}\,[f(x) + \sum_{i=1}^{m} g_i(x)\, u_i] \tag{3.8}$$

$$= L_f h_j + \sum_{i=1}^{m} (L_{g_i} h_j) u_i \tag{3.9}$$

If $L_{g_i} h_j(x) = 0$ for all i then the inputs have not appeared and one must differentiate further. This process is repeated until at least one input appears.

$$y_j^{(r_j)} = L_f^{r_j} h_j + \sum_{i=1}^{m} L_{g_i} L_f^{r_j - 1} h_j u_i \tag{3.10}$$

where r_j is the smallest integer such that at least one of the inputs appear. Here $L_{g_i} L_f^{r_j - 1} h_j(x) \neq 0$ for at least one i, $\forall x \in \Omega$, and Ω is a region around a point x_0. The integer r_j is known as the relative order of the j-th output with respect to the inputs.

Repeating the procedure for each output gives the following m equations:

$$\begin{bmatrix} y_1^{(r_1)} \\ \vdots \\ y_m^{(r_m)} \end{bmatrix} = \begin{bmatrix} L_f^{r_1} h_1(x) \\ \vdots \\ L_f^{r_m} h_m(x) \end{bmatrix} + E(x) \begin{bmatrix} u_1 \\ \vdots \\ u_m \end{bmatrix} \tag{3.11}$$

Here $E(x)$ is an $m \times m$ matrix :

$$E(x) = \begin{bmatrix} L_{g_1} L_f^{r_1-1} h_1(x) & \dots & L_{g_m} L_f^{r_1-1} h_1(x) \\ \vdots & \ddots & \vdots \\ L_{g_1} L_f^{r_m-1} h_m(x) & \dots & L_{g_m} L_f^{r_m-1} h_m(x) \end{bmatrix} \tag{3.12}$$

At this point the concept of *relative degree*, which is particularly important to the Input-Output Linearization procedure, is defined:

Definition The system (3.6) has a vector of relative degree $\{r_1, \dots, r_m\}$ at a point x_0 if there exists a neighbourhood Ω of x_0 such that $\forall x \in \Omega$:

1. $L_{g_i} L_f^k h_j(x) = 0 \qquad 0 \le k < r_j - 1 \qquad 1 \le i, j \le m$
2. $E(x)$ is non-singular

Point 1 in this definition indicates that no component of the input vector appears before the r_j-th derivative of the j-th output y_j. The non-singularity of matrix $E(x)$ in point 2 implies that each of the $j = 1 \dots m$ row vectors

$$\left[L_{g_1} L_f^{r_j-1} h_j(x) \, , \, L_{g_2} L_f^{r_j-1} h_j(x) \, , \, \dots \, L_{g_m} L_f^{r_j-1} h_j(x) \right]$$

associated with each output y_j, has at least one non-zero element. This means that at least one of the inputs appear in the r_j-th time derivative of y_j. Moreover, the order of appearance of the outputs must be such that the matrix $E(x)$ resulting from the above m row vectors is invertible. The importance of this non-singularity condition will be interpreted later.

The procedure of successive differentiation yields functions that may be used as a new set of state variables. This may be verified by showing that if a system has a (vector) relative degree of $\{r_1 \dots r_m\}$ at x_0, then the gradients of these functions, forming the following row vectors, are linearly independent.

$$\begin{array}{cccc} \frac{\partial h_1}{\partial x} \, , & \frac{\partial L_f h_1}{\partial x} \, , & \dots \, , & \frac{\partial L_f^{r_1-1} h_1}{\partial x} \\ \frac{\partial h_2}{\partial x} \, , & \frac{\partial L_f h_2}{\partial x} \, , & \dots \, , & \frac{\partial L_f^{r_2-1} h_2}{\partial x} \\ & & \vdots & \\ \frac{\partial h_m}{\partial x} \, , & \frac{\partial L_f h_m}{\partial x} \, , & \dots \, , & \frac{\partial L_f^{r_m-1} h_m}{\partial x} \end{array}$$

The proof of this statement is given in Isidori [34] and implies that $r_1 + r_2 + \dots r_m = r$ linearly independent vectors have been found. A consequence of this is that r is

necessarily less than or equal to n, since it is impossible to have more than n linearly independent vectors in an n-dimensional space. So:

$$r_1 + r_2 + \ldots + r_m \leq n \tag{3.13}$$

The r functions, generated by differentiation of the outputs, are now renamed as follows:

$$\begin{aligned} \phi_1^i(x) &= h_i(x) \\ \phi_2^i(x) &= L_f h_i(x) \\ &\vdots \\ \phi_{r_i}^i(x) &= L_f^{r_i-1} h_i(x) \end{aligned} \tag{3.14}$$

for $1 \leq i \leq m$

If $r = n$ then the following mapping:

$$\Phi(x) = col[\phi_1^1(x), \ldots, \phi_{r_1}^1(x), \ldots, \phi_1^m(x), \ldots, \phi_{r_m}^m(x)]$$

has a nonsingular Jacobian matrix at x_0 since the gradients of functions $\phi_j^i(x)$ are linearly independent as shown earlier. This implies that the mapping $\Phi(x)$ qualifies as a local state space coordinates transformation in a neighbourhood of x_0 as pointed out in the earlier lemma. Note that the coordinates transformation is global if the relative degree is defined for all x and the Jacobian matrix is nonsingular for all x.

It is more usual however, that $r < n$. In this case it is always possible to find $(n-r)$ more functions, $\{ \phi_{r+1}(x), \ldots, \phi_n(x) \}$, such that the mapping:

$$\Phi = col[\phi_1^1(x), \ldots, \phi_{r_1}^1(x), \ldots, \phi_1^m(x), \ldots, \phi_{r_m}^m(x), \phi_{r+1}(x), \ldots, \phi_n(x)]$$

has a nonsingular Jacobian matrix and therefore qualifies as a coordinates transformation.

For the general case $r \leq n$ a new state vector can be defined as $\{\zeta^1, \ldots, \zeta^m, \eta\}$, where:

$$\zeta^i = \begin{bmatrix} \zeta_1^i \\ \vdots \\ \zeta_{r_i}^i \end{bmatrix} = \begin{bmatrix} \phi_1^i(x) \\ \vdots \\ \phi_{r_i}^i(x) \end{bmatrix} \qquad \text{For} \quad 1 \leq i \leq m \tag{3.15}$$

$$\eta = \begin{bmatrix} \eta_1 \\ \vdots \\ \eta_{n-r} \end{bmatrix} = \begin{bmatrix} \phi_{r+1}(x) \\ \vdots \\ \phi_n(x) \end{bmatrix} \tag{3.16}$$

The system may now be described in the new coordinates by differentiating the state vector; for $1 \leq i \leq m$

$$\begin{aligned}
\frac{d\zeta_1^i}{dt} &= \frac{\partial \phi_1^i}{\partial x}\frac{dx}{dt} = \frac{\partial h_i}{\partial x}\dot{x} = L_f h_i = \phi_2^i = \zeta_2^i \\
\frac{d\zeta_2^i}{dt} &= \frac{\partial \phi_2^i}{\partial x}\frac{dx}{dt} = \frac{\partial L_f h_i}{\partial x}\dot{x} = L_f^2 h_i = \phi_3^i = \zeta_3^i \\
&\vdots \\
\frac{d\zeta_{r_i-1}^i}{dt} &= \frac{\partial \phi_{r_i-1}^i}{\partial x}\frac{dx}{dt} = \frac{\partial L_f^{r_i-2} h_i}{\partial x}\dot{x} = L_f^{r_i-1} h_i = \phi_{r_i}^i = \zeta_{r_i}^i \\
\frac{d\zeta_{r_i}^i}{dt} &= \frac{\partial \phi_{r_i}^i}{\partial x}\frac{dx}{dt} = \frac{\partial L_f^{r_i-1} h_i}{\partial x}\dot{x} = L_f^{r_i} h_i + \sum_{j=1}^{m}(L_{g_j} L_f^{r_i-1} h_i)\, u_j
\end{aligned} \tag{3.17}$$

The dynamic equations in the new state variables are:

$$\begin{aligned}
\dot{\zeta}_1^i &= \zeta_2^i \\
&\vdots \\
\dot{\zeta}_{r_i-1}^i &= \zeta_{r_i}^i \\
\dot{\zeta}_{r_i}^i &= a_i(\zeta,\eta) + \sum_{j=1}^{m} b_i^j(\zeta,\eta) u_j \\
y_i &= \zeta_1^i
\end{aligned} \tag{3.18}$$

where

$$\left.\begin{aligned}
a_i(\zeta,\eta) &= L_f^{r_i} h_i(\Phi^{-1}(\zeta,\eta)) \\
b_i^j(\zeta,\eta) &= L_{g_j} L_f^{r_i-1} h_i(\Phi^{-1}(\zeta,\eta))
\end{aligned}\right\} \quad \text{for} \quad \begin{aligned} i &= 1,2,\ldots,m \\ j &= 1,2,\ldots,m \end{aligned}$$

The dynamic equations corresponding to the remaining set of new states is given by

$$\dot{\eta} = w(\zeta,\eta) + p(\zeta,\eta)\, u \tag{3.19}$$

where

$$\left.\begin{aligned}
w_k(\zeta,\eta) &= L_f \eta_k(\Phi^{-1}(\zeta,\eta)) \\
p_{k,i}(\zeta,\eta) &= L_{g_i} \eta_k(\Phi^{-1}(\zeta,\eta))
\end{aligned}\right\} \quad \text{for} \quad \begin{aligned} i &= 1,2,\ldots,m \\ k &= 1,2,\ldots,n-r \end{aligned}$$

Recall that by virtue of the fact that system (3.6) has a relative degree, matrix $E(x)$ is nonsingular and the following nonlinear control law is evident from equation (3.11)

$$\begin{bmatrix} u_1 \\ \vdots \\ u_m \end{bmatrix} = -E^{-1}\begin{bmatrix} L_f^{r_1} h_1(x) \\ \vdots \\ L_f^{r_m} h_m(x) \end{bmatrix} + E^{-1}\begin{bmatrix} v_1 \\ \vdots \\ v_m \end{bmatrix} \tag{3.20}$$

where $\{ v_1 \ \ldots \ v_m \}$ is the new input vector to be designed.

In new coordinates the control law becomes:

$$\begin{bmatrix} u_1 \\ \vdots \\ u_m \end{bmatrix} = E^{-1}(\Phi^{-1}(\zeta, \eta)) \begin{bmatrix} v_1 - L_f^{r_1} h_1(\Phi^{-1}(\zeta, \eta)) \\ \vdots \\ v_m - L_f^{r_m} h_m(\Phi^{-1}(\zeta, \eta)) \end{bmatrix} \tag{3.21}$$

Note that by definition of system (3.18)

$$a(\zeta, \eta) = \begin{bmatrix} L_f^{r_1} h_1(\Phi^{-1}(\zeta, \eta)) \\ \vdots \\ L_f^{r_m} h_m(\Phi^{-1}(\zeta, \eta)) \end{bmatrix} \qquad \text{and} \qquad b(\zeta, \eta) = E(\Phi^{-1}(\zeta, \eta))$$

Applying the control law (3.21) to system (3.18) yields:

$$\begin{aligned} \dot{\zeta}_1^i &= \zeta_2^i \\ &\vdots \\ \dot{\zeta}_{r_i-1}^i &= \zeta_{r_i}^i \\ \dot{\zeta}_{r_i}^i &= v_i \qquad\qquad \text{for } i = 1, 2, \ldots, m \\ \\ y_i &= \zeta_1^i \end{aligned} \tag{3.22}$$

$$\dot{\eta} = w(\zeta, \eta) + p(\zeta, \eta)\, E^{-1}(\Phi^{-1}(\zeta, \eta)) \{ v - a(\zeta, \eta) \}$$

At this point one can see that applying the diffeomorphic transformation $\Phi(x)$ and the nonlinear feedback control law, decomposes the nonlinear system into a linear controllable system described by state variables (ζ) in addition to a nonlinear subsystem describing the remaining dynamics through states (η).

Note that the outputs are given only in terms of the linear states, this implies that the nonlinear states are not observable at the output. In other words the decomposition renders the nonlinear subsystem, (*the internal dynamics*), unobservable.

The main attraction of control law (3.21) is that *Noninteracting Control* is achieved. This means that each output channel, $y_i = \zeta_1^i$ is affected only by the corresponding

input channel v_i and not by v_j if $j \neq i$. This is illustrated by Figure 3.1 below, where the output y_i is controlled only by the input v_i through a chain of r_i integrators.

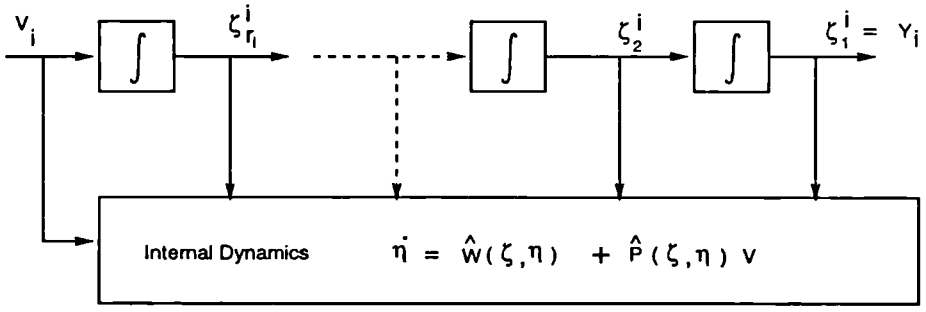

Figure 3.1: Schematic of System in New Coordinates

Control law (3.21) is often called a decoupling control law and the matrix E is known as the decoupling matrix. Since each input-output channel is decoupled, it is possible to use linear single-input single-output design, such as Pole-Placement, on each $y_i - v_i$ channel without it affecting the others. If on the other hand decoupling were not achieved then the design of input v_i would affect not only the y_i output but all other outputs. In this case linear multivariable designs would be required to provide a satisfactory decoupled response. This is may be considered undesirable due to the considerable theoretical analysis and design complexity typically required.

An interesting case occurs when $r = n$, then the entire nonlinear system (3.6) is transformed to a linear equivalent system without any internal dynamics. This is the ideal case since no nonlinear subsystem is present to *complicate* the control system design as indicated later.

Figure 3.2 shows, the Input-Output Linearization process leads to the decomposition of a nonlinear system into a linear part *(external dynamics)* and a reduced order nonlinear part *(internal dynamics)*. Using the external part and known linear techniques one can then design the input v so that the output y achieves a desired response. The problem that still remains is that of the behaviour of the hidden internal dynamics. Since the overall control law should account for the entire system dynamics, careful

attention should be paid to the internal dynamics.

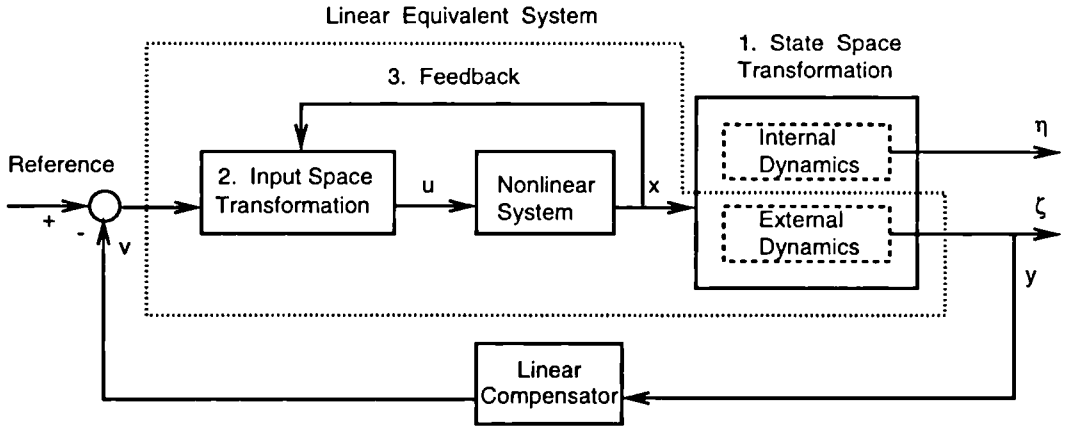

Figure 3.2: Entire Closed Loop System

It is worth noting here that the control law (3.21) may only be used provided that $E(x)$ is invertible. If this is not the case then a *dynamic* control law may be considered to achieve noninteraction. The dynamic compensator takes the following form:

$$u = \alpha(\delta, x) + \beta(\delta, x)\, v \tag{3.23}$$

$$\dot{\delta} = \gamma(\delta, x) + \psi(\delta, x)\, v \tag{3.24}$$

Dynamic extension, which is used to produce the dynamic control law, essentially involves adding integrators to the dynamics. The controller is then no longer static; for a detailed description of the procedure see Isidori [34].

3.3 Zero Dynamics

While the zero dynamics concept is outlined below, Isidori [34] provides more details. Recall that for the system in new coordinates (3.22), the internal dynamics is given by:

$$\begin{aligned} \dot{\eta} &= w(\zeta, \eta) + p(\zeta, \eta)\, E^{-1}(\Phi^{-1}(\zeta, \eta))\, \{ v - a(\zeta, \eta) \} \\ &= \hat{w}(\zeta, \eta) + \hat{p}(\zeta, \eta)\, v \end{aligned} \tag{3.25}$$

To determine the behaviour of the internal dynamics involves solving the nonlinear

equations given by (3.25) subject to the effect of the control v which is designed to ensure that the external dynamics satisfy certain criteria. In general nonlinear differential equations are difficult to solve however the concept of *Zero Dynamics* greatly assists in identifying the behaviour of the nonlinear hidden dynamics. To gain an understanding of the significance of the zero dynamics it is beneficial to start with the linear case and then to infer parallels with the nonlinear case.

Consider the following single-input single-output system:

$$\frac{y}{u} = \frac{b_0 + b_1\, s + \ldots + b_p\, s^p}{a_0 + a_1\, s + a_2\, s^2 + \ldots + a_{n-1}\, s^{n-1} + s^n} \tag{3.26}$$

Note that the only cases of interest are when the output $y = C\,x$ is a function of the state and not the input, to be consistent with the nonlinear systems considered. This necessarily restricts the order of the numerator polynomial, (p), to be less than the order of the denominator polynomial, (n). The difference, $n - p = r$, is known as the relative order or relative degree.

A state space realization of the transfer function is

$$\begin{bmatrix} \dot{x}_1 \\ \dot{x}_2 \\ \vdots \\ \dot{x}_{n-1} \\ \dot{x}_n \end{bmatrix} = \begin{bmatrix} 0 & 1 & 0 & \ldots & 0 \\ 0 & 0 & 1 & \ldots & 0 \\ \vdots & \vdots & \vdots & \ddots & \vdots \\ 0 & 0 & 0 & \ldots & 1 \\ -a_0 & -a_1 & -a_2 & \ldots & -a_{n-1} \end{bmatrix} \begin{bmatrix} x_1 \\ x_2 \\ x_3 \\ \vdots \\ x_n \end{bmatrix} + \begin{bmatrix} 0 \\ 0 \\ \vdots \\ 0 \\ 1 \end{bmatrix} u \tag{3.27}$$

$$y = \begin{bmatrix} b_0 & b_1 & \ldots & b_p & 0 & \ldots & 0 \end{bmatrix} \begin{bmatrix} x_1 \\ x_2 \\ \vdots \\ x_{p+1} \\ x_{p+2} \\ \vdots \\ x_n \end{bmatrix}$$

The Input-Output Linearization procedure is now carried out starting with successive differentiations of the output in order to find the explicit relationship between the input and the output.

$$\begin{aligned} y &= b_0\, x_1 + b_1\, x_2 + \ldots + b_p\, x_{p+1} \\ \dot{y} &= b_0\, x_2 + b_1\, x_3 + \ldots + b_p\, x_{p+2} \\ &\vdots \end{aligned} \tag{3.28}$$

$$\begin{aligned} y^{(n-p-1)} &= b_0 x_{n-p} + b_1 x_{n-p+1} + \ldots + b_p x_n \\ y^{(n-p)} &= b_0 x_{n-p+1} + b_1 x_{n-p+2} + \ldots + \\ & \quad b_p (-a_0 x_1 - a_1 x_2 - a_2 x_3 - \ldots - a_{n-1} x_n) + b_p u \end{aligned}$$

The output appears after $(n-p)$ differentiations of the output, i.e. after r (the relative degree) number of differentiations.

Part of the state space mapping can now be constructed from the following functions

$$\begin{aligned} \phi_1 = \zeta_1 &= b_0 x_1 + b_1 x_2 + \ldots + b_p x_{p+1} = y \\ \phi_2 = \zeta_2 &= b_0 x_2 + b_1 x_3 + \ldots + b_p x_{p+2} = \dot{y} \\ &\vdots \\ \phi_r = \zeta_r &= b_0 x_r + b_1 x_{r+1} + \ldots + b_p x_n = y^{(r-1)} \end{aligned} \tag{3.29}$$

The remaining non-unique functions

$$\begin{aligned} \phi_{r+1} &= \eta_1 = x_{r+1} \\ \phi_{r+2} &= \eta_2 = x_{r+2} \\ &\vdots \\ \phi_n &= \eta_p = x_n \end{aligned} \tag{3.30}$$

are chosen to ensure that the following Jacobian matrix

$$\frac{\partial \Phi(x)}{\partial x} = \begin{bmatrix} b_0 & b_1 & b_2 & \cdots & \cdots & \cdots & \cdots & b_p & 0 & \cdots & 0 \\ 0 & b_0 & b_1 & b_2 & \cdots & \cdots & \cdots & \cdots & b_p & \cdots & 0 \\ \vdots & \vdots & \ddots & \ddots & \ddots & \cdots & \cdots & \cdots & \cdots & \ddots & \vdots \\ 0 & 0 & \cdots & b_0 & b_1 & b_2 & \cdots & \cdots & \cdots & \cdots & b_p \\ 0 & 0 & \cdots & 0 & 1 & 0 & \cdots & \cdots & \cdots & \cdots & 0 \\ 0 & 0 & \cdots & 0 & 0 & 1 & \cdots & \cdots & \cdots & \cdots & 0 \\ \vdots & \vdots & \cdots & \vdots & \vdots & \vdots & \ddots & \cdots & \cdots & \cdots & \vdots \\ \vdots & \vdots & \cdots & \vdots & \vdots & \vdots & \cdots & \ddots & \cdots & \cdots & \vdots \\ \vdots & \vdots & \cdots & \vdots & \vdots & \vdots & \cdots & \cdots & \ddots & \cdots & \vdots \\ \vdots & \vdots & \cdots & \vdots & \vdots & \vdots & \cdots & \cdots & \cdots & \ddots & \vdots \\ 0 & 0 & \cdots & 0 & 0 & 0 & \cdots & \cdots & \cdots & \cdots & 1 \end{bmatrix} \tag{3.31}$$

is nonsingular, thus enabling Φ to be used as a coordinates transformation.

The system described partially in new coordinates is

$$\dot{\zeta}_1 = \zeta_2$$

$$\begin{aligned}
\dot{\zeta}_2 &= \zeta_3 \\
&\vdots \\
\dot{\zeta}_r &= b_0 x_{r+1} + b_1 x_{r+2} + \ldots + b_{p-1} x_n + \\
&\quad b_p (-a_0 x_1 - a_1 x_2 - \ldots - a_{n-1} x_n) + b_p u \\
\dot{\eta}_1 &= x_{r+2} \\
\dot{\eta}_2 &= x_{r+3} \\
&\vdots \\
\dot{\eta}_p &= (-a_0 x_1 - a_1 x_2 - \ldots - a_{n-1} x_n) + u
\end{aligned} \tag{3.32}$$

Letting the control law be:

$$u = \frac{v - b_0 x_{r+1} - b_1 x_{r+2} - \ldots - b_p (-a_0 x_1 - a_1 x_2 - \ldots - a_{n-1} x_n)}{b_p} \tag{3.33}$$

and applying it to system (3.32) yields:

$$\begin{aligned}
\dot{\zeta}_1 &= \zeta_2 \\
\dot{\zeta}_2 &= \zeta_3 \\
&\vdots \\
\dot{\zeta}_r &= v
\end{aligned} \tag{3.34}$$

$$\begin{aligned}
\dot{\eta}_1 &= \eta_2 \\
\dot{\eta}_2 &= \eta_3 \\
&\vdots \\
\dot{\eta}_p &= -\frac{b_0}{b_p} \eta_1 - \frac{b_1}{b_p} \eta_2 - \ldots - \frac{b_{p-1}}{b_p} \eta_p + \frac{v}{b_p}
\end{aligned} \tag{3.35}$$

If v is now designed to provide tracking of $\zeta_1 = y$, or for stabilization of the external dynamics, then v takes the following form

$$v = -k_1 \zeta_1 - k_2 \zeta_2 - \ldots - k_r \zeta_r + v \tag{3.36}$$

such that the eigenvalues of the matrix below, given in terms of k_i, have negative real

part.

$$\begin{bmatrix} \dot{\zeta}_1 \\ \dot{\zeta}_2 \\ \vdots \\ \dot{\zeta}_{r-1} \\ \dot{\zeta}_r \end{bmatrix} = \begin{bmatrix} 0 & 1 & 0 & \dots & 0 \\ 0 & 0 & 1 & \dots & 0 \\ \vdots & \vdots & \vdots & \ddots & \vdots \\ 0 & 0 & 0 & \dots & 1 \\ -k_1 & -k_2 & -k_3 & \dots & -k_r \end{bmatrix} \begin{bmatrix} \zeta_1 \\ \zeta_2 \\ \zeta_3 \\ \vdots \\ \zeta_r \end{bmatrix} + \begin{bmatrix} 0 \\ 0 \\ \vdots \\ 0 \\ 1 \end{bmatrix} v \quad (3.37)$$

Therefore the external dynamics achieves the desired control tasks, but the the behaviour of the hidden dynamics is still to be determined. Note that for stabilization or tracking tasks on the external dynamics, $\zeta_1, \dots \zeta_r$ and $\bar{v}$ are bounded. Therefore applying the control law (3.36) to the internal dynamics (3.35) gives:

$$\begin{aligned} \dot{\eta}_1 &= \eta_2 \\ \dot{\eta}_2 &= \eta_3 \\ &\vdots \\ \dot{\eta}_p &= -\frac{b_0}{b_p}\eta_1 - \frac{b_1}{b_p}\eta_2 - \dots - \frac{b_{p-1}}{b_p}\eta_p + \{\text{Bounded Function}\} \end{aligned} \quad (3.38)$$

Clearly this implies that the stability of the internal dynamics is determined only by the coefficients, $b_0, \dots b_p$, of the *zeros* polynomial. Bearing this in mind it is possible to define the *zero dynamics* of a linear system as linear dynamics with eigenvalues coinciding with the zeros of the transfer function matrix. It therefore follows that for linear systems, if the zero dynamics are stable then the internal dynamics are also stable.

It is now shown that the zero dynamics can be obtained directly by applying a feedback control that ensures that the output remains identically zero for all time. This implies that in the system given by (3.34) and (3.35), the output and all its derivatives are zero.

$$\begin{aligned} y &= \zeta_1 = 0 \\ \dot{y} &= \dot{\zeta}_1 = \zeta_2 = 0 \\ &\vdots \quad\quad \vdots \quad\quad \vdots \\ y^{(r-1)} &= \dot{\zeta}_{r-1} = \zeta_r = 0 \\ y^{(r)} &= \dot{\zeta}_r = v = 0 \end{aligned} \quad (3.39)$$

Subject to the above constraints (3.35) becomes the zero dynamics and is given by:

$$\dot{\eta}_1 = \eta_2$$

$$\begin{aligned} \dot{\eta}_2 &= \eta_3 \\ &\vdots \\ \dot{\eta}_p &= -\frac{b_0}{b_p}\eta_1 - \frac{b_1}{b_p}\eta_2 - \ldots - \frac{b_{p-1}}{b_p}\eta_p \end{aligned} \tag{3.40}$$

To translate these ideas into the nonlinear system framework consider the following nonlinear system:

$$\begin{aligned} \dot{x} &= f(x) + G(x)\,u \\ y &= h(x) \end{aligned} \tag{3.41}$$

where the equilibrium point is defined as (x_0, u_0) such that $y = h(x_0) = 0$.

Recall that part of the linear subsystem in new coordinates is:

$$\dot{\zeta}^i_{r_i} = v_i \tag{3.42}$$

From successive differentiation of the output the following relationship holds:

$$y_i^{(r_i)} = \dot{\zeta}^i_{r_i} \tag{3.43}$$

As in the linear case, the dynamics such that the output remains identically zero is the zero dynamics. This implies the following conditions:

$$\begin{aligned} y_i &= \zeta^i_1 = 0 \\ y_i^{(1)} &= \zeta^i_2 = 0 \\ &\vdots \quad\quad \vdots \\ y_i^{(r_i)} &= v_i = 0 \end{aligned} \tag{3.44}$$

The zero dynamics representation in new coordinates

$$\begin{aligned} \dot{\zeta} &= 0 \\ \dot{\eta} &= w(0, \eta) - p(0, \eta)\,E^{-1}(0, \eta)\,a(0, \eta) \end{aligned} \tag{3.45}$$

Alternatively in the original coordinates the nonlinear control law arising from the Input-Output Linearization procedure is

$$u = E^{-1}(x)\,[v - L_f^r h(x)] \tag{3.46}$$

Applying this control law to the nonlinear system and observing the output zeroing constraints (3.44), gives the zero dynamics as:

$$\dot{x} = f(x) + G(x)\, E^{-1}(x)\, [-L_f^r h(x)] \tag{3.47}$$

The equilibrium point $(x_0,\, u_0)$ defined earlier is a point such that $y = 0$, this implies that this point necessarily lies in the output zeroing submanifold over which the zero dynamics evolve. Or in the new coordinates the equilibrium point is $(\zeta_0,\, \eta_0,\, v_0)$, where by definition $\zeta_0 = 0$ and $\zeta_0^{(r)} = 0 = v$ which implies that the equilibrium point is given more simply as $(0,\, \eta_0,\, 0)$.

In linear systems the stability of the zero dynamics guarantees the global stability of the internal dynamics. In nonlinear systems, however, stability of the zero dynamics guarantees only local stability of the internal dynamics in a region around the equilibrium point in question. The proof of this is available in texts such as Isidori [34], however a brief inspection of the rationale follows next.

For the system in new coordinates, applying a feedback that ensures stability of the external dynamics gives the following system:

$$\begin{aligned} \dot{\zeta}_r^i &= -k_{i1}\, \zeta_1^i - \ \ldots\ - k_{i r_i}\, \zeta_{r_i}^i + \bar{v}_i \\ \dot{\eta} &= \hat{w}(\zeta, \eta) + \hat{p}(\zeta, \eta)\, (-k_1\, \zeta_1 - \ \ldots\ - k_r\, \zeta_r + v) \end{aligned} \tag{3.48}$$

If the zero dynamics are asymptotically stable then for sufficiently small $\bar{v}$ the trajectories of (3.48) are bounded. More precisely, using results from Centre Manifold Theory, for each ϵ there exists δ and K such that

$$||\, \zeta_0,\, \eta_0|| < \delta \qquad \text{and} \qquad |v_i| < K \qquad\qquad \forall\, t \geq 0\,,\ 1 \leq i \leq m \tag{3.49}$$

imply

$$||\, \zeta_t,\, \eta_t|| < \epsilon \qquad\qquad \forall\, t \geq 0 \tag{3.50}$$

i.e. the internal dynamics remain bounded.

An important point to note is that the nonlinear control law given in this chapter achieves noninteraction with stability provided the zero dynamics are stable. This condition is only a sufficient one and there may still exist systems whose zero dynamics

are not asymptotically stable in which the achievement of noninteractive control by means of an internally stable closed loop is still possible. More details of this are given in the literature review of Chapter 1.

3.4 Asymptotic Output Tracking

Isidori [34] shows the design of a tracking controller for the Input-Output Linearized system is essentially the design of a control law that will asymptotically stabilize an error system defined in terms of the actual system outputs and its desired trajectories. As proved in Isidori, if the zero dynamics are asymptotically stable this type of control law will ensure that the entire system remains stable and the tracking objectives met.

The outputs of the system are the variables required to track a prescribed trajectory y_d. Recall that the state vector of the linear subsystem is:

$$\begin{bmatrix} \zeta_1^i \\ \vdots \\ \zeta_{r_i}^i \end{bmatrix} = \begin{bmatrix} y_i(x) \\ \vdots \\ y_i^{(r_i-1)}(x) \end{bmatrix} \qquad \text{For} \quad 1 \le i \le m \tag{3.51}$$

Define the error corresponding to each output as:

$$e_1^i = y_i(x) - y_{i_d} = \zeta_1^i - y_{i_d} \qquad i = 1 \ldots m \tag{3.52}$$

Differentiating e^i repeatedly r_i times

$$\begin{array}{ccccccc} \dot{e}_1^i & = & \dot{\zeta}_1^i - \dot{y}_{i_d} & = & \zeta_2^i - \dot{y}_{i_d} & = & e_2^i \\ \dot{e}_2^i & = & \dot{\zeta}_2^i - y_{i_d}^{(2)} & = & \zeta_3^i - y_{i_d}^{(2)} & = & e_3^i \\ & \vdots & & \vdots & & \vdots & \\ \dot{e}_{r_i-1}^i & = & \dot{\zeta}_{r_i-1}^i - y_{i_d}^{(r_i-1)} & = & \zeta_{r_i}^i - y_{i_d}^{(r_i-1)} & = & e_{r_i}^i \\ \dot{e}_{r_i}^i & = & \dot{\zeta}_{r_i}^i - y_{i_d}^{(r_i)} & & & & \end{array} \tag{3.53}$$

From system (3.22), $\dot{\zeta}_{r_i}^i = v_i$, therefore the dynamic equations of the error system are:

$$\begin{array}{rcl} \dot{e}_1^i & = & e_2^i \\ & \vdots & \\ \dot{e}_{r_i-1}^i & = & e_{r_i}^i \\ \dot{e}_{r_i}^i & = & v_i - y_{i_d}^{(r_i)} \end{array} \tag{3.54}$$

Isidori [34] points out that a control law of the following form achieves asymptotic output tracking:

$$\begin{bmatrix} v_1 \\ v_2 \\ \vdots \\ v_m \end{bmatrix} = \begin{bmatrix} k_{11} \ldots k_{1r_1} & 0 & \ldots & 0 \\ 0 & k_{21} \ldots k_{2r_2} & \ldots & 0 \\ & & \ddots & \\ 0 & 0 & \ldots & k_{m1} \ldots k_{mr_m} \end{bmatrix} \begin{bmatrix} e_1^1 \\ \vdots \\ e_{r_1}^1 \\ e_1^2 \\ \vdots \\ e_{r_2}^2 \\ \vdots \\ e_1^m \\ \vdots \\ e_{r_m}^m \end{bmatrix} + \begin{bmatrix} y_{1_d}^{(r_1)} \\ y_{2_d}^{(r_2)} \\ \vdots \\ y_{m_d}^{(r_m)} \end{bmatrix} \tag{3.55}$$

Replacing v in control law (3.54) with (3.55) results in:

$$\begin{bmatrix} \dot{e}_1^i \\ \dot{e}_2^i \\ \vdots \\ \dot{e}_{r_i-1}^i \\ \dot{e}_{r_i}^i \end{bmatrix} = \begin{bmatrix} 0 & 1 & 0 & \ldots & 0 \\ 0 & 0 & 1 & \ldots & 0 \\ \vdots & \vdots & \vdots & \ddots & \vdots \\ 0 & 0 & 0 & \ldots & 1 \\ k_{i1} & k_{i2} & k_{i3} & \ldots & k_{ir_i} \end{bmatrix} \begin{bmatrix} e_1^i \\ e_2^i \\ e_3^i \\ \vdots \\ e_{r_i}^i \end{bmatrix} \tag{3.56}$$

The error dynamics of each of the m linear sub-systems will be stabilized if the coefficients k_{ij} are chosen so that the eigenvalues of the above error system matrix lie in the *Left Half Plane*. Because of the local nature of the zero dynamics stability, the control law given above guarantees the stability of the internal dynamics if the desired trajectories $y_d \ldots y_d^{(r-1)}$ have small magnitudes.

3.5 Summary

A solution to the nonlinear decoupling problem has been found using the theory of Input-Output Linearization. The steps below show the approach to the problem

- Determine the relative degree r of the n-th order system for the outputs given. This is done by differentiating the outputs until the inputs appear.
- This procedure gives rise to the decoupling matrix $E(x)$ and r functions that can be used as part of a state space coordinates transformation. It is then possible to find $n - r$ functions to complete the coordinates change.
- The state space transformation along with a nonlinear feedback control law involving the inverse of the decoupling matrix can then be applied to the system. This decomposes the original system into a linear decoupled subsystem of order r and a nonlinear subsystem of order $n - r$.
- The stability characteristics of the zero dynamics should then be determined.
- Finally a tracking control law for the decoupled outputs may be designed.

This system decomposition is used as the basis for the robustness analysis given in Chapter 4.

Chapter 4

Nonlinear Robust Control

This chapter is concerned with finding nonlinear tracking control laws that are robust to uncertainties. The control laws are derived within the Feedback Linearization framework. As mentioned in Chapter 1, three main approaches prevail for the treatment of uncertain systems; they are adaptive control, Sliding mode control and Lyapunov based control. Since adaptive schemes normally require costly on-line identification algorithms to monitor parameter values and disturbances, the latter two deterministic approaches were chosen in this work in order to limit the complexity of the controllers.

Methods employed to deal with uncertainties often require discontinuous control laws to ensure that the system is robust to uncertainties and that the control objective is met. The problem with discontinuous control is that implementation is impractical since control activity is usually unacceptably high. Both the Sliding mode and the Lyapunov techniques resort to saturation functions in order to eliminate the control discontinuity, this however affects the desired performance. In the case of tracking control, the guaranteed asymptotic tracking that discontinuous control provides is not achievable using the continuous control; in fact the best that can be attained is *uniform ultimate boundedness*. This essentially means that the steady state tracking error will be non-zero. The dynamic error will however be bounded and dependent on the positive constant ϵ, to be defined later, which is part of the saturation control law.

A more precise statement of the objective of this chapter can be stated as follows: given a desired trajectory y_d, design control laws incorporating the linearizing control of Chapter 3, so that the output error of the closed loop system will be bounded while maintaining the boundedness of all signals inside the loop regardless of the presence of uncertainties.

The first step in any analysis of uncertain systems is that of characterizing the uncertainties. This is done in Section 4.1 and is followed in Section 4.2 by the Lyapunov approach to the design of robust control laws. The Lyapunov approach utilizes Gutman's theory [24] for the nonlinear aspects of the system. Leitmann's approach [43] for linear systems is then used for the linear subsystem derived during Input-Output Linearization. The actual Feedback Linearization aspects are dealt with using ideas from Chen and Chen [10]. Finally the internal dynamics arising from Input-Output Linearization are discussed in terms of the contribution by Liao et al [45] to uncertain systems. Section 4.3 then concludes this chapter with a presentation of Sliding Mode Control. The design of the Sliding mode control within the Feedback Linearization environment makes use of the work of Fu and Liao [20].

4.1 System Uncertainty

Consider a nonlinear system:

$$\begin{aligned} \dot{x} &= f(x) + \Delta f(x) + \sum_{i=1}^{m} [\, g_i(x) + \Delta g_i(x) \,] \, u_i \\ &= f(x) + \Delta f(x) + [\, G(x) + \Delta G(x) \,] \, u \\ y_i &= h_i(x) \qquad i = 1 \ldots m \end{aligned} \tag{4.1}$$

with inputs u_i, outputs y_i and state x. Note also that $G(x) = [g_1(x) \ldots g_m(x)]$ and $\Delta G(x) = [\Delta g_1(x) \ldots \Delta g_m(x)]$

The *nominal* system refers to the case where the uncertainties, $\Delta f(x)$ and $\Delta G(x)$, are zero.

$$\Delta f(x) = \Delta G(x) = 0 \tag{4.2}$$

The uncertainty can always be divided into two parts, a *matched* part and a *mismatched* part as follows:

$$\begin{aligned} \Delta f(x) &= G(x)\, S(x) + f_{mm}(x) \\ \Delta G(x) &= \underbrace{G(x)\, T(x)}_{\text{matched}} + \underbrace{G_{mm}(x)}_{\text{mismatched}} \end{aligned} \tag{4.3}$$

i.e. the image space of the matched part lies within the span of the nominal g_i.

In the context of Feedback Linearization, the matched uncertainties are the uncertain terms that appear at the same order of differentiation as the inputs during the Input-Output Linearization procedure. This implies that the relative degree remains unchanged so that the matched uncertainties do not affect relative orders, tangent manifolds, coordinate transformations, etc. Arbitrarily large uncertainties of this kind can be compensated for by well designed robust control laws.

The design of robust control laws tends to be based entirely on the matched uncertainty. The mismatched uncertainty is usually tolerated provided its bound is less than a certain *critical threshold.* Uncertainties exceeding this threshold are likely to cause noticeable degradation in controller performance. The literature review in Chapter 1 gives more details of the work by Barmish and Leitmann [3] in this area. The uncertainties considered in this thesis are of the matched kind and Chapter 5 provides the justification of this for the helicopter problem. In view of this, the analysis that follows will omit any unmatched uncertainties, i.e. $f_{mm}(x)$ and $G_{mm}(x)$ will both be set equal to zero.

4.2 Lyapunov-Based Robust Control

The Lyapunov-based control adopted in this thesis utilizes the Lyapunov Min-Max approach presented by Gutman [24]. The robust control law designed by this method depends explicitly on finding a suitable Lyapunov function, which for nonlinear systems is generally quite difficult. However, as shown later, by starting with the Input-Output Linearization approach a Lyapunov function can be found readily. Before presenting the analysis for Input-Output Linearized systems it is essential to discuss Gutman's ideas and some of the later developments that are relevant to the design of robust control laws exploiting the Feedback Linearization concept.

First a few important definitions are stated using the following time varying system:

$$\dot{x} = f(x, t) \tag{4.4}$$

where a solution to (4.4) is given by $x(\cdot) : [t_0, \infty) \rightarrow \Re^n$ for every $x(t_0) = x_0$.

The equilibrium $x = 0$ of (4.4) is *Uniformly Stable* if for all $\epsilon > 0$ there exists a

$\delta(\epsilon) > 0$ such that:

$$\| x_0 \| < \delta(\epsilon) \quad \Rightarrow \quad \| x(t) \| < \epsilon \qquad \text{for all} \quad t \geq t_0 \geq 0 \tag{4.5}$$

The equilibrium $x = 0$ of (4.4) is *Uniformly Asymptotically Stable* if it is uniformly stable and, in addition, there exists a $T(r) > 0$, for all $r > 0$, and a $\gamma(r) > 0$ such that:

$$\| x_0 \| \leq \gamma(r) \quad \Rightarrow \quad \| x(t) \| \leq r \qquad \text{for all} \quad t \geq t_0 + T(r),\ t_0 \geq 0 \tag{4.6}$$

The solution $x(t)$ of (4.4) is *Uniformly Ultimately Bounded* with respect to a set $S \subset \Re^n$ if there exists a non-negative constant $T(x_0, S) < \infty$ such that:

$$x(t) \in S \qquad \text{for all} \quad t \geq t_0 + T(x_0, S) \tag{4.7}$$

4.2.1 Lyapunov Min-Max Approach

Gutman [24] considered the following type of uncertain system:

$$\begin{aligned} \dot{x} &= f(x,t) + B(x,t)\,u + \Delta f(x,t) + \Delta B(x,t)\,u \\ x(t_0) &= x_0, \qquad\qquad u \in U \end{aligned} \tag{4.8}$$

where

x is the state vector

u is a control vector

$x,\ f,\ \Delta f \in \Re^n$ and $B,\ \Delta B \in \Re^{n \times m}$

$f,\ \Delta f,\ B,\ \Delta B$ are continuous in all their arguments

It is also assumed that for all $(x,t) \in \Re^n \times \Re^1_+$, there exists a continuous vector function $h(x,t) \in \Re^m$ and a continuous matrix function $E(x,t) \in \Re^{m \times m}$ such that:

$$\Delta f(x,t) = B(x,t)\,h(x,t) \tag{4.9}$$

$$\Delta B(x,t) = B(x,t)\,E(x,t) \tag{4.10}$$

Using the above matching conditions, (4.9, 4.10), it is possible to rewrite system (4.8) as:

$$\dot{x} = f(x,t) + B(x,t)\,(u + \eta) \tag{4.11}$$

where $\eta = h(x,t) + E(x,t)\,u$

Define:

$$M = \{ \eta \in \Re^m : \|\eta\| \leq \rho(x,t) \} \tag{4.12}$$

which represents a set of norm-bounded uncertain signals.

The problem can now be stated as follows: given system (4.11) where $x(t)$ is a solution of (4.11) at t generated by $u(t)$, find a control strategy $p(\cdot) : \Re^n \times \Re^1_+ \rightarrow \Re^m$ satisfying $u(t) = p(x(t), t)$ such that the origin $\{0\}$ is uniformly asymptotically stable in the large for all $e(\cdot) : \Re^n \times \Re^1_+ \rightarrow \Re^m$ satisfying $\eta(t) = e(x(t), t) \in M$.

Note that (4.12) effectively specifies the maximum possible bound on the uncertainties. This does not preclude cases where uncertainties exceed this bound, it does mean however, that under those circumstances the control law's performance will not be guaranteed.

To find the control strategy that ensures uniform asymptotic stability, it is necessary to assume that there exists a scalar function $V : \Re^n \times \Re^1_+ \rightarrow \Re^1$ satisfying:

- $V(x,t)$ is positive definite, i.e. $V(0,t) = 0$ for all $t \geq 0$ and there exist continuous, increasing scalar functions $\gamma(\cdot)$ and $\beta(\cdot)$ with $\gamma(0) = 0$ and $\beta(0) = 0$, such that $\forall\, t \in \Re^1_+$ and $\forall\, x \in \Re^n$: $\gamma(\|x\|) \leq V(x,t) \leq \beta(\|x\|)$.
- $\gamma(\|x\|) \rightarrow \infty$ as $\|x\| \rightarrow \infty$.
- $-W_0(x,t)$ is positive definite where $W_0(x,t) = (\frac{\partial V}{\partial t} + \nabla_x V \cdot f)$.

This assumption implies that the free system $\dot{x} = f(x,t)$ is uniformly asymptotically stable in the large. If it does not have this property but (4.11) is stabilizable, then this is first stabilized.

The next step is to choose V as a Lyapunov function to system (4.11), then differentiating V along a solution $x(\cdot)$ of (4.11) generated by $\{u, \eta\}$ gives:

$$\frac{\partial V}{\partial t} + \nabla_x V \cdot \dot{x} = \frac{\partial V}{\partial t} + \nabla_x V \cdot f + \nabla_x V \cdot B(u + \eta) \tag{4.13}$$

$$= W_0(x(t), t) + \nabla_x V \cdot B(u + \eta) \tag{4.14}$$

If

$$\min_{u \in U} \max_{\eta \in M} [\nabla_x V \cdot B(u + \eta)] \leq 0 \qquad \forall\, (x,t) \in \Re^{n+1} \tag{4.15}$$

then $V(\cdot)$ decreases along a solution $x(\cdot)$ of (4.11) and is therefore a Lyapunov function for the system which is stable. Condition (4.15) is satisfied by choosing:

$$u(t) = p(x(t), t) \tag{4.16}$$

$$\text{where} \quad p(x,t) = -\rho(x,t)\frac{\alpha(x,t)}{\|\alpha(x,t)\|} \tag{4.17}$$

$$\text{and} \quad \alpha(x,t) \triangleq B^T(x,t)\nabla_x^T V(x,t) \tag{4.18}$$

Since $p(\cdot)$ is undefined for $\alpha(x,t) = 0$ then $p^*(\cdot)$ is introduced as:

$$p^*(x,t) = \begin{cases} -\rho(x,t)\frac{\alpha(x,t)}{\|\alpha(x,t)\|} & \text{if} \quad \|\alpha(x,t)\| \neq 0 \\ \{u \in \Re^m : \|u\| \leq \rho(x,t)\} & \text{if} \quad \|\alpha(x,t)\| = 0 \end{cases} \tag{4.19}$$

This control law ensures that the system remains asymptotically stable for all admissible uncertainties, the proof of this is readily available in Gutman [24]. This control law is in fact discontinuous and direct implementation would lead to *chattering* of the control when the state reaches the discontinuous region, i.e. the control would oscillate at very high frequency between its limits. Under such conditions control actuators fail prematurely due to fatigue. Leitmann [43] showed that a continuous approximation to the discontinuous control derived above no longer guarantees uniform asymptotic stability but assures a performance that is arbitrarily close to it, i.e. uniform ultimate boundedness. That study also demonstrated the application of the Min-Max approach, i.e. the approach outlined above, to linear systems.

Due to the presence of a linear subsystem arising from the application of the Input-Output Linearization technique, it is necessary to consider Leitmann's specialization of the Min-Max approach to linear systems. This will become clear in Section 4.2.2 when the analysis is applied to Input-Output Linearized systems. First a brief description of Leitmann's contribution is given.

Leitmann [43] considered a linear system of the form given below. Note however that error in the measurement of the state and uncertainty in the input, which are present in the original system, are omitted here since they are not necessary to the analysis considered later:

$$\dot{x}(t) = [A + \Delta A(r(t))]x(t) + [B + \Delta B(s(t))]u(t) \tag{4.20}$$

$$x(t_0) = x_0 \qquad (\text{not known})$$

where

A	$n \times n$ matrix	$x \in \Re^n$	$\Delta A(r)$	$n \times n$ matrix	$r \in \Re^p$
B	$n \times m$ matrix	$u \in \Re^m$	$\Delta B(s)$	$n \times m$ matrix	$s \in \Re^q$

The following assumptions are made:

- $\Delta A(\cdot)$ and $\Delta B(\cdot)$ are prescribed functions which are continuous on $\Re^p$ and $\Re^q$ respectively.
- Uncertainty parameters $r(\cdot) : \Re^1 \rightarrow R$ and $s(\cdot) : \Re^1 \rightarrow S$ are Lebesgue measurable where $R \subset \Re^p$ and $S \subset \Re^q$.
- (A, B) is controllable.
- The matching assumptions are met:

$$\begin{array}{rcll} \Delta A(r) & = & B\,D(r) & \forall r \in R \\ \Delta B(s) & = & B\,E(s) & \forall s \in S \end{array} \tag{4.21}$$

Using the above matching conditions system (4.20) can be rewritten as:

$$\dot{x}(t) = A\,x(t) + B\,(u(t) + \eta) \tag{4.22}$$

where $\eta = D(r) + E(s)\,u(t)$

This system suggests a state feedback control given by:

$$u = K\,x + P_{rob} \qquad \forall x \in \Re^n \tag{4.23}$$

where K is a matrix such that $\bar{A} \triangleq A + B\,K$ is stable. Clearly the control law contains an element responsible for stabilizing the nominal system, $\dot{x} = A\,x + B\,u$, in the case that it is not already stable. After stabilization of the nominal system it is possible to determine a matrix P, which will be of use later, the solution to the following Lyapunov equation:

$$P\,\bar{A} + A^T\,P + Q = 0 \tag{4.24}$$

for any constant positive definite matrix Q.

Now the saturation control, $P_{rob}(\cdot) : \Re^n \rightarrow \Re^m$, that compensates for the uncertainty is given by:

$$P_{rob}(x) = \begin{cases} -\frac{\mu}{\|\mu\|}\,\rho_v(x) & \text{if} \quad \|\mu\| > \epsilon \\ -\frac{\mu}{\epsilon}\,\rho_v(x) & \text{if} \quad \|\mu\| \leq \epsilon \end{cases} \tag{4.25}$$

where

$\mu = B^T P x$

ϵ is a prescribed positive constant

and $\rho_v(\cdot) : \Re^n \rightarrow \Re^1_+$ is determined in the following way. Rewriting (4.22) with control u of (4.23) as:

$$\dot{x}(t) = \bar{A}\, x(t) + B\, P_{rob}(x) + B\, \delta(x,t) \tag{4.26}$$

where, for all $(x,t) \in \Re^n \times \Re^1$

$$\delta(x,t) \triangleq D(r)\, x + E(s)\, K\, x + E(s)\, P_{rob}(x) \tag{4.27}$$

ρ_v is defined by applying matrix norms to (4.27) in order to bound the maximum uncertainty:

$$\|\delta(x,t)\| \leq \max_{r \in R} \|D(r)\, x\| + \max_{s \in S} \|E(s)\, K\, x\| + \max_{s \in S} \|E(s)\|\, \rho_v(x) \triangleq \rho_v(x)$$

This equation can be solved for $\rho_v(x)$ if $[1 - \max_{s \in S} \|E(s)\|] > 0$. Then:

$$\rho_v(x) \triangleq [1 - \max_{s \in S} \|E(s)\|]^{-1} \{ \triangleq \|D(r)\, x\| + \max_{s \in S} \|E(s)\, K\, x\| \} \tag{4.28}$$

The proof of the stabilizing nature of the control law appears in Leitmann's paper.

Corless and Leitmann [14] generalized this to the design a control law for the non-linear system below:

$$\dot{x}(t) = f(x(t),t) + B(x(t),t)u(t) + B(x(t),t)e(x(t),t) \tag{4.29}$$

$$x(t_o) = x_o \tag{4.30}$$

where $t \in \Re$ is time, $x(t) \in \Re^n$ is the state and $u(t) \in \Re^m$ is the control. A matched uncertain element is given by $e(x(t),t)$ and its norm is bounded by a known function, that is for all $(x,t) \in \Re^n \times \Re$, $\|e(x,t)\| \leq \rho(x,t)$.

The control which guarantees ultimate boundedness of all possible system responses within an arbitrarily small neighbourhood of the zero state is given by:

$$P_{rob}(x,t) = \begin{cases} -\frac{\mu(x,t)}{\|\mu(x,t)\|}\, \rho(x,t) & \text{if } \|\mu(x,t)\| > \epsilon \\ -\frac{\mu(x,t)}{\epsilon}\, \rho(x,t) & \text{if } \|\mu(x,t)\| \leq \epsilon \end{cases} \tag{4.31}$$

where $\mu(x,t) \triangleq B^T(x,t)\nabla_x^T V(x,t)\rho(x,t)$

This was later developed by Chen [11] for the following system:

$$\dot{x}(t) = f(x(t),t) + \Delta f(x(t),\sigma(t),t) + \{B(x(t),t) + \Delta B(x(t),\sigma(t),t)\}u(t) \quad (4.32)$$

where $t \in \Re$ is time, $x(t) \in \Re^n$ is the state and $u(t) \in \Re^m$ is the control. The time-varying parameter $\sigma(t) \in \Re^p$ represents the uncertainty. The uncertainty parameter $\sigma(\cdot) : \Re^1 \to \Sigma$ is Lebesgue measurable where $\Sigma \subset \Re^p$. The uncertain elements are matched and are given by:

$$\Delta B(x,\sigma,t) = B(x,t)E(x,\sigma,t) \quad (4.33)$$

$$\Delta f(x,\sigma,t) = B(x,t)D(x,\sigma,t) \quad (4.34)$$

In addition it is assumed that $\max_{\sigma \in \Sigma} \|E(x,\sigma,t)\| \triangleq \lambda(x,t) < 1$

It was proved that the following control law guaranteed uniform ultimate boundedness of all system responses:

$$P_{rob}(x,t) = \begin{cases} -\frac{\mu(x,t)}{\|\mu(x,t)\|}\rho_v(x,t) & \text{if } \|\mu(x,t)\| > \epsilon \\ -\frac{\mu(x,t)}{\epsilon}\rho_v(x,t) & \text{if } \|\mu(x,t)\| \leq \epsilon \end{cases} \quad (4.35)$$

where

$$\mu(x,t) \triangleq B^T(x,t)\nabla_x^T V(x,t)\rho_v(x,t) \quad (4.36)$$

$$\rho_v(x,t) \triangleq [1-\lambda(x,t)]^{-1}\,[\max_{\sigma \in \Sigma} \|D(x,\sigma,t)\|] \quad (4.37)$$

To summarize, using the Lyapunov Min-Max approach of Gutman, robust saturation type control laws were derived by Leitmann, Corless and Leitmann and Chen, for both nonlinear and linear systems. The next stage is therefore to show how these ideas can be utilized in conjunction with Feedback Linearization to produce control laws that are robust to the effects of uncertain dynamics.

4.2.2 Input-Output Linearization Framework

The study by Chen and Chen [10] shows how the Min-Max approach is used in the design of a robust controller for the stabilization of single-input single-output nonlinear

systems. The nonlinear systems considered include a nominal part that is fully linearizable using Input-State Linearization. Even though this thesis is concerned with the the multivariable Input-Output Linearization problem, some of the ideas from Chen and Chen have been helpful to the analysis that follows.

In order to combine and directly apply the ideas of Chen (nonlinear) and Leitmann (linear) described in the previous section, it is necessary to express the Input-Output Linearized system in Leitmann's form given below, i.e. (4.26):

$$\dot{x}(t) = \bar{A}\,x(t) + B\,P_{rob}(x) + B\,\delta(x,t)$$

First consider the nonlinear system (4.1):

$$\begin{aligned} \dot{x} &= f(x) + \Delta f(x) + \sum_{i=1}^{m} [\,g_i(x) + \Delta g_i(x)\,]\,u_i \\ &= f(x) + \Delta f(x) + [\,G(x) + \Delta G(x)\,]\,u \\ y_i &= h_i(x) \qquad i = 1 \ldots m \end{aligned} \tag{4.38}$$

where the following matching assumptions hold:

$$\begin{aligned} \Delta f(x) &= G(x)\,S(x) \\ \Delta G(x) &= G(x)\,T(x) \end{aligned} \tag{4.39}$$

and, in addition, where the nominal system:

$$\begin{aligned} \dot{x} &= f(x) + G(x)\,u \\ y_i &= h_i(x) \qquad i = 1 \ldots m \end{aligned} \tag{4.40}$$

is Input-Output Linearizable.

Applying a partial coordinates change to system (4.38) gives:

$$\begin{aligned} \dot{\zeta}_1^i &= \zeta_2^i \\ &\ldots \\ \dot{\zeta}_{r_i-1}^i &= \zeta_{r_i}^i \\ \dot{\zeta}_{r_i}^i &= L_f^{r_i} h_i(x) + E_{row\,i}\,u + \Delta L_f^{r_i} h_i(x) + \Delta E_{row\,i}\,u \\ \\ \dot{\eta} &= p(x) + q(x)\,u + \Delta p(x) + \Delta q(x)\,u \end{aligned} \tag{4.41}$$

where:

$$E(x) = \begin{bmatrix} L_{g_1}L_f^{r_1-1}h_1(x) & \dots & L_{g_m}L_f^{r_1-1}h_1(x) \\ \vdots & \ddots & \vdots \\ L_{g_1}L_f^{r_m-1}h_m(x) & \dots & L_{g_m}L_f^{r_m-1}h_m(x) \end{bmatrix} \tag{4.42}$$

$$\Delta L_f^r h(x) = \begin{bmatrix} L_{\Delta f}^{r_1}h_1(x) \\ \vdots \\ L_{\Delta f}^{r_m}h_m(x) \end{bmatrix} \tag{4.43}$$

$$\Delta E(x) = \begin{bmatrix} L_{\Delta g_1}L_f^{r_1-1}h_1(x) & \dots & L_{\Delta g_m}L_f^{r_1-1}h_1(x) \\ \vdots & \ddots & \vdots \\ L_{\Delta g_1}L_f^{r_m-1}h_m(x) & \dots & L_{\Delta g_m}L_f^{r_m-1}h_m(x) \end{bmatrix} \tag{4.44}$$

For the entire system, the external dynamics of (4.41) can be written as:

$$\begin{Bmatrix} \dot{\zeta}^1 \\ \dot{\zeta}^2 \\ \vdots \\ \dot{\zeta}^m \end{Bmatrix} = \begin{bmatrix} A_1 & 0 & \dots & 0 \\ 0 & A_2 & & 0 \\ 0 & 0 & \ddots & \vdots \\ 0 & 0 & \dots & A_m \end{bmatrix} \begin{Bmatrix} \zeta^1 \\ \zeta^2 \\ \vdots \\ \zeta^m \end{Bmatrix} + \begin{bmatrix} B_1 & 0 & \dots & 0 \\ 0 & B_2 & & 0 \\ 0 & 0 & \ddots & \vdots \\ 0 & 0 & \dots & B_m \end{bmatrix}$$
$$\begin{Bmatrix} L_f^{r_1}h_1(x) + E_{row\,1}\,u + \Delta L_f^{r_1}h_1(x) + \Delta E_{row\,1}\,u \\ L_f^{r_2}h_2(x) + E_{row\,2}\,u + \Delta L_f^{r_2}h_2(x) + \Delta E_{row\,2}\,u \\ \vdots \\ L_f^{r_m}h_m(x) + E_{row\,m}\,u + \Delta L_f^{r_m}h_m(x) + \Delta E_{row\,m}\,u \end{Bmatrix} \tag{4.45}$$

or more compactly as:

$$\dot{\zeta} = A\,\zeta + B\,\{L_f^r h(x) + E\,u + \Delta L_f^r h(x) + \Delta E\,u\} \tag{4.46}$$

where $A_i = \begin{bmatrix} 0 & 1 & 0 & \dots & 0 \\ 0 & 0 & 1 & \dots & 0 \\ \vdots & \vdots & \vdots & \ddots & \vdots \\ 0 & 0 & 0 & \dots & 1 \\ 0 & 0 & 0 & \dots & 0 \end{bmatrix}$ $B_i = \begin{Bmatrix} 0 \\ 0 \\ \vdots \\ 0 \\ 1 \end{Bmatrix}$ $\zeta^i = \begin{Bmatrix} \zeta_1^i \\ \zeta_2^i \\ \vdots \\ \zeta_{r_i-1}^i \\ \zeta_{r_i}^i \end{Bmatrix}$

and A_i is a $r_i \times r_i$ matrix while B_i is a $r_i \times 1$ vector and $i = 1 \dots m$.

Recall from Section 3.4 that output tracking is achieved by stabilizing the error system. With the error coordinates defined as: $e_1^i = y_i(x) - y_{i_d} = \zeta_1^i(x) - y_{i_d}$ for $i = 1 \dots m$. The error system dynamics are given by:

$$\dot{e} = A\,e + B\,\{L_f^r h(x) + E\,u + \Delta L_f^r h(x) + \Delta E\,u - y_d^{(r)}\} \tag{4.47}$$

If the nominal system's Input-Output Linearizing control law:

$$u = E^{-1}\left[-L_f^r h(x) + v\right] \tag{4.48}$$

is applied to system (4.47), the following is obtained:

$$\dot{e} = A\,e + B\left\{v + \Delta L_f^r h(x) + \Delta E\,E^{-1}\left(-L_f^r h(x) + v\right) - y_d^{(r)}\right\} \tag{4.49}$$

System (4.49) is now in the form of Leitmann's (4.22), therefore similarly to Leitmann's control (4.23), the control variable v can be chosen as:

$$v \;=\; K\,e + y_d^{(r)} + P_{rob} \tag{4.50}$$

where $K\,e + y_d^{(r)}$ is a stabilizing and output tracking control for the nominal part of the system, and the *robustifying term* P_{rob} can be designed to ensure that effects of the uncertainties are minimised.

To find P_{rob} the control law (4.50) is substituted into (4.49):

$$\begin{aligned}\dot{e} \;=\; & \bar{A}\,e + B\,P_{rob} + B\left\{\Delta L_f^r h(x) \;+\right. \\ & \left.\Delta E\,E^{-1}\left(-L_f^r h(x) + K\,e + y_d^{(r)} + P_{rob}\right)\right\}\end{aligned} \tag{4.51}$$

where $\bar{A} = A + B\,K$.

Noting now, that error system (4.51) is equivalent to Leitmann's (4.26) and taking into account the nonlinear uncertainty, Chen [80], present in this case it is possible to use the following saturation control for the error system:

$$P_{rob} \;=\; -\rho_v(x)\,sat(\mu(x)) \;=\; \begin{cases} -\frac{\mu(x)}{\|\mu(x)\|}\,\rho_v(x) & \text{if} \quad \|\mu(x)\| > \epsilon \\ \\ -\frac{\mu(x)}{\epsilon}\,\rho_v(x) & \text{if} \quad \|\mu(x)\| \leq \epsilon \end{cases} \tag{4.52}$$

where

$$\mu(x) \;=\; B^T P\,e\,\rho_v(x) \tag{4.53}$$

and the matrix $P > 0$ is the solution of (4.24) where Q is an arbitrary constant positive definite $r \times r$ matrix. The positive constant ϵ affects the size of the achievable steady state tracking error as will become clearer later.

To determine $\rho_v(\cdot) : \Re^n \to \Re^1_+$, compare (4.51) to (4.26) and then note that Leitmann's δ is equivalent to M given below:

$$M \;=\; \Delta L_f^r h(x) + \Delta E\,E^{-1}\left(-L_f^r h(x) + K\,e + y_d^{(r)} + P_{rob}\right) \tag{4.54}$$

Taking the norm of (4.54) and defining $\rho_v(x)$ leads to:

$$\begin{aligned} \|M\|_2 \quad &\leq \quad \|\Delta L_f^r h(x) + \Delta E\, E^{-1}\,(-L_f^r h(x) + K\, e + y_d^{(r)})\|_2 + \\ &\quad \|\Delta E\, E^{-1}\|_2\, \rho_v(x) \quad \triangleq \quad \rho_v(x) \end{aligned} \tag{4.55}$$

Note that all vector norms are Euclidean and the matrix norms are defined by: $\|A\|_2 = [\lambda_{max}(A^*A)]^{\frac{1}{2}}$ were A^* denotes the conjugate transpose of A and λ_{max} is the maximum eigenvalue.

So, provided that $[1 - \|\Delta E\, E^{-1}\|_2] > 0$, then

$$\begin{aligned} \rho_v(x) \quad &= \quad [1 - \|\Delta E\, E^{-1}\|_2]^{-1} \\ &\quad [\,\|\Delta L_f^r h(x) + \Delta E\, E^{-1}\,(-L_f^r h(x) + K\, e + y_d^{(r)})\|_2\,] \end{aligned} \tag{4.56}$$

Finally the saturation control law, where $P_{rob}(x)$ is given by (4.52), is as follows:

$$u = E^{-1}\,[-L_f^r h(x) + K\, e + y_d^{(r)} + P_{rob}\,] \tag{4.57}$$

This control law guarantees that the states of the external system and the output tracking errors are bounded for all initial conditions. In fact the tracking errors will converge to a ball around 0 whose radius is affected by the positive constant ϵ, as seen in the next section.

Note that, like the basic Input-Output Linearization, this control law does not directly address the internal dynamics, these modes must however, be inspected, to ensure that their behaviour is at least predictable. This issue is discussed further in the section entitled Internal Dynamics.

Guaranteed Boundedness of Tracking Errors

In this section the error dynamics are examined and it is shown that the control law derived in the previous section will ensure that the external dynamics are robustly stable and the steady state tracking error is necessarily non zero as a result of the saturation control.

Consider a Lyapunov function for the error dynamics as follows:

$$V(e) = e^T\, P\, e \tag{4.58}$$

Differentiating $V(e)$ along trajectory (4.51) gives:

$$\begin{aligned}\dot{V} &= e^T (P A + A^T P) e + 2 e^T P B \{\Delta L_f^r h + \Delta E E^{-1} (-L_f^r h \\ &\quad + K e + y_d^{(r)})\} - 2 e^T P B \rho_v (I + \Delta E E^{-1}) sat(\mu) \end{aligned} \tag{4.59}$$

Noting that

$$e^T (P \bar{A} + \bar{A}^T P) e = -e^T Q e \tag{4.60}$$

and

$$\lambda_{min}(Q) \|e\|^2 \leq e^T Q e \leq \lambda_{max}(Q) \|e\|^2 \tag{4.61}$$

and also using $\mu(x)$ from (4.53) and $\rho_v(x)$ from (4.56) leads to the following inequality:

$$\begin{aligned}\dot{V} &\leq -\lambda_{min}(Q) \|e\|^2 + 2 \|\mu\|_2 [1 - \|\Delta E E^{-1}\|_2] \\ &\quad - 2 \|\mu\|_2 \| I + \Delta E E^{-1} \|_2 \|sat(\mu)\|_2 \end{aligned} \tag{4.62}$$

Since

$$\| I + \Delta E E^{-1} \|_2 \geq \|I\|_2 - \| \Delta E E^{-1} \|_2 \tag{4.63}$$

Then

$$-\| I + \Delta E E^{-1} \|_2 \leq -[1 - \| \Delta E E^{-1} \|_2] \tag{4.64}$$

Also noting that $\| sat(\mu) \| = sat(\|\mu\|)$ allows (4.62) to be rewritten as:

$$\dot{V} \leq -\lambda_{min}(Q) \|e\|^2 + 2 [1 - \|\Delta E E^{-1}\|_2] \{ \|\mu\|_2 - \|\mu\|_2 \, sat(\|\mu\|_2) \} \tag{4.65}$$

With the saturation function $sat(\mu)$ given by:

$$sat(\mu) = \begin{cases} \frac{\mu}{\|\mu\|} & \text{if } \|\mu\| > \epsilon \\ \frac{\mu}{\epsilon} & \text{if } \|\mu\| \leq \epsilon \end{cases} \tag{4.66}$$

Then $sat(\|\mu\|)$ is as follows:

$$sat(\|\mu\|) = \begin{cases} \frac{\|\mu\|}{\|\mu\|} & \text{if } \|\mu\| > \epsilon \\ \frac{\|\mu\|}{\epsilon} & \text{if } \|\mu\| \leq \epsilon \end{cases} \tag{4.67}$$

Now considering the second term in (4.65) i.e.

$$2\,[\,1 - \|\Delta E\,E^{-1}\|_2\,]\,\{\,\|\mu\|_2 - \|\mu\|_2\,sat(\,\|\mu\|_2\,)\,\} \tag{4.68}$$

if $\|\mu\|_2 > \epsilon$ then the above term (4.68) becomes zero. If on the other hand $\|\mu\|_2 \leq \epsilon$ then (4.68) becomes:

$$2\,[\,1 - \|\Delta E\,E^{-1}\|_2\,]\,\{\,\|\mu\|_2 - \frac{\|\mu\|_2\,\|\mu\|_2}{\epsilon}\,\} \tag{4.69}$$

The maximum valve of $\{\|\mu\|_2 - \frac{\|\mu\|_2\,\|\mu\|_2}{\epsilon}\}$, found by differentiating and setting the derivative to zero, is given by $\frac{\epsilon}{4}$. Since the maximum value of $\{1 - \|\Delta E\,E^{-1}\|\}$ is 1 then:

$$\text{Max}\ \{\,2\,[\,1 - \|\Delta E\,E^{-1}\|_2\,]\,\{\,\|\mu\|_2 - \|\mu\|_2\,\|sat(\mu)\|_2\,\}\,\} \;=\; \frac{\epsilon}{2} \tag{4.70}$$

Finally, using the above statements:

$$\dot{V} \;\leq\; -\lambda_{min}(Q)\,\|e\|^2 + \frac{\epsilon}{2} \tag{4.71}$$

Clearly for $\dot{V}$ to remain negative definite then:

$$\|e\|^2 \;>\; \frac{\epsilon}{2\,\lambda_{min}(Q)} \tag{4.72}$$

which implies that the introduction of the saturation control to ensure the error system stability leads to the existence of a tracking error that depends on the size of ϵ.

Internal Dynamics

This section examines the problem of the internal dynamics with uncertainties and the effect of the robust control law on them. It will be shown that, provided the internal dynamics of the nominal system is stable, then the internal dynamics of the uncertain system will remain within a bounded set B_R a ball in $\Re^n$ with radius R, where R depends on the size of the uncertainties affecting the internal dynamics. The analysis that follows utilizes and generalizes some of the ideas developed by Liao et al [45] for dealing with the internal dynamics of single-input single-output nonlinear systems with mismatched uncertainties.

The internal dynamics of the uncertain system is given by:

$$\dot{\eta} = p(\zeta, \eta) + q(\zeta, \eta)\, u + \Delta p(\zeta, \eta) + \Delta q(\zeta, \eta)\, u \tag{4.73}$$

where the Input-Output Linearization control law is:

$$u = E^{-1}\left[-L_f^r h + v\right] \tag{4.74}$$

Applying control law (4.74) to system (4.73) results in:

$$\dot{\eta} = \hat{p}(\zeta, \eta) + \hat{q}(\zeta, \eta)\, v + \Delta\hat{p}(\zeta, \eta) + \Delta\hat{q}(\zeta, \eta)\, v \tag{4.75}$$

At this point certain assumptions are made, the crucial one being that the zero dynamics of the nominal system are exponentially stable.

Recall from Chapter 3 that the zero dynamics of the nominal system are

$$\dot{\eta} = \hat{p}(0\,\eta) \tag{4.76}$$

If (4.76) is exponentially stable then by a converse theorem of Lyapunov, Hahn [26], there exists a Lyapunov function $V_0(\eta)$ which satisfies the following inequalities:

$$k_1 \|\eta\|^2 \leq V_0(\eta) \leq k_2 \|\eta\|^2 \tag{4.77}$$

$$\frac{\partial V_0}{\partial \eta}\hat{p}(0, \eta) \leq -k_3 \|\eta\|^2 \tag{4.78}$$

$$\left\| \frac{\partial V_0}{\partial \eta} \right\| \leq k_4 \|\eta\| \tag{4.79}$$

where $k_1 \ldots k_4$ are appropriate positive constants.

In addition, if $\hat{p}(\zeta, \eta)$ is assumed to be locally Lipschitz in ζ and η, then there exists a positive constant L such that:

$$\|\hat{p}(\zeta^1, \eta^1) - \hat{p}(\zeta^2, \eta^2)\| \leq L\left(\|\zeta^1 - \zeta^2\| + \|\eta^1 - \eta^2\|\right) \tag{4.80}$$

Now substituting control law (4.50) into (4.75) produces:

$$\dot{\eta} = \hat{p}(\zeta, \eta) + \phi(\zeta, \eta, v) \tag{4.81}$$

where:

$$\begin{aligned} \phi(\zeta, \eta, v) = {} & \hat{q}(\zeta, \eta)\left\{K e + y_d^{(r)} + P_{rob}\right\} + \Delta\hat{p}(\zeta, \eta) + \\ & \Delta\hat{q}(\zeta, \eta)\left\{K e + y_d^{(r)} + P_{rob}\right\} \end{aligned} \tag{4.82}$$

If G, Δf and ΔG are smooth then constants l_1 and l_2 will exist such that $\forall\ (\zeta,\ \eta) \in \Re^n$:

$$\|\phi(\zeta,\ \eta,\ v)\| \ \leq\ l_1\,(\|\zeta\| + \|\eta\|) + l_2 \tag{4.83}$$

This assumption will be satisfied within a compact set B_R; a ball in $\Re^n$ with radius R, where l_1 and l_2 depend on R which can be arbitrarily large. The desired output trajectory $y_d(t)$ and its first r derivatives are all assumed to be bounded and satisfy:

$$\|\,(y_d,\ y_d^{(1)},\ \ldots,\ y_d^{(r)})\,\| \ \leq\ b_d \tag{4.84}$$

for some positive constant b_d. Finally, it is also assumed that

$$\|\zeta\| \ \leq\ \|e\| + b_d \tag{4.85}$$

To obtain the boundedness result for the internal dynamics, choose a Lyapunov function:

$$V(\zeta,\ \eta) = \mu\, V_0(\eta) \tag{4.86}$$

where μ is a positive constant to be determined later.

Differentiating $V_0(\eta)$ along trajectory (4.81) and using inequalities (4.77) to (4.79) along with (4.83) to (4.85) gives:

$$\begin{aligned}
\dot{V}_0(\eta) \ &=\ \frac{\partial V_0}{\partial \eta}\,\{\hat{p}(\zeta,\ \eta) + \phi(\zeta,\ \eta,\ v)\} && (4.87)\\
&=\ \frac{\partial V_0}{\partial \eta}\,\{\hat{p}(0,\ \eta) + \hat{p}(\zeta,\ \eta) - \hat{p}(0,\ \eta) + \phi(\zeta,\ \eta,\ v)\} && (4.88)\\
&\leq\ -\,k_3\,\|\eta\|^2 + k_4\,L\,\|\eta\|\,\|\zeta\| + k_4\,\|\eta\|\,\{l_1\,(\|\zeta\| + \|\eta\|) + l_2\} && (4.89)\\
&\leq\ -\,k_3\,\|\eta\|^2 + k_4\,l_1\,\|\eta\|^2 + k_4\,(L + l_1)\,\|\eta\|\,\|e\| \\
&\quad + k_4\,(l_2 + (L + l_1)\,b_d)\,\|\eta\| && (4.90)
\end{aligned}$$

Therefore the derivative of the Lyapunov function for the internal dynamics is given by:

$$\begin{aligned}
\dot{V} \ &\leq\ -\,\mu\,(k_3 - k_4\,l_1)\,\|\eta\|^2 + \mu\,k_4\,(L + l_1)\,\|\eta\|\,\|e\| \\
&\quad + \mu\,k_4\,(l_2 + (L + l_1)\,b_d)\,\|\eta\| && (4.91)\\
&\leq\ -\,\mu\,(\frac{3}{4}\,k_3 - k_4\,l_1)\,\|\eta\|^2 + \frac{\|e\|^2}{4} - \left\{\,\frac{\|e\|}{2} - \mu\,k_4\,(L + l_1)\,\|\eta\|\,\right\}^2
\end{aligned}$$

$$+ (\mu k_4 (L + l_1))^2 \|\eta\|^2 - \mu k_3 \left\{ \frac{\|\eta\|}{2} - \frac{k_4 (l_2 + (L + l_1) b_d)}{k_3} \right\}^2 + \mu \frac{\{k_4 (l_2 + (L + l_1) b_d)\}^2}{k_3} \quad (4.92)$$

Removing the two negative terms, i.e. the third and the fifth, from the right hand side of the above inequality, leaves:

$$\dot{V} \leq -\mu (\frac{3}{4} k_3 - k_4 l_1) \|\eta\|^2 + \frac{\|e\|^2}{4} + (\mu k_4 (L + l_1))^2 \|\eta\|^2 + \mu \frac{\{k_4 (l_2 + (L + l_1) b_d)\}^2}{k_3} \quad (4.93)$$

Now μ must be chosen to ensure that:

$$-\mu (\frac{3}{4} k_3 - k_4 l_1) + (\mu k_4 (L + l_1))^2 < 0 \quad (4.94)$$

Therefore

$$\mu < \frac{\frac{3}{4} k_3 - k_4 l_1}{{k_4}^2 (L + l_1)^2} \quad (4.95)$$

but since μ is a positive constant

$$0 < \frac{\frac{3}{4} k_3 - k_4 l_1}{{k_4}^2 (L + l_1)^2} \quad (4.96)$$

$$k_4 l_1 < \frac{3}{4} k_3 \quad (4.97)$$

$$l_1 < \frac{3 k_3}{4 k_4} \quad (4.98)$$

So making

$$l_1 = \frac{k_3}{4 k_4} \quad (4.99)$$

satisfies (4.98) and therefore

$$\mu < \frac{8 k_3}{(4 k_4 L + k_3)^2} \quad (4.100)$$

is positive and ensures that (4.94) is true.

By choosing

$$\mu = \frac{2 k_3}{(4 k_4 L + k_3)^2} \quad (4.101)$$

and substituting μ and l_1 back into (4.93):

$$\dot{V} \leq -\mu \frac{3}{8} k_3 \|\eta\|^2 + \frac{\|e\|^2}{4} + \mu \frac{\{k_4 (l_2 + (L + l_1) b_d)\}^2}{k_3} \tag{4.102}$$

Since the tracking error e is quite small the second term of the right hand side of (4.102) is negligible so, as long as η is comparatively large, $\dot{V}$ is negative and the internal dynamics are bounded.

4.3 Robust Sliding Mode Control

Slotine and Li [69] and Zinober [82] provide good references for the Sliding mode technique. Sliding mode control employs a high speed feedback control law to drive the nonlinear plant's state trajectory onto a specified and user chosen surface in the state space (called the sliding or the switching surface) and to maintain the plant's state trajectory on this surface for all subsequent time. This property of the state trajectory remaining on the switching surface once intercepted is called a *sliding mode.* The surface is called a switching surface because if the state trajectory is *above* the surface a control path has one gain which switches sign if the trajectory drops *below* the surface. By proper design of the switching surface, Sliding mode control attains conventional goals of control such as stabilization and tracking.

Sliding mode control essentially involves a two phase procedure

1. Construction of a switching surface so that the original system restricted to the surface responds in a desired manner.

2. Development of a switching control law (i.e. appropriate switched feedback gains) which satisfy a set of sufficient conditions for the existence and reachability of a sliding mode, i.e. such that the system state is on the switching surface.

The objective in this section is to design a high speed switching control law, within the Input-Output Linearization domain, which will compensate for uncertainties and at the same time provide an asymptotic tracking force. Before examining this, the Sliding mode control (SMC) concept is illustrated by considering the following n-th order single-input single-output dynamic system:

$$x^{(n)}(t) = f(x,t) + b(x,t)\, u(t) + d(t) \tag{4.103}$$

$$y = x$$

The function $f(x,t)$ is generally nonlinear and uncertain, the extent of the imprecision $|\Delta f|$ on $f(x,t)$ is upper bounded by some known continuous function of x and t. Similarly the control gain $b(x,t)$ is uncertain but is of known sign and is bounded by some known continuous function of x and t. Both $f(x,t)$ and $b(x,t)$ are assumed to be continuous in x. Now the disturbance $d(t)$ is unknown but bounded in absolute value by a known continuous function of time.

The control objective is to have the output y track a specified reference trajectory y_d in the presence of model imprecision. Defining:

$$e = y - y_d \tag{4.104}$$

For asymptotic tracking choose a switching surface in the state space $\Re^n$ defined by the scalar equation:

$$s(x,t) = 0 \tag{4.105}$$

such that the state trajectory restricted to this surface achieves the control objective. One such surface can be defined as follows:

$$s(x,t) = \beta_0 e + \beta_1 \dot{e} + \ldots + \beta_{n-2} e^{(n-2)} + e^{(n-1)} \tag{4.106}$$

Clearly, choosing β_i for $i = 0 \ldots n-1$ so that the polynomial:

$$\beta_0 + \beta_1 s + \ldots + \beta_2 \dot{s} + \ldots + \beta_{n-2} s^{(n-3)} + s^{(n-2)} \tag{4.107}$$

is Hurwitz, ensures that on the surface, i.e. when $s(x,t) = 0$:

$$\beta_0 e + \beta_1 \dot{e} + \ldots + \beta_{n-2} e^{(n-2)} + e^{(n-1)} = 0 \tag{4.108}$$

(4.108) implies that $e^{(i)} \to 0$ as $t \to \infty$ for $i = 0 \ldots n-1$, thus asymptotic tracking is achieved.

After designing the switching surface, the next step is to guarantee the existence of a sliding mode. An ideal sliding mode exists only when the state trajectory $x(t)$ of the controlled plant satisfies $s(x,t) = 0$ at every $t \geq t_0$ for some t_0. Following the tutorial in

De Carlo et al [15], an ideal sliding mode exists if the tangent or the velocity vectors of the state trajectory always points towards the switching surface. Consequently, if the state trajectory intersects the sliding surface it remains on the surface for all subsequent time. Note that if a sliding mode exists on $s(x,t) = 0$ then this surface is termed a sliding surface.

Now ensuring the existence of a sliding mode requires infinitely fast switching. In practice all facilities responsible for switching control functions have imperfections such as delay, hysteresis, etc. which forces switching to occur at finite frequency. The value of the state trajectory then oscillates within a neighbourhood of the switching surface. This oscillation is called chattering and is shown in Figure 4.1 for a second order system. Also shown is an ideal case in which sliding actually occurs. The problems associated with chattering will be dealt with later.

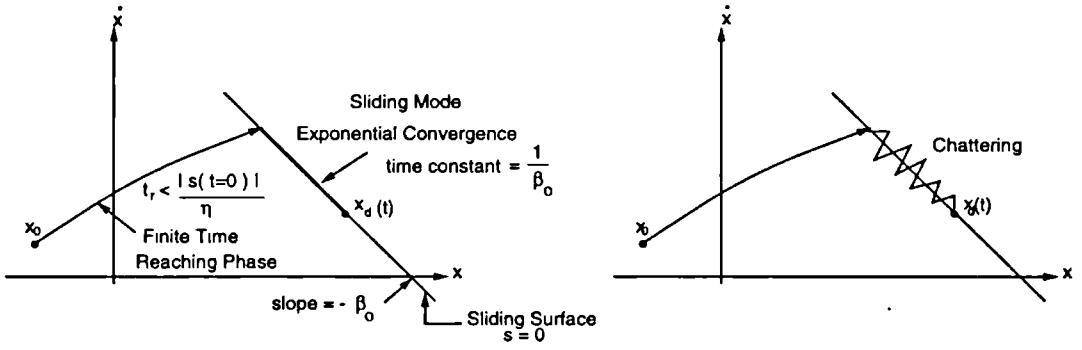

Figure 4.1: Ideal Sliding along with Chattering

The existence of a sliding mode requires stability of the state trajectory to the sliding surface $s(x,t) = 0$. This problem resembles a generalized stability problem, hence existence of a sliding mode requires selection of a generalized Lyapunov function $V(x,t)$ which is positive definite and has a negative definite time derivative.

A candidate Lyapunov function is:

$$V = \frac{1}{2} s^2 \tag{4.109}$$

Ensuring that the time derivative of V is negative definite, guarantees that $s(x,t) \rightarrow 0$ since:

$$\frac{1}{2} \frac{d}{dt} s^2(x,t) = s\,\dot{s} \leq 0 \tag{4.110}$$

Examination of (4.110) shows that $\dot{s}$ must have the following form $\dot{s} = -\alpha\, sgn(s)$, where α is non-negative. Since $\dot{s}$ is a function of the control it implies that the control must include the switching function $sgn(s)$ to ensure that the controlled system remains on the sliding surface.

Condition (4.110) may be rewritten as

$$\frac{1}{2}\frac{d}{dt}s^2(x,t) \leq -\eta|s| \tag{4.111}$$

where η is a positive constant to adjust the speed at which the state trajectory reaches the surface, see Figure 4.1 for the second order case.

The *Sliding Condition* (4.111) geometrically states that the squared distance to the surface as measured by s^2 decreases along all system trajectories. Thus it constrains trajectories to point towards the surface $s(x,t) = 0$. Once on the surface the system trajectories remain on the surface and the system behaviour is then in the *Sliding Mode*. Thus, satisfying the *sliding condition* (4.111) makes the surface an *invariant set* and, as we shall see later, this implies that some disturbances or dynamic uncertainties can be tolerated while the surface remains an invariant set.

Returning to the problem of chattering, this phenomenum is undesirable since it involves high control activity and possible excitation of high frequency dynamics neglected during modelling. This chattering may be eliminated by smoothing the control discontinuity in a thin *boundary layer* neighbouring the switching surface. Define the set:

$$B(t) = \{x,\ |\, s(x,t)\,| \leq \epsilon\} \qquad \epsilon > 0 \tag{4.112}$$

as the boundary layer. This is shown schematically in Figure 4.2 for a second order system.

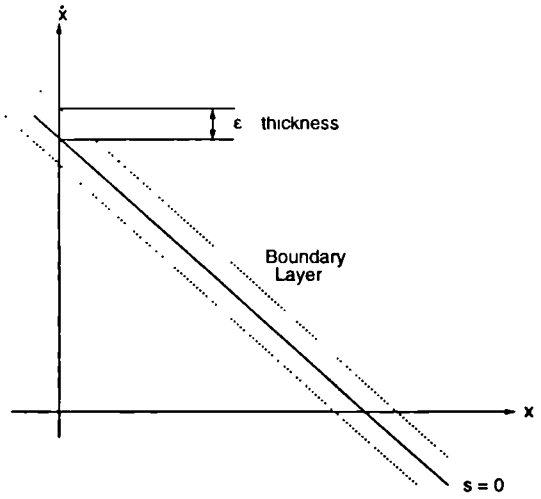

Figure 4.2: Boundary Layer

When a boundary layer is introduced, instead of ensuring that $s(x,t) = 0$ is attractive, it is the boundary layer that is made to be attractive, hence invariant. Therefore all trajectories starting inside $B(t = 0)$ remain inside $B(t)$ for all $t > 0$. The control may then be chosen to satisfy the sliding condition and hence guarantee that the boundary layer is attractive. However, inside the boundary layer the control is no longer switching but is interpolated by replacing $sgn(s)$ by $\frac{s}{\epsilon}$, replacing the *signum* function by the *saturation* function shown below in Figure 4.3.

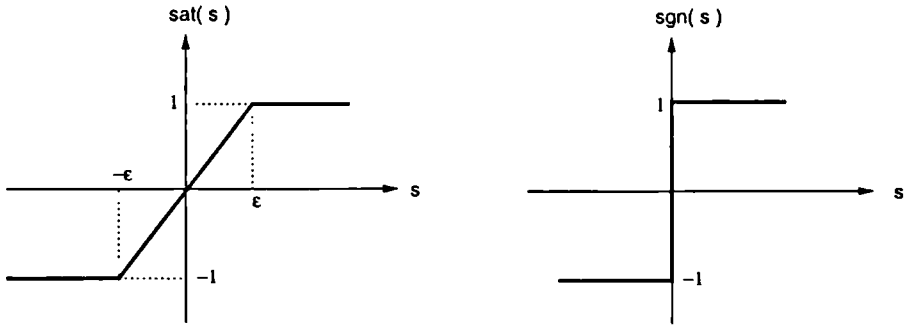

Figure 4.3: Saturation and Signum Functions

The result of this smoothing is the introduction of a trade-off between chattering and tracking accuracy. Tracking is guaranteed within a certain precision determined

by the boundary layer width.

4.3.1 Robust Tracking of Input-Output Linearizable Systems

The control law derivation presented next exploits many of the ideas presented in Fu and Liao [20] where a Sliding mode control was used in conjunction with an Input-Output Linearizing control. The system was a square multi-input multi-output system added to which the nominal internal dynamics were stable. The structure of the system considered and the matching conditions ensured that the internal dynamics of the uncertain system were exactly the same as those of the nominal system.

The control presented here as in the section on Lyapunov based control, is directly concerned only with the external dynamics. Therefore the control presented by Fu and Liao [20] suffices for this purpose. However, unlike Fu and Liao, the internal dynamics is treated as uncertain and an analysis similar to that carried out earlier in the section on internal dynamics should demonstrate the boundedness of these dynamics provided the previous conditions are satisfied.

The following development is a two step procedure, where the first task is to define a set of sliding surfaces, $s(x,t) = 0$, that represent the desired dynamics of the errors. The set $s(x,t)$ is defined as a function of the output space vector, the initial conditions and time.

$$s = \left\{ \begin{array}{c} s_1 \\ \vdots \\ s_m \end{array} \right\} = \left\{ \begin{array}{c} y_1^{(r_1-1)} - y_{1_d}^{(r_1-1)} + \sum_{j=0}^{r_1-2} \beta_j^1 \left(y_1^{(j)} - y_{1_d}^{(j)} \right) \\ \vdots \\ y_m^{(r_m-1)} - y_{m_d}^{(r_m-1)} + \sum_{j=0}^{r_m-2} \beta_j^m \left(y_m^{(j)} - y_{m_d}^{(j)} \right) \end{array} \right\} \tag{4.113}$$

where $y^{(0)} = y$ and β_j^i, for $j = 0 \ldots r_i - 2$ and $i = 1 \ldots m$, are appropriate constants to be specified.

Rewriting s in error coordinates:

$$\left\{ \begin{array}{c} s_1 \\ \vdots \\ s_m \end{array} \right\} = \left\{ \begin{array}{c} e_1^{(r_1-1)} + \sum_{j=0}^{r_1-2} \beta_j^1 e_1^{(j)} \\ \vdots \\ e_m^{(r_m-1)} + \sum_{j=0}^{r_m-2} \beta_j^m e_m^{(j)} \end{array} \right\} \tag{4.114}$$

Now β_j^i are chosen so that the polynomials:

$$H_i(s) = \beta_0^i + \beta_1^i s + \ldots + \beta_2^i \dot{s} + \ldots + \beta_{r_i-2}^i s^{(r_i-3)} + s^{(r_i-2)} \quad i = 1 \ldots m \tag{4.115}$$

are Hurwitz. Thus when the output error trajectories reach the sliding surface, $s = 0$, and stay on it:

$$\beta_0^i e + \beta_1^i \dot{e} + \ldots + \beta_{r_i-2}^i e^{(r_i-2)} + e^{(r_i-1)} = 0 \quad i = 1 \ldots m \tag{4.116}$$

This implies that $e_i^{(j)} \to 0$ as $t \to \infty$ for $j = 1 \ldots (r_i - 1)$ and $i = 1 \ldots m$. This obviously includes the control objective of $e = (y - y_d) \to 0$ as $t \to \infty$.

The sliding condition for the multivariable case which guarantees the existence of a sliding mode, i.e. that the error trajectories reach the switching surface and remain on it, can be derived in a similar way to that given in the previous section.

In this case with m surfaces a possible candidate Lyapunov function is:

$$V = \frac{1}{2} s^T s \tag{4.117}$$

Ensuring that the time derivative of V is negative definite, guarantees that $s(x,t) \to 0$, therefore the following is a valid sliding condition:

$$s^T \dot{s} \leq -\eta \|s\|_2 \tag{4.118}$$

Since $\dot{s}$ appears in the sliding condition, (4.114) is differentiated to give:

$$\begin{Bmatrix} \dot{s}_1 \\ \vdots \\ \dot{s}_m \end{Bmatrix} = \begin{Bmatrix} e_1^{(r_1)} + \sum_{j=0}^{r_1-2} \beta_j^1 e_1^{(j+1)} \\ \vdots \\ e_m^{(r_m)} + \sum_{j=0}^{r_m-2} \beta_j^m e_m^{(j+1)} \end{Bmatrix} \tag{4.119}$$

The second stage of the design is to find a control law for the nonlinear system such that the sliding condition is verified. Consider part of the uncertain nonlinear system after Input-Output Linearization:

$$y^{(r)} = L_f^r h(x) + \Delta L_f^r h(x) + [E(x) + \Delta E(x)] u \tag{4.120}$$

Substituting (4.120) into (4.119) gives:

$$\dot{s} = -y_d^{(r)} + L_f^r h(x) + \Delta L_f^r h(x) + [E(x) + \Delta E(x)] u + e_p \tag{4.121}$$

where

$$e_p = \begin{Bmatrix} \sum_{j=0}^{r_1-2} \beta_j^1 e_1^{(j+1)} \\ \vdots \\ \sum_{j=0}^{r_m-2} \beta_j^m e_m^{(j+1)} \end{Bmatrix} \tag{4.122}$$

To achieve tracking control, the sliding condition with (4.121), suggests a control law of the form:

$$u = E^{-1}(\hat{u} - K\,sgn(s)) \tag{4.123}$$

where

$$\hat{u} = y_d^{(r)} - L_f^r h(x) - e_p \tag{4.124}$$

This is a predictor-corrector control law where $E^{-1}\hat{u}$ accounts for the nominal system and $-E^{-1}K\,sgn(s)$ is the switching control part responsible for robustness to uncertainty. K is a non-negative real number selected to ensure that the sliding condition is satisfied.

To design K, substituting $\dot{s}$ of (4.121) into the sliding condition (4.118) yields:

$$\begin{aligned} s^T\{-y_d^{(r)} + L_f^r h(x) + \Delta L_f^r h(x) + \\ [E(x) + \Delta E(x)]E^{-1}(\hat{u} - K\,sgn(s)) + e_p\} \leq -\eta\|s\|_2 \end{aligned} \tag{4.125}$$

Now substituting for $\hat{u}$ and expanding gives:

$$\begin{aligned} s^T\{\Delta L_f^r h(x) - K\,sgn(s) + \\ \Delta E\,E^{-1}(y_d^{(r)} - L_f^r h(x) - e_p - K\,sgn(s))\} \leq -\eta\|s\|_2 \end{aligned} \tag{4.126}$$

If ξ is defined to be

$$\xi = y_d^{(r)} - e_p \tag{4.127}$$

then:

$$\begin{aligned} s^T\{\Delta L_f^r h(x) + \Delta E\,E^{-1}\xi - \Delta E\,E^{-1}L_f^r h(x)\} - \\ K\,s^T sgn(s) - K\,s^T\Delta E\,E^{-1}sgn(s) \leq -\eta\|s\|_2 \end{aligned} \tag{4.128}$$

At this point the above expressions are simplified in stages using the matrix norm technique of Chang [8]. The first step is to write:

$$\begin{aligned} s^T\{\Delta L_f^r h(x) + \Delta E\,E^{-1}\xi - \Delta E\,E^{-1}L_f^r h(x)\} \leq \\ \|s\|_2\,\|\Delta L_f^r h(x) + \Delta E\,E^{-1}\xi - \Delta E\,E^{-1}L_f^r h(x)\|_2 \end{aligned} \tag{4.129}$$

If ψ_2 is such that:

$$\|\Delta L_f^r h(x) + \Delta E\, E^{-1}\, \xi - \Delta E\, E^{-1}\, L_f^r h(x)\|_2 \;\leq\; \psi_2 \tag{4.130}$$

then

$$s^T \{\, \Delta L_f^r h(x) + \Delta E\, E^{-1}\, \xi - \Delta E\, E^{-1}\, L_f^r h(x) \,\} \;\leq\; \|s\|_2\, \psi_2 \tag{4.131}$$

For the second step note that:

$$-K\, s^T\, sgn(s) \;=\; -K\, \|s\|_1 \tag{4.132}$$

Since $\|\cdot\|_1 \geq \|\cdot\|_2$ then (4.132) can be replaced by:

$$-K\, s^T\, sgn(s) \;\leq\; -K\, \|s\|_2 \tag{4.133}$$

Finally, for the third step:

$$-K\, s^T\, \Delta E\, E^{-1}\, sgn(s) \;=\; K\, s^T\, \Delta E\, E^{-1}\, sgn(-s) \tag{4.134}$$

$$K\, s^T\, \Delta E\, E^{-1}\, sgn(-s) \;\leq\; K\, \|s\|_2\; \|\Delta E\, E^{-1}\, sgn(-s)\|_2 \tag{4.135}$$

Since the following is true:

$$\|\Delta E\, E^{-1}\, sgn(-s)\|_2 \;=\; \|\Delta E\, E^{-1}\, sgn(s)\|_2 \tag{4.136}$$

then this too is assured:

$$-K\, s^T\, \Delta E\, E^{-1}\, sgn(s) \;\leq\; K\, \|s\|_2\; \|\Delta E\, E^{-1}\, sgn(-s)\|_2 \tag{4.137}$$

In which case:

$$\|\Delta E\, E^{-1}\, sgn(-s)\|_2 \;\leq\; \psi_1 \tag{4.138}$$

It is now apparent that:

$$-K\, s^T\, \Delta E\, E^{-1}\, sgn(s) \;\leq\; K\, \|s\|_2\, \psi_1 \tag{4.139}$$

Therefore equation (4.128) becomes:

$$\psi_2 - K + K\, \psi_1 \;\leq\; -\eta \tag{4.140}$$

Rearranging (4.140):

$$K\,(1-\psi_1) \;\geq\; \eta+\psi_2 \tag{4.141}$$

Since K is a non-negative real number then it is well defined if $\psi_1 < 1$.

$$K \;>\; \frac{\eta+\psi_2}{1-\psi_1} \tag{4.142}$$

The discontinuous control law derived from the above analysis is now smoothed and the resulting nonlinear Sliding mode control law is:

$$u \;=\; E^{-1}\,(\,y_d^{(r)} - L_f^r h(x) - e_p - K\,sat(s)\,) \tag{4.143}$$

where $sat(s)$ depends on the positive constant ϵ.

To understand the action of the smoothing function, consider the system trajectory inside the boundary layer which can be expressed by $\dot{s}$ as follows. Applying (4.143) to (4.121) yields:

$$\dot{s} + K\,(1+\Delta E\,E^{-1})\,sat(s) \;=\; \Delta L_f^r h + \Delta E\,E^{-1}\,(y_d^{(r)} - L_f^r h - e_p) \tag{4.144}$$

Inside the boundary layer $sat(s) = \frac{s}{\epsilon}$, therefore (4.144) becomes:

$$\dot{s} + \frac{K}{\epsilon}\,(1+\Delta E\,E^{-1})\,s \;=\; \Delta L_f^r h + \Delta E\,E^{-1}\,(y_d^{(r)} - L_f^r h - e_p) \tag{4.145}$$

From (4.145) it is apparent that the variable s, (where s is a measure of the distance to the surface $s(x,t)=0$), can be viewed as the output of a low pass filter.

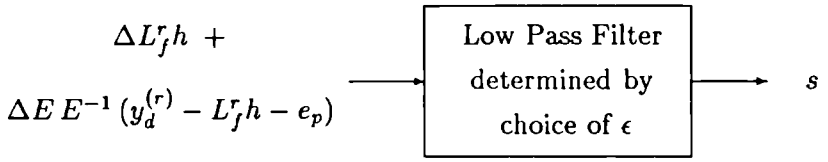

The filter structure enables chattering to be eliminated. The choice of ϵ allows the tuning of the control law so as to achieve a tradeoff between tracking accuracy and robustness to unmodelled dynamics. In fact ϵ is selected to ensure that the unmodelled high frequencies are not excited while still maintaining an acceptable degree of tracking precision.

Although not presented here the analysis given in the Section on Internal Dynamics is valid for the treatment of the internal dynamics of the system subject to the Sliding mode control.

In summary, two robust control laws have been presented within the Input-Output Linearization framework. The framework actually facilitates the robust control law design using the Lyapunov based and the Sliding mode control methods. The application of these ideas follow in Chapter 5 where robust control laws are designed for a helicopter. The performance of these designs is examined by means of computer simulation and these results are presented in Chapter 6.

Chapter 5

Helicopter Control System Design

This chapter describes the procedure involved in the design of robust control laws for helicopter systems. The first section is concerned with the application of Input-Output Linearization to the nonlinear helicopter model without uncertainties. The nonlinear control terms that appear in the helicopter model are effectively dealt with by a new iterative scheme that reduces design complexity by enabling the standard Input-Output Linearization Theory to be applied. The uncertainty considered is assumed to arise as a result of deficient rotor modeling and as such this representation of uncertainty is matched due to the structure of the dynamic equations. The level of uncertainty selected in this work is compared directly to previous uncertainty representations in H_∞ studies. The Lyapunov design described in Chapter 4 is next applied to the uncertain system inorder to increase the robustness properties of the closed loop system. In addition a second robust controller based on Sliding mode control is constructed. The internal dynamics of the system are also examined and it is shown that an outer loop design can practically control these modes by exploiting the time scale separation between the translational velocities and the angular velocities.

5.1 Tracking Control Using Input-Output Linearization

Before designing the tracking controller based on Input-Output Linearization, the outputs required to track desired trajectories must be specified. In the case of a helicopter, the most demanding flight regime is during low speed and hover. To provide maximum control benefit under these conditions an Attitude Command - Attitude Hold ($ACAH$) and a Rate Command (RC) system is required. This type of system should comply with the recommendations of the U.S. Handling Quality Requirements document [1].

Since four inceptors:

Main Rotor Collective	θ_o
Tail Rotor Collective	θ_{ot}
Longitudinal Cyclic	θ_{ls}
Lateral Cyclic	θ_{lc}

are available to the pilot then only four outputs can be directly controlled. The outputs selected for tracking are:

y_1	$=$	θ			Pitch Angle	(ACAH)
y_2	$=$	ϕ			Bank Angle	(ACAH)
y_3	$=$	$\dot{\psi}$	$=$	$[q \sin\phi + r \cos\phi] \sec\theta$	Heading Rate	(RC)
y_4	$=$	$\dot{h}$	$=$	$u \sin\theta - v \sin\phi \cos\theta - w \cos\phi \cos\theta$	Altitude Rate	(RC)

These outputs are consistent with the *ACAH* and *RC* system of the Aeronautical Design Standard [1] for the low speed and hover flight regimes. These outputs are also the same as those selected in the H_∞ design study by Yue and Postlethwaite [81]. The study by Yue and Postlethwaite is important since it represents the state of the art in linear robust helicopter control and as such provides a useful benchmark for qualitative comparisons. Furthermore the uncertainty model derived later in this chapter is compared directly to the level of uncertainty introduced in the H_∞ study.

To apply Feedback Linearization the system is generally assumed to be in the form

$$\begin{aligned} \dot{x} &= f(x) + g_1(x)\, u_1 + \ldots + g_m(x)\, u_m \\ \dot{x} &= f(x) + G(x)\, u \end{aligned} \tag{5.1}$$

This form implies that the differential equations are linear in the control variable u. This setting is often assumed since many systems can be expressed in this manner and because the additional complexity required in direct application of differential geometric methods to more general nonlinear systems is considerable. Nijmeijer and van der Shaft [54] provide further insight into the analysis required for general nonlinear systems. Unfortunately the helicopter system is not actually linear in the control, therefore, utilizing a knowledge of the system's properties, an iterative scheme is proposed to overcome this problem without significant increase in complexity. Essentially the problem is to transform the helicopter equations into the form of (5.1) by *grouping* the nonlinear coefficients of the control variables into a physically meaningful arrangement.

To show how this is done and to understand the subsequent role of the iterative scheme, it is necessary to examine the general helicopter equations presented in chapter 2.

Recall that the general form of the dynamic equations is as follows:

$$\begin{aligned}\dot{x} &= f(x) + g_1(x)\,\theta_o + g_2(x)\,\theta_{ls} + g_3(x)\,\theta_{lc} + g_4(x)\,\theta_o\,\theta_{ls} + g_5(x)\,\theta_o\,\theta_{lc} \\ &\quad + g_6(x)\,\theta_o^2 + g_7(x)\,\theta_{ls}\,\theta_{lc} + g_8(x)\,\theta_{ls}^2 + g_9(x)\,\theta_{lc}^2 + g_{10}(x)\,\theta_{ot} \qquad (5.2)\end{aligned}$$

$$\dot{x} = f(x) + G(x, \Theta) \qquad (5.3)$$

where $\Theta = [\theta_o,\ \theta_{ls},\ \theta_{lc},\ \theta_{ot}]^T$ is the input vector. Note also that only the equation describing the normal acceleration has the unique form:

$$\dot{w} = f_z(x) + g_{z_1}(x)\,\theta_o + g_{z_2}(x)\,\theta_{ls} + g_{z_3}(x)\,\theta_{lc} \qquad (5.4)$$

The problem arises because of the presence, in the other equations, of the following input product terms:

$$g_4(x)\,\theta_o\,\theta_{ls},\quad g_5(x)\,\theta_o\,\theta_{lc},\quad g_6(x)\,\theta_o^2,\quad g_7(x)\,\theta_{ls}\,\theta_{lc},\quad g_8(x)\,\theta_{ls}^2,\quad g_9(x)\,\theta_{lc}^2$$

It is first proposed that such terms are represented as:

$$\begin{aligned} g_6(x)\,\theta_o^2 &\rightarrow [g_6(x)\,\bar{\theta}_o]\,\theta_o \\ g_8(x)\,\theta_{ls}^2 &\rightarrow [g_8(x)\,\bar{\theta}_{ls}]\,\theta_{ls} \\ g_9(x)\,\theta_{lc}^2 &\rightarrow [g_9(x)\,\bar{\theta}_{lc}]\,\theta_{lc} \end{aligned}$$

where the square bracketed terms are the new system input vectors g_i and θ_* is a nominal value of θ_*. In the iterative scheme proposed, one uses the value of θ_* from the previous time-step for $\bar{\theta}_*$. During simulation such an *iterative* scheme, described fully later, is such that the performance of the controller remains very satisfactory despite the replacement of θ_*^2 with $\theta_*\,\theta_*$ and the continual updating of θ_*.

The other product terms are represented as follows:

$$\begin{aligned} g_4(x)\,\theta_o\,\theta_{ls} &\rightarrow [g_4(x)\,\bar{\theta}_o]\,\theta_{ls} \\ g_5(x)\,\theta_o\,\theta_{lc} &\rightarrow [g_5(x)\,\theta_o]\,\theta_{lc} \\ g_7(x)\,\theta_{ls}\,\theta_{lc} &\rightarrow [g_7(x)\,\bar{\theta}_{ls}]\,\theta_{lc} \end{aligned}$$

The first two representations provide a computationally stable iteration loop since variations in the collective θ_o tend to be smaller than either the longitudinal cyclic θ_{ls} or the lateral cyclic θ_{lc}. The final representation is also computationally stable as is:

$$g_7(x)\,\theta_{ls}\,\theta_{lc} \;\rightarrow\; [g_7(x)\,\bar{\theta}_{lc}]\,\theta_{ls}$$

This is so, because θ_{ls} and θ_{lc} both vary significantly. Further, simulation using both representations has been to found to converge and provide the same results in both cases. However for the control laws presented here the first option was used. Appendix B gives the full $G(x, \bar{\Theta})$ matrix incorporating the representations discussed above.

The state equations can now be written as:

$$\dot{x} = f(x) + g_1(x,\Theta)\,\theta_o + g_2(x,\Theta)\,\theta_{lc} + g_3(x,\Theta)\,\theta_{ls} + g_4(x,\Theta)\,\theta_{ot} \tag{5.5}$$

where $\Theta = [\,\theta_o\,,\ \theta_{ls}\,,\ \theta_{lc}\,,\ \theta_{ot}\,]^T$ is the input vector.

For Input-Output Linearization, the vector Θ appearing in the nonlinear vectors $g_i(x,\Theta)$, is assumed to be constant. Therefore the system to which Input-Output Linearization is applied is:

$$\dot{x} = f(x) + g_1(x,\bar{\Theta})\,\theta_o + g_2(x,\bar{\Theta})\,\theta_{lc} + g_3(x,\Theta)\,\theta_{ls} + g_4(x,\Theta)\,\theta_{ot} \tag{5.6}$$

During simulation the constant Θ is the value of Θ from the previous time-step.

For the actual dynamic equations given in Appendix B, the Input-Output Linearization computations were carried out *symbolically* using a program written in the **Mathematica** programming language.

- The outputs were differentiated repeatedly until the inputs $[\,\theta_o\,,\ \theta_{lc}\,,\ \theta_{ls}\,,\ \theta_{ot}\,]^T$ appeared.
- The relative degree and the decoupling matrix were then found.
- Finally the input space transformation was determined.

The vector of relative degree is $\mathbf{r} = \{2, 2, 1, 1\}$ for the output vector selected. Since there are eight states and $\sum_{i=1}^{4} \mathbf{r}_i = 6$, this implies the presence of two unobservable states. Part of the nonlinear state space transformation is given by:

$$\phi_1^1 \;=\; \theta \tag{5.7}$$

$$\phi_2^1 = q\cos\phi - r\sin\phi \tag{5.8}$$

$$\phi_1^2 = \phi \tag{5.9}$$

$$\phi_2^2 = p + [q\sin\phi + rcos\phi]\tan\theta \tag{5.10}$$

$$\phi_1^3 = [q\sin\phi + r\cos\phi]\sec\theta \tag{5.11}$$

$$\phi_1^4 = u[\sin\theta] - v[\sin\phi\cos\theta] - w[\cos\phi\cos\theta] \tag{5.12}$$

To describe the hidden part of the system it is possible to find $n - r = 2$ more functions ϕ_7 and ϕ_8 such that the mapping:

$$\Phi = col[\phi_1^1(x), \phi_2^1(x), \phi_1^2(x), \phi_2^2(x), \phi_1^3(x), \phi_1^4(x), \phi_7(x), \phi_8(x)]$$

has a nonsingular Jacobian matrix at x_0 and therefore qualifies as a state space coordinates transformation, for example $\phi_7 = u$ and $\phi_8 = v$. The Jacobian matrix is shown in Appendix B and has a determinant of $\cos\phi$. Thus the matrix is only singular if $\phi = \pm 90$ degrees. Since a bank angle of 90 degrees is an uncommon helicopter flight mode, then the coordinates transformation Φ is, practically speaking, global. Thus the system in new coordinates is a globally valid representation of the original system. The new state defined by the nonlinear state-space transformation is given by:

$$\zeta_1^i = \phi_1^i \tag{5.13}$$

$$\vdots \quad \vdots \qquad \text{for } i = 1\ldots4 \tag{5.14}$$

$$\zeta_{r_i}^i = \phi_{r_i}^i \tag{5.15}$$

$$\eta_1 = \phi_7 \tag{5.16}$$

$$\eta_2 = \phi_8 \tag{5.17}$$

As a result of the repeated differentiations, the input-space transformation is given by:

$$\begin{bmatrix} u_1 \\ \vdots \\ u_m \end{bmatrix} = E^{-1} \begin{bmatrix} v_1 - L_f^{r_1} h_1(x) \\ \vdots \\ v_m - L_f^{r_m} h_m(x) \end{bmatrix} \tag{5.18}$$

where E and $L_f^r h(x)$ are given in Appendix B.

The validity of this control law depends on the invertibility of E, however, for the system concerned proof of the non-singularity of E is not trivial. Further discussion of this is postponed until Chapter 6, where the setting is more appropriate for such ideas.

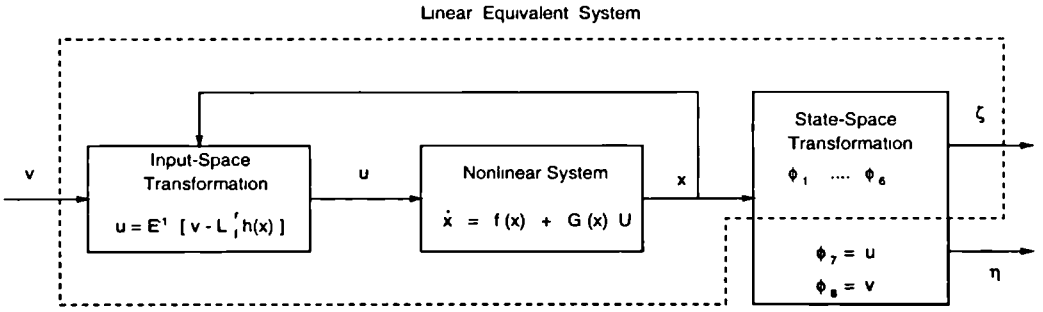

Figure 5.1: Transformed System

Applying the state space and the input space transformations decomposes the system as shown schematically in Figure 5.1.

The resulting dynamic system is:

$$\begin{bmatrix} \dot{\zeta}_1^1 \\ \dot{\zeta}_2^1 \\ \dot{\zeta}_1^2 \\ \dot{\zeta}_2^2 \\ \dot{\zeta}_1^3 \\ \dot{\zeta}_1^4 \end{bmatrix} = \begin{bmatrix} 0 & 1 & 0 & 0 & 0 & 0 \\ 0 & 0 & 0 & 0 & 0 & 0 \\ 0 & 0 & 0 & 1 & 0 & 0 \\ 0 & 0 & 0 & 0 & 0 & 0 \\ 0 & 0 & 0 & 0 & 0 & 0 \\ 0 & 0 & 0 & 0 & 0 & 0 \end{bmatrix} \begin{bmatrix} \zeta_1^1 \\ \zeta_2^1 \\ \zeta_1^2 \\ \zeta_2^2 \\ \zeta_1^3 \\ \zeta_1^4 \end{bmatrix} + \begin{bmatrix} 0 & 0 & 0 & 0 \\ 1 & 0 & 0 & 0 \\ 0 & 0 & 0 & 0 \\ 0 & 1 & 0 & 0 \\ 0 & 0 & 1 & 0 \\ 0 & 0 & 0 & 1 \end{bmatrix} \begin{bmatrix} v_1 \\ v_2 \\ v_3 \\ v_4 \end{bmatrix} \tag{5.19}$$

$$\dot{\eta}_1 = \dot{u} = f_u(x) + g_u(x, E^{-1}[v - L_f^r h(x)]) \tag{5.20}$$

$$\dot{\eta}_2 = \dot{v} = f_v(x) + g_v(x, E^{-1}[v - L_f^r h(x)]) \tag{5.21}$$

The linear subsystem is given by (5.19) while equations (5.20) and (5.21) represent the nonlinear internal dynamics. Note that the internal dynamics are given in the original state coordinates for simplicity.

For the tracking control law described in Chapter 3 the helicopter error system is first defined.

$$\begin{aligned} e_1^1 &= y_1 - y_{d_1} = \theta - \theta_d = \zeta_1^1 - \theta_d \\ e_2^1 &= \dot{y}_1 - \dot{y}_{d_1} = \dot{\theta} - \dot{\theta}_d = \zeta_2^1 - \dot{\theta}_d \\ e_1^2 &= y_2 - y_{d_2} = \phi - \phi_d = \zeta_1^2 - \phi_d \\ e_2^2 &= \dot{y}_2 - \dot{y}_{d_2} = \dot{\phi} - \dot{\phi}_d = \zeta_2^2 - \dot{\phi}_d \\ e_1^3 &= y_3 - y_{d_3} = \dot{\psi} - \dot{\psi}_d = \zeta_1^3 - \dot{\psi}_d \\ e_1^4 &= y_4 - y_{d_4} = \dot{h} - \dot{h}_d = \zeta_1^4 - \dot{h}_d \end{aligned} \tag{5.22}$$

The matrix K is chosen to provide adequate speed of response, and the tracking control is given by:

$$\begin{bmatrix} v_1 \\ v_2 \\ v_3 \\ v_4 \end{bmatrix} = \begin{bmatrix} k_{11} & k_{12} & 0 & 0 & 0 & 0 \\ 0 & 0 & k_{21} & k_{22} & 0 & 0 \\ 0 & 0 & 0 & 0 & k_{31} & 0 \\ 0 & 0 & 0 & 0 & 0 & k_{41} \end{bmatrix} \begin{bmatrix} e_1^1 \\ e_2^1 \\ e_1^2 \\ e_2^2 \\ e_1^3 \\ e_1^4 \end{bmatrix} + \begin{bmatrix} y_{1_d}^{(2)} \\ y_{2_d}^{(2)} \\ y_{3_d}^{(1)} \\ y_{4_d}^{(1)} \end{bmatrix} \tag{5.23}$$

Recall from Chapter 3 that the Input-Output Linearization control law decomposes the original system into $m = 4$ linear decoupled subsystems where the order of each i-th subsystem is given by r_i. This explains why the K matrix has this special decoupled form.

5.1.1 Iterative Scheme

With the control law:

$$u = E^{-1}(x,u)\,[v - L_f^r h_(x)] \tag{5.24}$$

an iterative scheme is useful in finding u and $E^{-1}(x,u)$ simultaneously. To be more explicit about what is actually being achieved, begin by rearranging (5.24) as follows:

$$v = L_f^r h_(x) + E(x,u)\,u \tag{5.25}$$

where $u = [\,\theta_o\ \theta_{ls}\ \theta_{lc}\ \theta_{ot}\,]^T$.

Each of the four rows of the above matrix equation is given by:

$$\begin{aligned} v_i = {} & L_f^r h_(x)_i + E_{i1}(x)\,\theta_o + E_{i2}(x)\,\theta_{ls} + E_{i3}(x)\,\theta_{lc} + E_{i4}(x)\,\theta_o\,\theta_{ls} + E_{i5}(x)\,\theta_o\,\theta_{lc} \\ & + E_{i6}(x)\,\theta_o^2 + E_{i7}(x)\,\theta_{ls}\,\theta_{lc} + E_{i8}(x)\,\theta_{ls}^2 + E_{i9}(x)\,\theta_{lc}^2 + E_{i10}(x)\,\theta_{ot} \end{aligned}$$

Given v_i for $i = 1 \ldots 4$ at each timestep it is necessary to find each component of u. As discussed earlier values of u are assumed from the previous time-step to begin the iterative solution as follows:

$$v_i = L_f^r h_(x)_i +$$

$$[\,E_{i1} + E_{i6}\,\bar{\theta}_o \mid E_{i3}(x) + E_{i5}\,\bar{\theta}_o + E_{i7}\,\bar{\theta}_{ls} + E_{i9}\,\bar{\theta}_{lc} \mid E_{i2}(x) + E_{i4}\,\theta_o + E_{i8}\,\bar{\theta}_{ls} \mid E_{i10}(x)\,]\begin{bmatrix} \theta_o \\ \theta_{lc} \\ \theta_{ls} \\ \theta_{ot} \end{bmatrix}$$

where θ_* is the value of the particular control from the previous time-step.

The entire E matrix is assembled this way and then inverted leading to an iterative solution of (5.24) as the schematic below, Figure 5.2, shows.

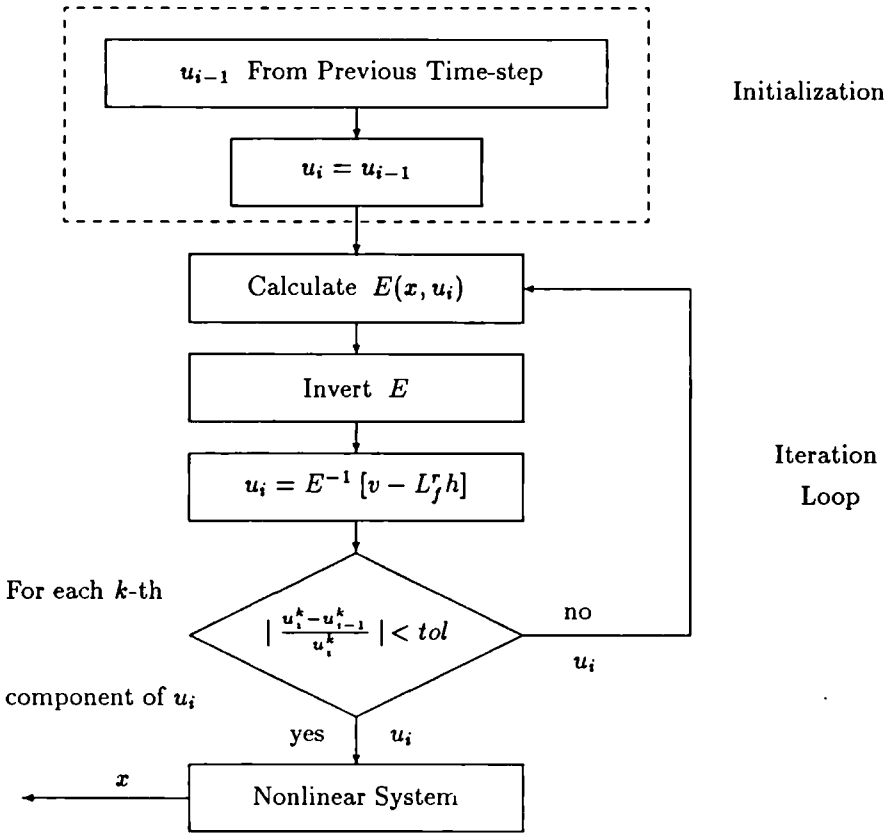

Figure 5.2: Iteration Scheme

At the beginning of each time-step, the value of u is passed from the previous time-step to compute E. The value of u is then updated by computing E^{-1} and applying (5.24). The iteration loop is terminated when the updated input u_i is within some specified tolerance of the previous value u_{i-1}

A controller based on Input-Output Linearization has been designed for a helicopter system. The incorporation of an iterative scheme facilitated the application of the theory to a system that is not linear in the control variable. This controller will next

be used in conjunction with robust techniques to ensure that the final controller's performance does not degrade significantly in the presence of uncertainties. At this point the internal dynamics have not been investigated, however this will be discussed at the end of the chapter since the robust techniques also affect the behaviour of the internal dynamics.

5.1.2 Full State Feedback

The full state feedback used in this study was based on the availability of the following measured variables, Mullen [53]: $\dot{h}$ q p r θ ϕ as well as the normal and lateral accelerations. In addition to the measured variables good estimates of the other states, namely u v w, are required.

5.2 Robust Controller Design

The robust helicopter control system designs are outlined in this section. There are two designs: one derived from the Lyapunov theory of Section 4.2 and the other from the Sliding mode control theory of Section 4.4. Both control laws utilize the Input-Output Linearization decomposition of the nonlinear system as the basis for the design procedure.

5.2.1 Uncertainty Characterization

For the helicopter, the dynamic equations for the iterative scheme are expressed as

$$\dot{x} = f(x) + g_1(x, \bar{\Theta})\,\theta_o + g_2(x, \Theta)\,\theta_{lc} + g_3(x, \bar{\Theta})\,\theta_{ls} + g_4(x, \Theta)\,\theta_{ot} \tag{5.26}$$

or

$$\dot{x} = f(x) + G(x, u)\,u \tag{5.27}$$

Note that $g_i(x)$ for $i = 1 \ldots 4$ are coefficients containing aerodynamic force and moment contributions. Additionally $f(x)$ can be decomposed as follows

$$f(x) = f_{rb}(x) + f_{aer}(x) \tag{5.28}$$

into rigid body and aerodynamic components. Appendix B gives the component parts of the full equations.

Here we assume that $G(x,u)$ and $f_{aer}(x)$ are uncertain with regard only to their norms.

Therefore the system is given by

$$\dot{x} = f_{rb}(x) + f_{aer}(x) + \Delta f_{aer}(x) + G(x,u)\,u + \Delta G(x,u)\,u \tag{5.29}$$

where

$$\Delta f_{aer}(x) = \Psi f_{aer}(x) \tag{5.30}$$

$$\Delta G(x,\bar{u}) = \Psi G(x,\bar{u}) \tag{5.31}$$

As we shall see later Ψ is necessarily upper bounded by 1, i.e. $\Psi < 1$.

To justify this choice of uncertainty representation, comparisons were made with previous work on H_∞ helicopter control, namely that of Yue and Postlethwaite [81]. In order carry out this comparison it is necessary to outline the structure of the perturbed system in Yue and Postlethwaite [81].

Figure 5.3 below shows how the uncertainty, mostly due to deficient modelling of the rotor dynamics, is characterized as an unstructured input multiplicative perturbation.

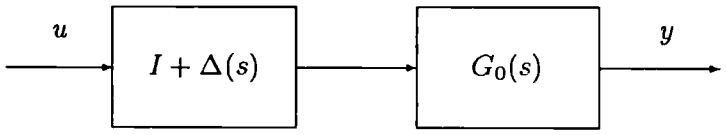

Figure 5.3: Input Multiplicative Uncertainty

where $G_0(s)$ is the transfer function matrix of the nominal system, u is the input vector and y is the output vector. The matrix $\Delta(s)$ represents the unstructured uncertainty.

The actual system is given by $G(s)$ and is defined as follows:

$$G(s) \;=\; G_0(s)\,(\,I + \Delta(s)\,) \tag{5.32}$$

Thus rearranging:

$$G_0(s)\,\Delta(s) \;=\; G(s) - G_0(s) \tag{5.33}$$

Typically a measure of the uncertainty in a system is given by plotting the maximum singular value of $\Delta(j\omega)$, i.e. $\sigma[\Delta(j\omega)]$, against frequency.

For the nonlinear models, i.e. with uncertainty and without, used in this thesis, small perturbation linearization about the trimmed hover position yields a linear systems in state space form. The following transfer functions matrices can be calculated using this state space form:

$G_0(s)$ for the nominal system, i.e. ($\Psi = 0$).

$G(s)$ for the actual system including uncertain terms.

For the system considered here it was possible only to find $G_0(s)$ and $G(s)$, therefore to find $\bar{\sigma}[\Delta(j\omega)]$, it was necessary to express $\bar{\sigma}[\Delta(j\omega)]$ in terms of $G_0(s)$ and $G(s)$. Begin by noting that the Hilbert or the Spectral norm is defined in Maciejowski [48] as:

$$\|\Delta(j\omega)\|_s = \bar{\sigma}[\Delta(j\omega)] \tag{5.34}$$

now observe that

$$\|G_m - G_{m_0}\|_s = \|G_{m_0}\,\Delta_m\|_s \tag{5.35}$$

Using norm inequalities

$$\|G_{m_0}\,\Delta_m\|_s \leq \|G_{m_0}\|_s\,\|\Delta_m\|_s \tag{5.36}$$

So substituting (5.36) into (5.35) gives:

$$\frac{\|G_m - G_{m_0}\|_s}{\|G_{m_0}\|_s} \leq \|\Delta_m\|_s \tag{5.37}$$

Plotting the left hand side of the inequality (5.37) against frequency, (noting that this is actually less than or equal to the uncertainty term), and comparing it to the results of the H_∞ design, gives an indication of the validity of the uncertainty representation.

Figure 5.4 below shows several singular value plots with varying levels of uncertainty determined by the magnitude of Ψ.

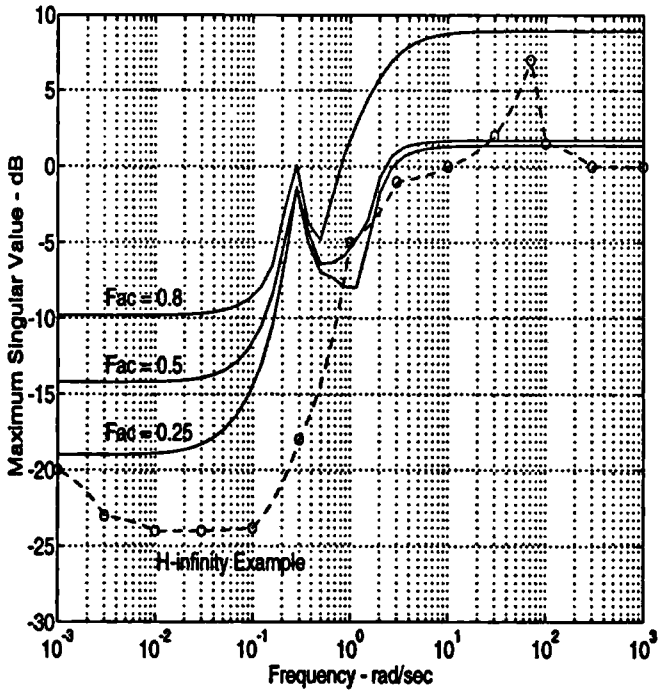

Figure 5.4: Comparison of Uncertainty Levels at hover

It is evident that the uncertainty levels designed for in this thesis is at least comparable if not greater than that of previous robust controller designs. In the designs that follow, a *large* uncertainty factor of $\Psi = 0.8$ was chosen as the level of imprecision in the model. This factor actually represents an 80 % magnitude variation over the nominal aerodynamic contributions to the system.

5.2.2 Robust Controller Using a Lyapunov-Based Design

With the model including uncertainty given by:

$$\dot{x} = f_{rb}(x) + f_{aer}(x) + 0.8\, f_{aer}(x) + G(x, \bar{u})\, u + 0.8\, G(x, \bar{u})\, u \tag{5.38}$$

differentiating the output set, $y = [\,\theta\ \phi\ \dot{\psi}\ \dot{h}\,]$, and noting the particular structure of f_{aer} in Appendix B leads to the following input-output relationship for this model:

$$y^{(r)} = L^r_{f_{rb}} h(x) + L^r_{f_{aer}} h(x) + 0.8\, L^r_{f_{aer}} h(x) + [E(x) + 0.8\, E(x)]\, u \tag{5.39}$$

Since the uncertainty is matched, the vector of relative degree remains the same as the nominal case, {2, 2, 1, 1} and the error dynamics is given by:

$$\{\dot{e}\} = [A]\{e\} + [B]\{L^r_{f_{rb}}h(x)L^r_{f_{aer}}h(x) + E\,u + 0.8\,L^r_{f_{aer}}h(x) + 0.8\,E\,u - y_d^{(r)}\} \quad (5.40)$$

where matrices A and B are

$$A = \begin{bmatrix} 0 & 1 & 0 & 0 & 0 & 0 \\ 0 & 0 & 0 & 0 & 0 & 0 \\ 0 & 0 & 0 & 1 & 0 & 0 \\ 0 & 0 & 0 & 0 & 0 & 0 \\ 0 & 0 & 0 & 0 & 0 & 0 \\ 0 & 0 & 0 & 0 & 0 & 0 \end{bmatrix} \qquad B = \begin{bmatrix} 0 & 0 & 0 & 0 \\ 1 & 0 & 0 & 0 \\ 0 & 0 & 0 & 0 \\ 0 & 1 & 0 & 0 \\ 0 & 0 & 1 & 0 \\ 0 & 0 & 0 & 1 \end{bmatrix}$$

Comparing equation (5.40) with those presented in Chapter 4, indicates that $\Delta E = 0.8\,E$.

Substituting the following control law:

$$u = E^{-1}[-L^r_{f_{rb}}h(x) - L^r_{f_{aer}}h(x) + K\{e\} + y_d^{(r)} + P_{rob}] \quad (5.41)$$

into (5.40) gives:

$$\{\dot{e}\} = [\bar{A}]\{e\} + [B]P_{rob} + [B]\{0.8\,L^r_{f_{aer}}h(x) + \quad (5.42)$$

$$0.8\,[I]\{-L^r_{f_{rb}}h(x) - L^r_{f_{aer}}h(x) + K\{e\} + y_d^{(r)} + P_{rob}\}\} \quad (5.43)$$

where $\bar{A} = A + B\,K$, and K given below is chosen to ensure that the eigenvalues of A lie in the open Left Half Plane.

$$K = \begin{bmatrix} k_{11} & k_{12} & 0 & 0 & 0 & 0 \\ 0 & 0 & k_{21} & k_{22} & 0 & 0 \\ 0 & 0 & 0 & 0 & k_{31} & 0 \\ 0 & 0 & 0 & 0 & 0 & k_{41} \end{bmatrix} \quad \text{for} \quad k_{i,j} \leq 0 \quad (5.44)$$

Since $\Delta E = 0.8E$, then:

$$\Delta E E^{-1} = 0.8\,[I] \qquad \text{and} \qquad \|\,0.8\,[I]\,\|_2 = 0.8$$

Additionally ρ_v is given by:

$$\rho_v = \frac{\|\,0.8\,[I]\{-L^r_{f_{rb}}h(x) - L^r_{f_{aer}}h(x) + K\{e\} + y_d^{(r)}\} + 0.8\,L^r_{f_{aer}}h(x)\,\|_2}{[1 - 0.8]} \quad (5.45)$$

P is the solution to the Lyapunov equation $P\bar{A} + \bar{A}^T P = -Q$.

Since there appears to be no optimal choice for Q when only matched uncertainties are present, it was nevertheless chosen to be $Q = I$, since Chen and Leitmann [12] showed that $Q = I$ maximises a certain mismatch threshold.

Using the above K and Q matrices, P is found to be:

$$\begin{bmatrix} \frac{k_{11}^2+k_{12}^2-K_{11}}{2k_{11}k_{12}} & \frac{-k_{12}}{2k_{11}k_{12}} & 0 & 0 & 0 & 0 \\ \frac{-k_{12}}{2k_{11}k_{12}} & \frac{1-k_{11}}{2k_{11}k_{12}} & 0 & 0 & 0 & 0 \\ 0 & 0 & \frac{k_{21}^2+k_{22}^2-K_{21}}{2k_{21}k_{22}} & \frac{-k_{22}}{2k_{21}k_{22}} & 0 & 0 \\ 0 & 0 & \frac{-k_{22}}{2k_{21}k_{22}} & \frac{1-k_{21}}{2k_{21}k_{22}} & 0 & 0 \\ 0 & 0 & 0 & 0 & \frac{1}{2k_{31}} & 0 \\ 0 & 0 & 0 & 0 & 0 & \frac{1}{2k_{41}} \end{bmatrix} \tag{5.46}$$

By choosing different values of ϵ for each decoupled channel, independent regulation of the robustness to tracking trade-off in each channel is achieved. Hence

$$P_{rob_i} = \begin{cases} -\frac{\mu_i(x)}{|\mu_i(x)|}\rho_v(x) & \text{if} |\mu_i(x)| > \epsilon_i \\ -\frac{\mu_i(x)}{\epsilon_i}\rho_v(x) & \text{if} |\mu_i(x)| \leq \epsilon_i \end{cases} \tag{5.47}$$

where

$$\mu_i(x) = \{B^T P e \rho_v\}_i \tag{5.48}$$

For $i = 1 \ldots 4$.

ϵ can be chosen to provide a trade-off between tracking accuracy and robustness as a result of using the saturation control law.

5.2.3 Robust Controller Based on Sliding Mode Control Theory

For the system with relative degree $\{2, 2, 1, 1\}$, the set of sliding surfaces can be defined as:

$$s = \begin{Bmatrix} s_1 \\ s_2 \\ s_3 \\ s_4 \end{Bmatrix} = \begin{Bmatrix} \dot{e}_1 + \beta_0^1 e_1 \\ \dot{e}_2 + \beta_0^2 e_2 \\ e_3 \\ e_4 \end{Bmatrix} = 0 \tag{5.49}$$

In keeping with the error notation given earlier, note that:

$$\begin{aligned} e_1 &= e_1^1 & \dot{e}_1 &= e_2^1 \\ e_2 &= e_1^2 & \dot{e}_2 &= e_2^2 \end{aligned} \tag{5.50}$$

Now from Chapter 4, the control law is of the following form:

$$u = E^{-1}\left[\, y_d^{(r)} - L_f^r h(x) - e_p - K\, sat(s)\,\right] \tag{5.51}$$

where:

$$e_p = \left\{ \begin{array}{c} \beta_0^1\, \dot{e}_1 = \beta_0^1\, e_1^2 \\ \beta_0^2\, \dot{e}_2 = \beta_0^2\, e_2^2 \\ 0 \\ 0 \end{array} \right\} \tag{5.52}$$

K is then designed as:

$$K = \frac{\eta + \psi_2}{1 - \psi_1} \tag{5.53}$$

where

$$\psi_2 = \| \, 0.8\, L_{f_{aer}}^r h(x) + 0.8\,[I]\,\{-L_{f_{rb}}^r h(x) - L_{f_{aer}}^r h(x) - e_p + y_d^{(r)}\} \, \|_2 \tag{5.54}$$

$$\psi_1 = \| \, 0.8\,[I]\, sgn(-s) \, \|_2 \tag{5.55}$$

η can be varied to change the time taken to reach the switching surface, while the boundary layer thickness for the saturation control ϵ, is selected to provide a good tradeoff between tracking performance and robustness.

5.3 Internal Dynamics

Recall that that the internal dynamics are given by the $\dot{u}$ and the $\dot{v}$ equations. In a theoretical sense these are unstable. Practically however, a helicopter is flown under these conditions because a pilot controls the fore-aft motion by pitch angle demands and the lateral translational motion by bank angle demands. In the context of Input-Output Linearization the pilot may be thought of as an outer loop feedback control that uses the external dynamics to control the internal system behaviour. This is possible because the angular rates evolve much faster than the translational velocities.

Linear studies such as Low et al [47] and Manness et al [49] in which controllers were designed to provide tracking of θ, ϕ, $\dot{h}$, $\dot{\psi}$, have stabilised the modes associated with the longitudinal and the lateral motion. It was found however that the best that could be achieved, without compromising certain controller properties such as decoupling and tracking performance, is placement of the eigenvalues associated with these modes at:

λ_u	λ_v	
-0.002	-0.005	Low et al [47]
-0.006	-0.008	Manness et al [49]

with λ_u for the longitudinal motion mode and λ_v for the lateral motion mode.

For *mathematical completeness* these modes may also be stabilized in the nonlinear case by again using an outer loop feedback control that can be designed as follows. Recall the equations associated with the internal dynamics:

$$\dot{u} = \bar{f}_u(x) + G(x, U^*) - g \sin\theta \tag{5.56}$$

$$\dot{v} = \bar{f}_v(x) + G(x, U^*) + g \sin\phi\cos\theta \tag{5.57}$$

where

$$\bar{f}_u(x) = vr - wq + \frac{X_f(\mathbf{x})}{m} + \frac{X_{r_0}(\mathbf{x})}{m}$$

$$\bar{f}_v(x) = wp - ur + \frac{Y_f(\mathbf{x})}{m} + \frac{Y_{fn}(\mathbf{x})}{m} + \frac{Y_{r_0}(\mathbf{x})}{m} + \frac{Y_{t_0}(\mathbf{x})}{m}$$

$$U^* = \text{Inner Loop Robust Control Law Design}$$

The actual design will assume that the equations take the following form:

$$\dot{u} = -g \sin\theta \tag{5.58}$$

$$\dot{v} = g \sin\phi\cos\theta \tag{5.59}$$

This assumption is valid since the most significant terms in these equations are $-g \sin\theta$ and $g \sin\phi\cos\theta$. The objective is to stabilize these dynamic equations using θ and ϕ as controls. To follow the Input-Output Linearization approach, the output are selected as as $y_1 = u$ and $y_2 = v$. These are differentiated repeatedly until the inputs appear to yield the following input-output relationship:

$$\dot{y}_1 = -g \sin\theta \tag{5.60}$$

$$\dot{y}_2 = g \sin\phi\cos\theta \tag{5.61}$$

This suggests a control law of the form:

$$\theta = \arcsin\left(\frac{-V_1}{g}\right)$$

$$\phi = \arcsin\left(\frac{V_2}{g\cos\theta}\right) \tag{5.62}$$

where

$$V_1 = -0.005\,u \tag{5.63}$$

$$V_2 = -0.008\,v \tag{5.64}$$

The following block diagram, Figure 5.5, shows how this could be done.

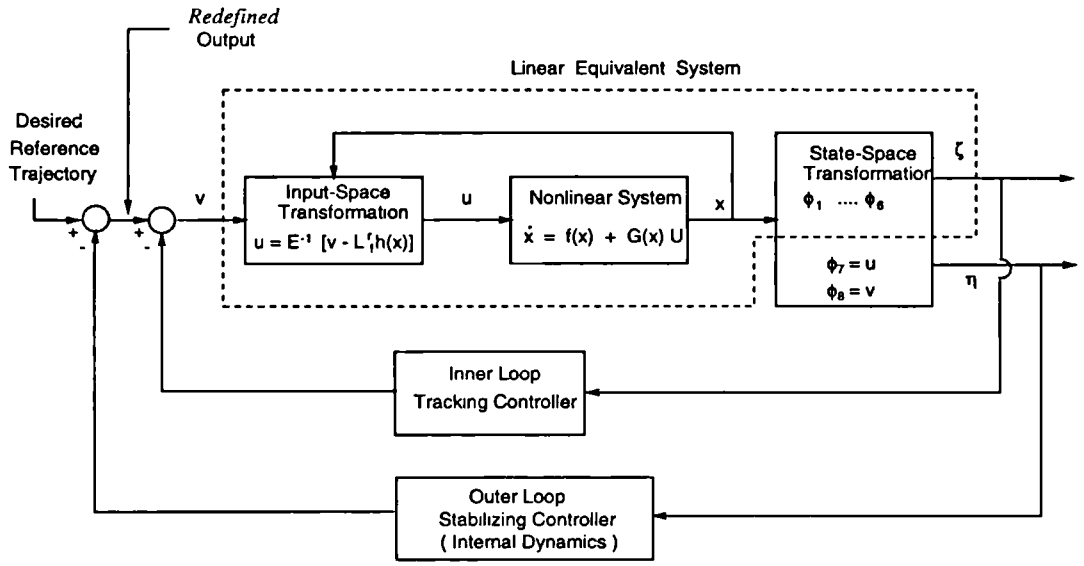

Figure 5.5: Internal Dynamics Outer Loop Stabilizing Feedback

If the effects of the neglected dynamics are felt to be of significance then the Feedback Linearization control law may be augmented by the Sliding mode or the Lyapunov techniques.

The outer loop design outlined above is somewhat similar to the more formal approach of Gopalswamy and Hedrick [23] in which the *output redefinition* approach is used to ensure that the internal dynamics are stable. Essentially their approach is to find analytically a new output such that tracking of it leads to approximate tracking of the actual desired output while at the same time ensuring that the internal dynamics are bounded.

The approach of Figure 5.5 *redefines* the output on-line and leads to a tradeoff between boundedness of the internal dynamics and decoupled tracking performance

of the external dynamics. The magnitude of the outer loop gains must therefore be restricted if good decoupled performance of the external dynamics is to be maintained. This restrictive condition is also recognised by Gopalswamy and Hedrick and shows further similarity in the methods.

Chapter 6

Discussion of Results

This chapter commences with a brief outline of the simulation model and describes the simulink block diagram constructed for this work. This is followed by time responses obtained due to step demands in each of the four decoupled axes. Results are presented for the helicopter model excluding uncertainty controlled by a standard Input-Output Linearization control law. These responses are then compared to those obtained when uncertainty is introduced into the model. Following this the robust control laws, i.e. the Lyapunov-based and the Sliding mode control laws are tested on the uncertain system to demonstrate the improvement in performance achieved when such techniques are used to augment the basic Input-Output Linearization control. In addition, an assessment of the closed loop system response is made with regard to the Handling Qualities Requirements of ADS 33-C. This is followed by other manœuvres such as a *bob-up* manœuvre to further illustrate the versatility of the designs. This chapter is concluded by examining the determinant of the decoupling matrix through simulation since analytical conclusions regarding the continuous invertability of the decoupling matrix have at present proved difficult make.

6.1 Model

The nonlinear helicopter model described in Padfield [55], was implemented in Matlab's Simulink. To reduce the workload involved in creating the entire model from the graphical Simulink blocks and for increased speed of execution, the equations of motion were programmed in the *C* Language and accessed in Simulink via *C-Mex* files. Figure 6.1, overleaf, shows the Simulink diagram for the entire system.

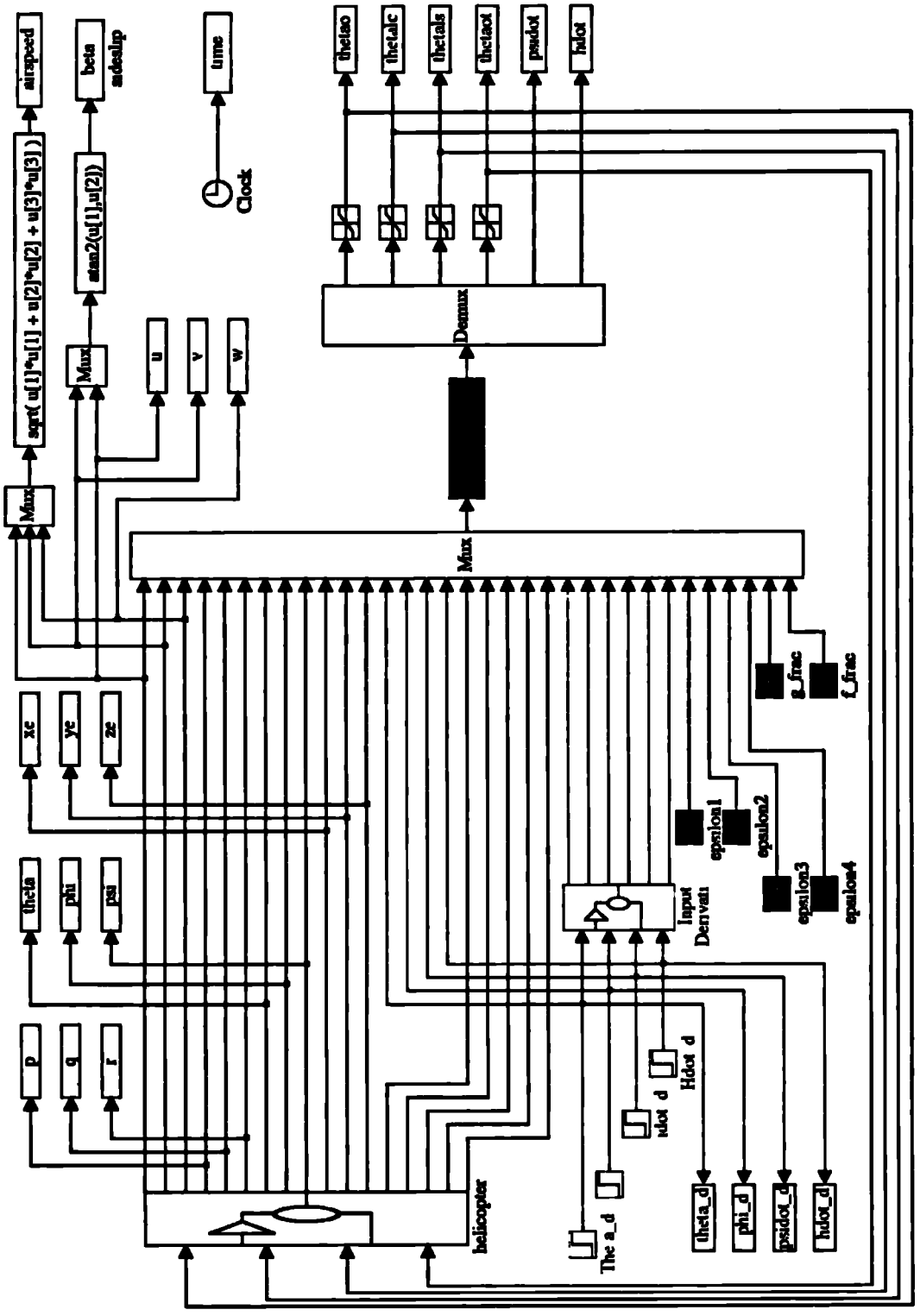

Figure 6.1: Closed Loop Simulink Block Diagram

Note the presence of the actuator authority limits on the main rotor collective and cyclic commands and the tail collective command. The following typical limits given in Smith [71] are used in the model:

Main rotor collective	θ_o	-5	to	$+20.3$	degrees
Longitudinal cyclic	θ_{ls}	-15.7	to	$+7.5$	degrees
Lateral cyclic	θ_{lc}	-7.5	to	$+7.5$	degrees
Tail rotor collective	θ_{ot}	-8.5	to	$+33.5$	degrees

The signals computed by the *controller* first pass through the actuator authority limiting blocks before entering the *helicopter* model. This model contains the dynamic equations and calculates the helicopter state which is fed to the controller. As well as the state, step (or other user defined) demands along with their time derivatives, of the order specified in Chapter 5, enter the flight control system block for the computation of the demand tracking control law.

In Figure 6.1 the reference signals have the following correspondence:

Theta_d	$\rightarrow$	Demand in pitch angle	θ
Phi_d	$\rightarrow$	Demand in roll angle	ϕ
Psidot_d	$\rightarrow$	Demand in heading rate	$\dot{\psi}$
Hdot_d	$\rightarrow$	Demand in altitude rate	$\dot{h}$

In addition to the above inputs to the controller, the tuning parameters from Chapter 5, associated with the use of a boundary layer to smooth the discontinuous control law, are given by:

epsilon1	$\rightarrow$	ϵ_1
epsilon2	$\rightarrow$	ϵ_2
epsilon3	$\rightarrow$	ϵ_3
epsilon4	$\rightarrow$	ϵ_4

The outputs sideslip and airspeed are calculated by:

$$\begin{aligned} \text{Sideslip} &= \arctan \frac{v}{u} \\ \text{Airspeed} &= \sqrt{u^2 + v^2 + w^2} \end{aligned}$$

Finally the model data used for the simulations is found in Padfield [55].

Most of the cases presented here represent aggressive manœuvring, in that large amplitude step inputs are demanded. These inputs often result in sizeable actuator displacements in order to satisfy the ferocity and amplitude of these demands. In real actuators only finite displacement is possible and therefore it was felt that the inclusion of these authority limits is necessary to provide a realistic view of how the system will perform under these conditions. It will become clear later that it is precisely this limiting of the actuator authority that causes much of the transient coupling that is observed.

6.2 Simulation Results

The computer simulation results presented in this section reveal the performance achievable by using the nonlinear control laws described in Chapters 3 and 4. The actuator authority limits are present in all cases unless otherwise stated. When uncertainty is introduced into the helicopter model as described in Chapter 5, a factor of $\Psi = 0.8$ is assumed. Recall from Chapter 5 that this represents a large uncertainty since, by virtue of the uncertain system theory applied to the factor case, Ψ_{max} must be less than 1. The first set of time domain simulation results serves to illustrate the tracking and decoupling properties of the control laws. To do this the following step demands are made:

- ± 30 degrees pitch angle
- ± 60 degrees/sec heading rate
- ± 40 degrees bank angle
- ± 30 ft/sec altitude rate

The pitch angle and heading rate demands represent the minimum requirement for Level 1 *aggressive large amplitude* manœuvring. The importance of this Level 1 requirement is discussed later. The bank angle demand is less than the ± 60 degrees minimum required for the above manœuvres. This was chosen however because for demands in excess of about ± 50 degrees actuator saturation occurs about one second after achieving the desired demand. This saturation causes the subsequent response to become unrepresentative of the real situation since in practice an additional trimming

control would be used to null the cockpit controller forces, i.e. the pilot input, at any achievable steady state attitude. Finally with the helicopter model data representative of a Lynx helicopter, the altitude rate level was chosen to be in line with the maximum vertical rate of climb of 25 ft/sec that is achievable by the Royal Navy Lynx helicopters [41].

In all the figures that follow, which begin on page 115, the results are presented in a uniform manner to facilitate ease of reading. Each figure consists of twelve sub-figures, presented in four rows. The first row shows the longitudinal axis responses given by pitch angle θ and pitch rate q also shown in this row is the control associated with this axis, i.e. the longitudinal cyclic θ_{ls}. The next row shows the lateral axis responses given by bank angle ϕ and roll rate p along with the control associated with this axis, i.e. the lateral cyclic θ_{lc}. The third row shows the yaw axis responses given by heading rate $\dot{\psi}$ and yaw rate r along with the control associated with this axis, i.e. the tail rotor collective θ_{ot}. The final row shows the normal axis response given by altitude rate $\dot{h}$ along with the control associated with this axis, i.e. the collective θ_o. The airspeed V_T is also shown in this final row for convenience. Note that the first sub-figure of each row represents a decoupled output that is intended to follow an appropriate tracking demand.

The first four figures show the basic Input-Output Linearization control law applied to a nominal system and also to a system containing uncertain terms. Note the following line styles that have been maintained in these four figures:

Nominal System	Positive Demand	→	Dot Dashed Line	· – · – ·
Nominal System	Negative Demand	→	Dotted Line	· · · · · ·
Uncertain System	Positive Demand	→	Solid Line	————
Uncertain System	Negative Demand	→	Dashed Line	– – – –

The other figures showing the Lyapunov based control and the Sliding mode control laws applied to the uncertain system, follow the convention below:

Positive Demand	→	Solid Line	————
Negative Demand	→	Dot Dashed Line	· – · – ·

6.2.1 Input-Output Linearization Control Law

Figures 6.2 to 6.5 show a comparison between the nominal Input-Output Linearization tracking control law applied to the nominal system and the same nominal control law applied to the uncertain system. First considering Figure 6.2 where the nominal control law controls the nominal system, a positive step demand in pitch angle (the dash-dot line) is achieved in about 1.75 seconds. The other axes corresponding to roll angle, heading rate and altitude rate produce very small amplitude transient responses and are therefore well decoupled. The maximum value of the longitudinal cyclic actuator θ_{ls}, that is the authority limit placed on that actuator, is reached at the beginning of the manœuvre due to the substantial power required for such a large amplitude step input. This causes an unobtrusive delay to the pitch angle, θ, in reaching its steady state value which is physically expected. The responses to a corresponding negative step demand (the dotted lines) are similarly decoupled. Under these circumstances however the pitch angle demand is achieved in less time, about 1.2 seconds. This is a direct consequence of greater actuator displacement allowable for negative travel as indicated by negative limit of 15.25 degrees of travel compared to the positive limit of 7.5 degrees of travel.

The inclusion of uncertainty into the helicopter model causes the nominal control law's performance to degrade noticeably. Even though pitch angle continues to track the demand very well, small coupling in the roll and yaw axis arise while rather larger excursions in altitude rate occur. To explain these observations it is necessary to return to the equations of motion.

$$\dot{x} = f_r(x) + f_{aer}(x) + G(x\,u) \qquad \text{Nominal System} \qquad (6.1)$$

$$\dot{\tilde{x}} = f_r(\tilde{x}) + (1+\Psi)\, f_{aer}(\tilde{x}) + (1+\Psi)\, G(\tilde{x}\,u) \qquad \text{Uncertain System} \qquad (6.2)$$

where $\Psi = 0.8$.

From these equations it is apparent that for some value of the control variable u the state derivative in the uncertain system $\dot{\tilde{x}}$ is greater than that of the nominal system $\dot{x}$ due to the presence of the uncertainty factor $\Psi = 0.8$. Roughly speaking, for tracking systems this implies that $\tilde{x}$ reaches its desired value following a step demand in less time than it would take x for an identical demand. This mechanism is clearly visible for the pitch angle response where θ achieves the input demand θ_d for the system with uncertainty faster than in the case of the nominal system. This further means that the

actuator signal θ_{ls}, in the uncertainty case, decreases quicker than in the nominal case since the system achieves a steady state in less time.

The large excursion in altitude rate is also attributable to the uncertainty factor. Recall that the vertical rate equation is given by:

$$\dot{h} = u\sin\theta - v\sin\phi\cos\theta - w\cos\phi\cos\theta \tag{6.3}$$

For this manœuvre the $-v\sin\phi\cos\theta$ component in $\dot{h}$ is small since ϕ is small. The term $u\sin\theta$ is small at the beginning of the manœuvre while θ is small and u which depends on the evolution of θ is also small. Therefore the main component in equation (6.3) is $-w\cos\phi\cos\theta$ with w given by:

$$\dot{w} = uq - vp + g\cos\theta\cos\phi + \Psi f_{aer}(x) + \Psi G(x,u) \tag{6.4}$$

Without uncertainty, i.e $\Psi = 0$, the nominal control law produces w such as to counteract the small effects in (6.3) thus ensuring that $\dot{h}$ remains at zero. With the uncertainty factor however, w changes faster under the nominal control law than the small effects in equation (6.3) thus causing $\dot{h}$ to drift away from zero. As the altitude rate drifts, the collective pitch θ_o decreases in order to reduce the main rotor lift and ultimately retard the altitude rate development. The decrease in collective causes a corresponding decrease in the torque generated by the main rotor, therefore the yaw compensation provided by the tail rotor collective for the reduced torque is itself reduced to ensure that heading remains virtually unchanged.

Figure 6.3 depicts the responses to positive and negative 40 degree bank angle demands. Similar comments apply here with regard to nominal performance. For the uncertainty model tracking of the demand is still good under the nominal control law. Small coupling exists in all axes except the normal axes, where excursions are quite large and similar to that observed in Figure 6.2. The positive and negative demands produce symmetrical responses in this case because the actuator responsible for effecting changes in the roll axis, θ_{lc}, allows equal travel in both the negative and positive directions and because its dynamics effect is symmetrical.

The response to heading rate demands in Figure 6.4 shows that decoupling in the other axes is quite good despite the uncertainty, however as expected the normal axis coupling is still present. In addition, as mentioned earlier, the increase in tracking

speed due to the uncertainty factor is now quite visible. One anomaly that exists however is the drift in airspeed even when uncertainty is not present, that is when the nominal control law is applied to the nominal system. This is due to the very low damping of the modes associated with forward velocity u and lateral velocity v. With the dependence of these modes to variations in the body attitudes θ and ϕ, small perturbations introduced into these variables cause the observed drift in the airspeed. This deviation would normally be alleviated by the use of an additional trimming controller which ensures that under steady conditions the helicopter can be trimmed to achieve a state of equilibrium.

Apart from the, by now, anticipated responses to the ± 30 ft/sec demands in altitude rate of Figure 6.5, some interesting details arise as a result of the -30 ft/sec command. Consider the nominal system with nominal control (the dotted line). As the demand is made the collective pitch θ_o is reduced to bring about a decrease in lift thus enabling the helicopter to translate downwards. For this demand the θ_o actuator saturates which causes a delay in $\dot{h}$ achieving its demanded value. The tail rotor collective θ_{ot} also changes to provide a level of yaw compensation corresponding to the new torque developed as a result of the change in collective. However the θ_{ot} actuator also saturates and therefore provides insufficient compensation for this new torque, consequently a drift in $\dot{\psi}$ arises. This digression is rapidly eliminated during the first 0.5 seconds by further reduction in θ_{ot}.

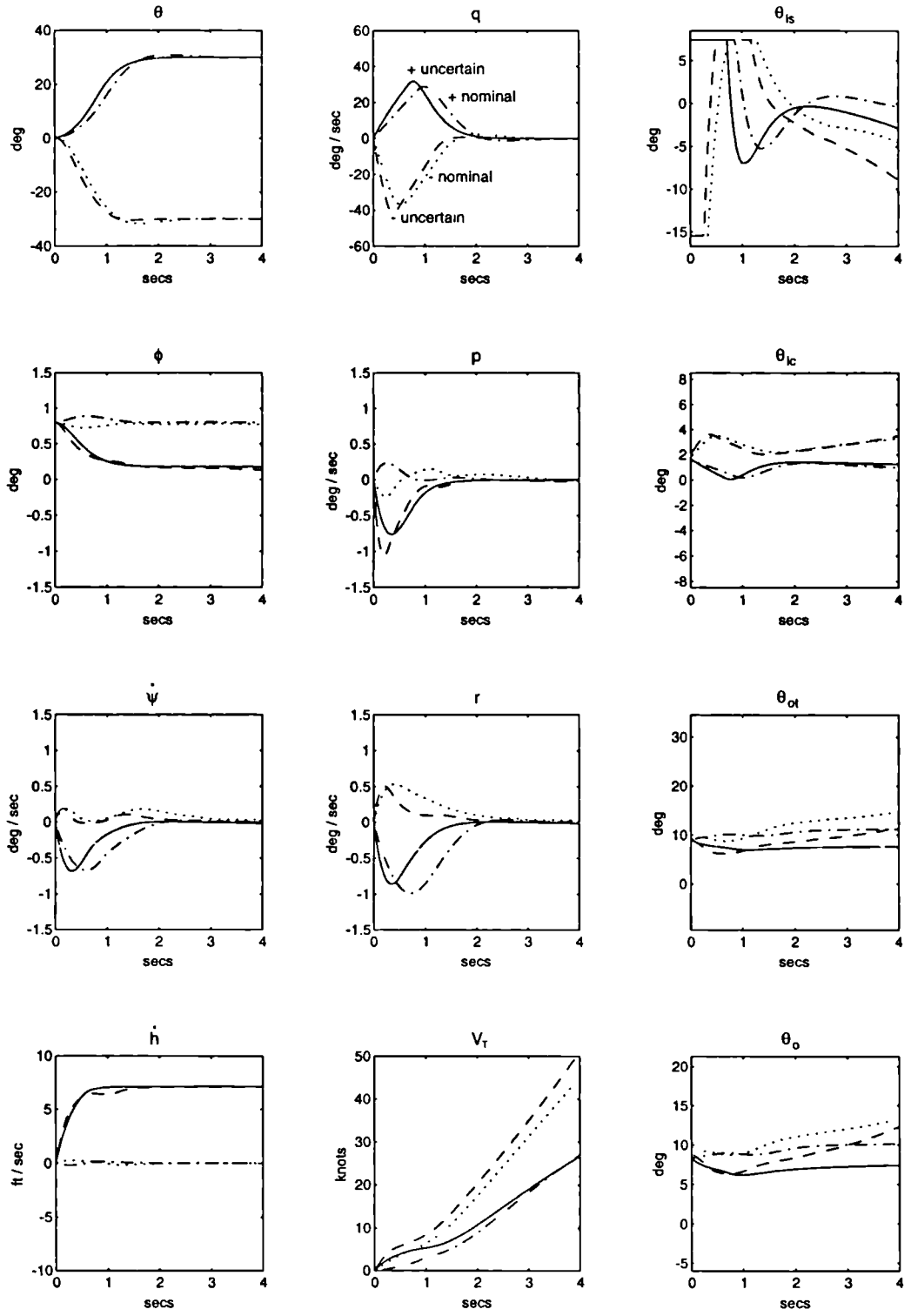

Figure 6.2: Nominal Controller: ±30 degrees Demand in Pitch Angle

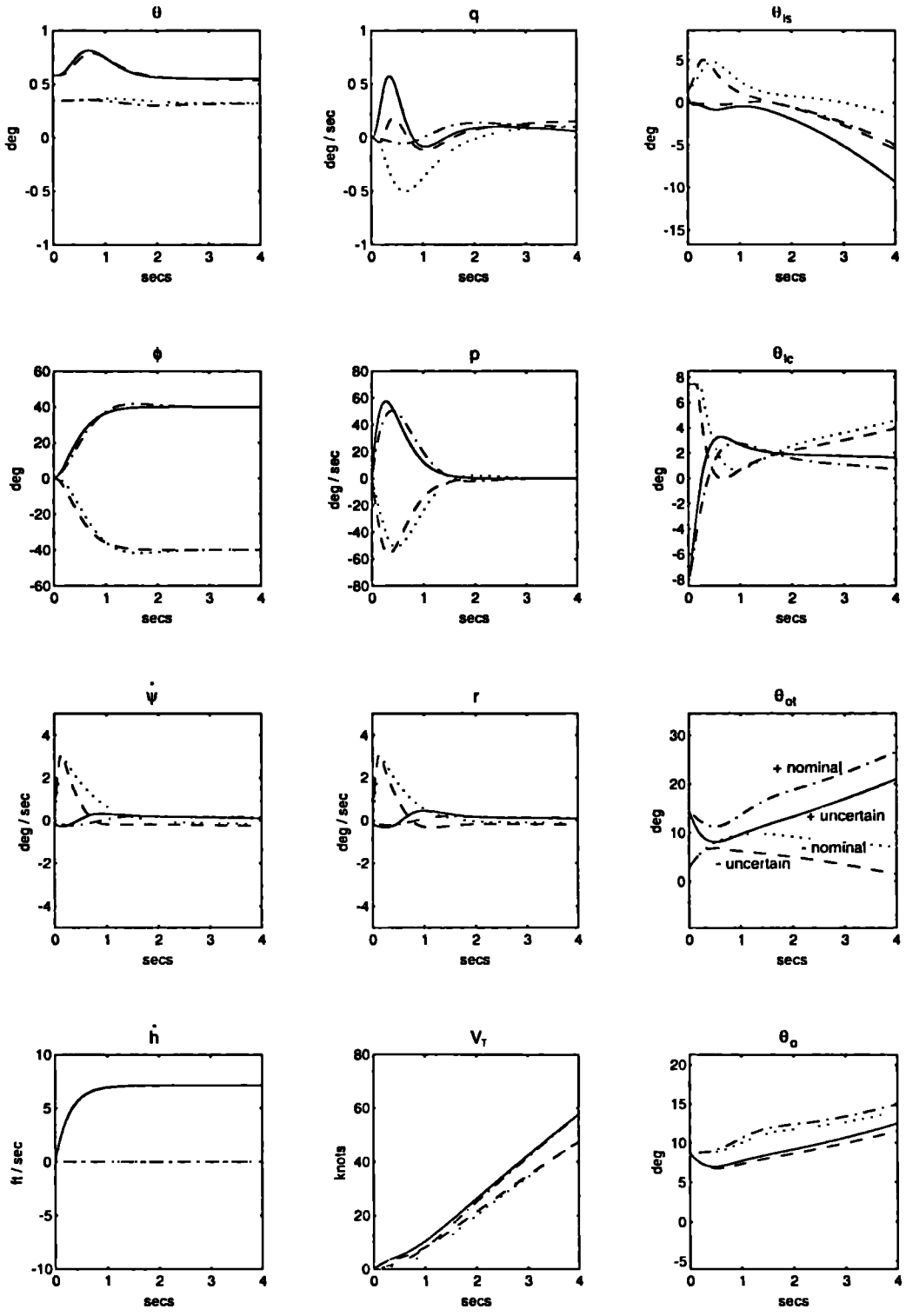

Figure 6.3: Nominal Controller: ±40 degrees Demand in Bank Angle

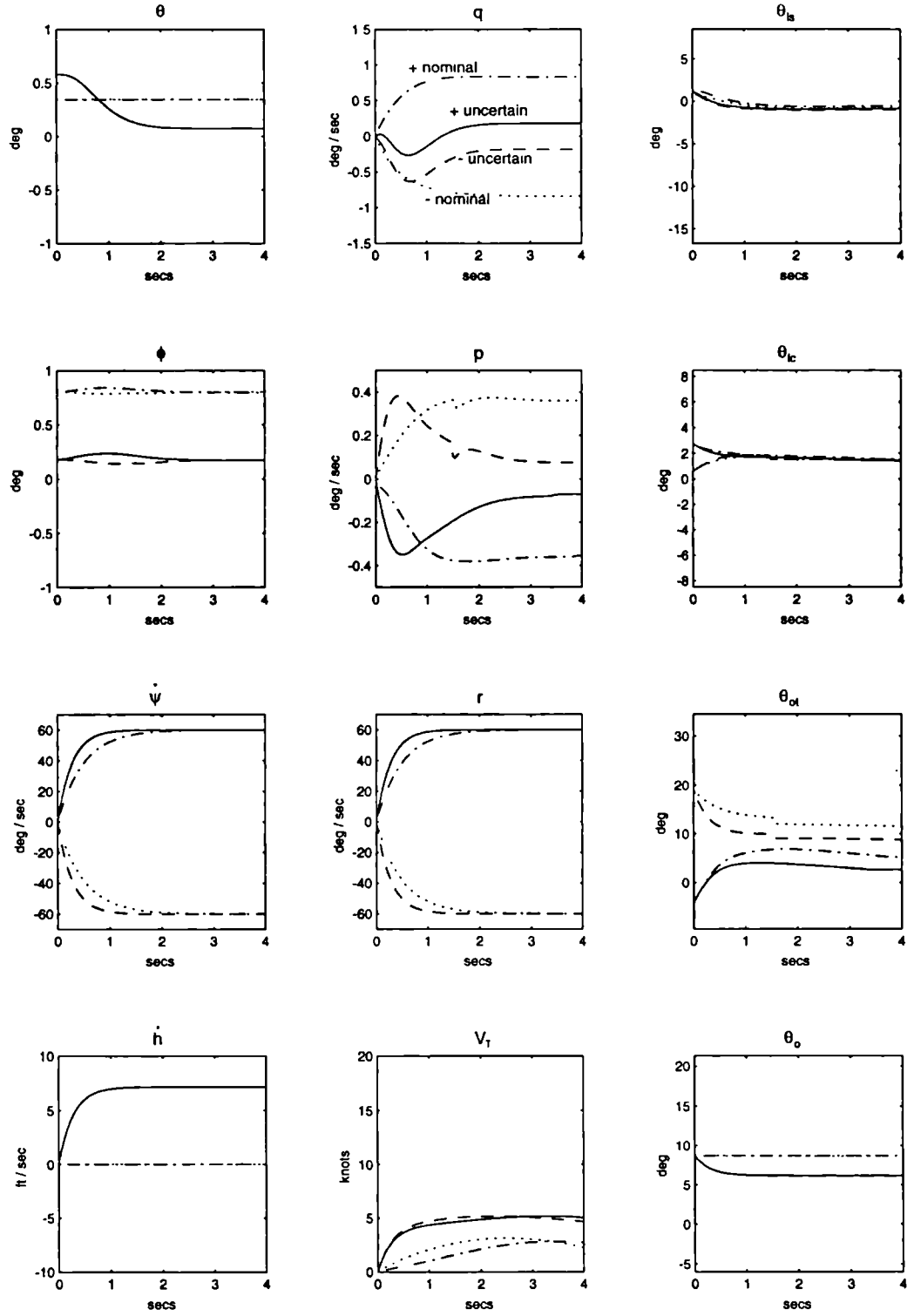

Figure 6.4: Nominal Controller: ±60 degrees/sec Demand in Heading Rate

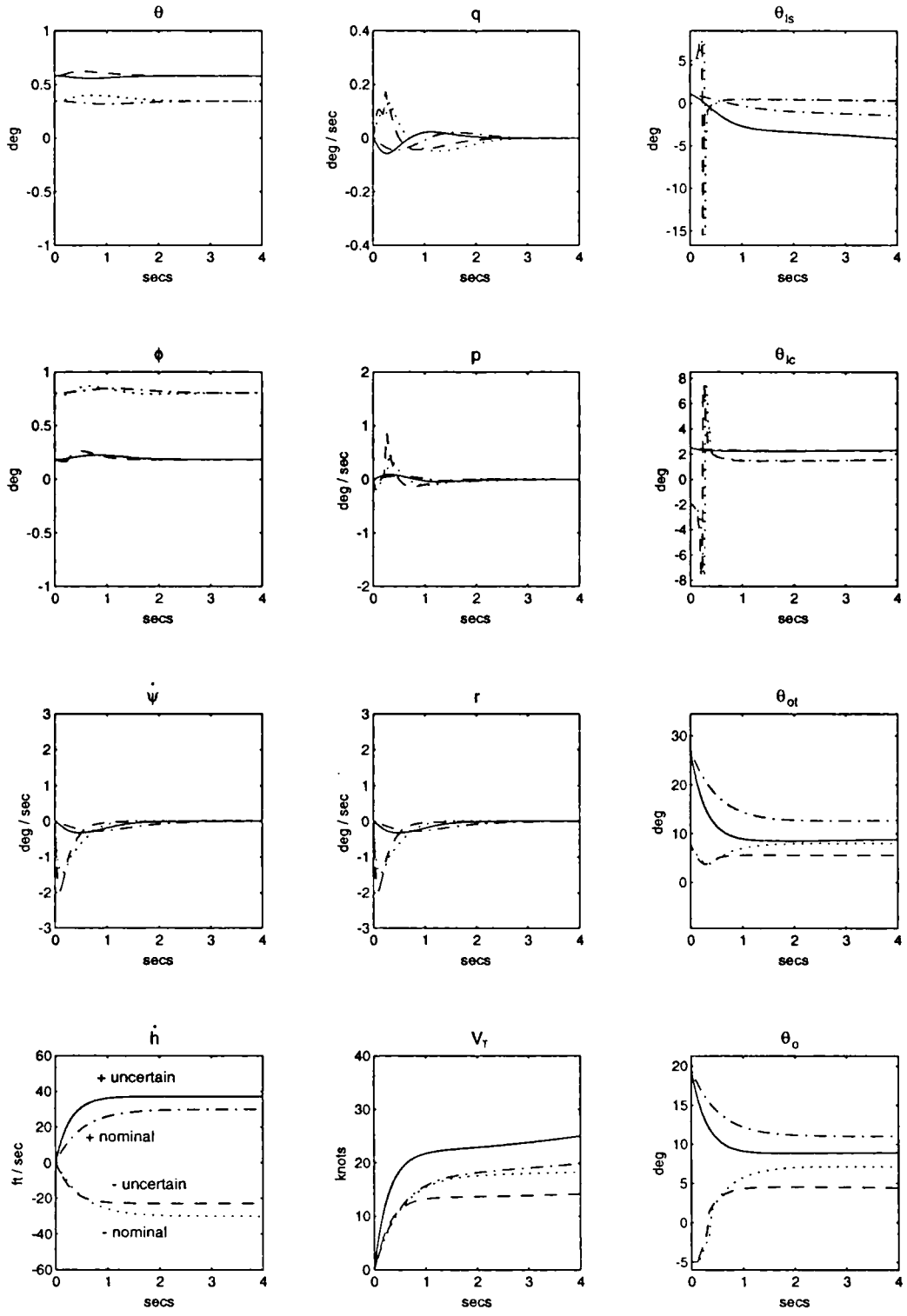

Figure 6.5: Nominal Controller: ±30 ft/sec Demand in Altitude Rate

6.2.2 Robust Control Laws

In this section comparisons of the performance of the nominal control law are made against that of the Sliding mode and the Lyapunov control laws. The eight manœuvres considered are the same as those illustrated in Figures 6.2 to 6.5. The figures begin on page 121.

Sliding Mode Control Law

For the system with uncertainty, the responses to pitch angle demands using the Sliding mode control law are given in Figure 6.6. The speed of response is still very good, greater control power is now needed to overcome the effects of uncertainties and this is clearly visible by the extended length of time that the θ_{ls} actuator remains at its limiting values. The most noticeable difference between the achievements of the nominal control law and this robust control law is the almost complete decoupling that is now possible in all the axes. The normal axes shows the most significant recovery with the steady state altitude rate reduced down to about 0.07 ft/sec compared to the level of 7 ft/sec when the only nominal control law was is use. This remaining level of coupling is small enough to be virtually ignored.

The bank angle responses in Figure 6.7 also illustrate the virtue of using the robust Sliding mode control law. However the effects of positive heading demands in Figure 6.8 are not quite as tidy as the last two cases. This is due to the presence of certain coupled transients in the pitch and roll axes which arise as a consequence of actuator saturation. The roll induced by yaw changes is not adequately countered because the lateral cyclic actuator θ_{lc} saturates at the beginning of the response. The presence of roll deviations itself induces pitching which again is not fully eliminated due to the saturation of the longitudinal cyclic θ_{ls}. Now by the time pitching develops the rolling motion begins to subside as θ_{lc} is no longer limited, this causes the effects of the roll induced pitching to be smaller. Since all the above coupling is transient and decays to zero in about 0.5 seconds these effects are not problematic. Note that in contrast almost no transients develop in response to a negative heading rate demand since the actuators only saturate momentarily.

To further illustrate the point Figure 6.9 shows the response of the helicopter with

Sliding mode control law to positive heading rate demands. Two cases are shown, one in which the actuator authority limits are present (the dash-dot line) and the second case where no limits are imposed (the solid line). With no limits specified no transients appear in either the pitch angle or the bank angle responses. In addition the desired heading rate is achieved almost instantaneously. However this ideal response is achieved because of the large actuator demands that occur almost instantaneously at the beginning of the manœuvre. The numbers on the scales of the actuator responses are indicative of these large maximum and minimum actuator demands. A small coupling still exists in altitude rate but this is due the smoothing of the control discontinuity in a thin boundary layer of thickness ϵ. Chapters 4 and 5, provide more details of this method which is required to eliminate the chattering associated with discontinuous control. The penalty incurred with this approach is that only ultimate boundedness as opposed to asymptotic tracking is achievable and this of course causes the persistence of a steady state error in $\dot{h}$.

Responses to the ± 30 ft/sec altitude rate demands are shown in Figure 6.10. Here all four actuators are saturated at the beginning of the response. Limiting the control power available to the collective θ_o causes a sluggish response in altitude rate. Transient excursions in θ, ϕ and $\dot{\psi}$ are noticeable due to the associated actuators saturating. As the collective θ_o changes in response to the step demand in altitude rate, the main rotor torque is then altered and must be compensated for by a change in yaw. This yaw compensation is not fully achieved because θ_{ot} is constrained thus inducing a certain amount of sideslip which is coupled to rolling motion. This rolling motion is itself not fully countered due to the saturation of the lateral cyclic θ_{lc}, this then causes the roll to pitch coupling to manifest itself under the momentary loss of full decoupling control. Fortunately all the coupling occurs in a very short period of time and is unlikely to cause the pilot difficulty.

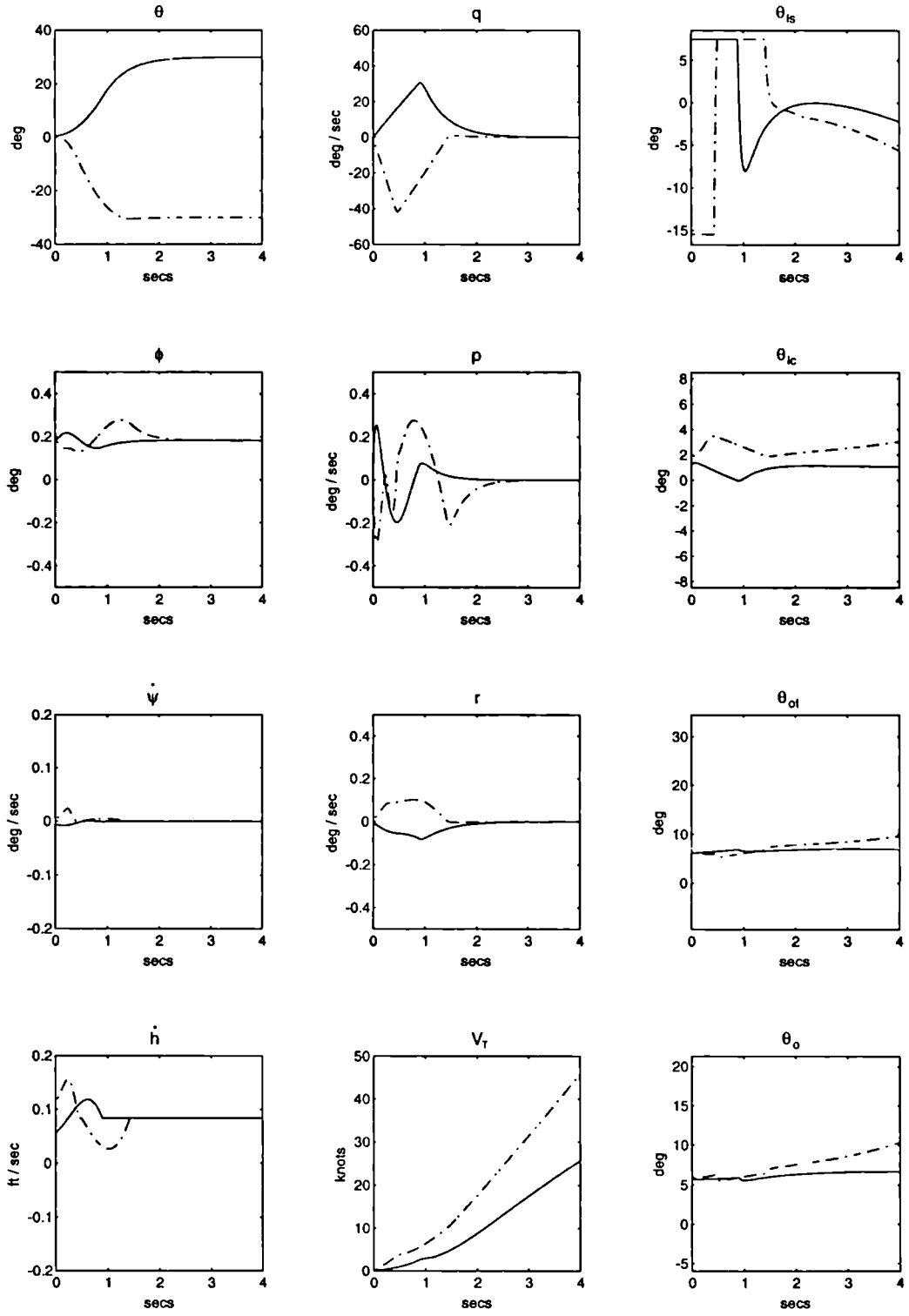

Figure 6.6: Sliding Mode Controller: ±30 degrees Demand in Pitch Angle

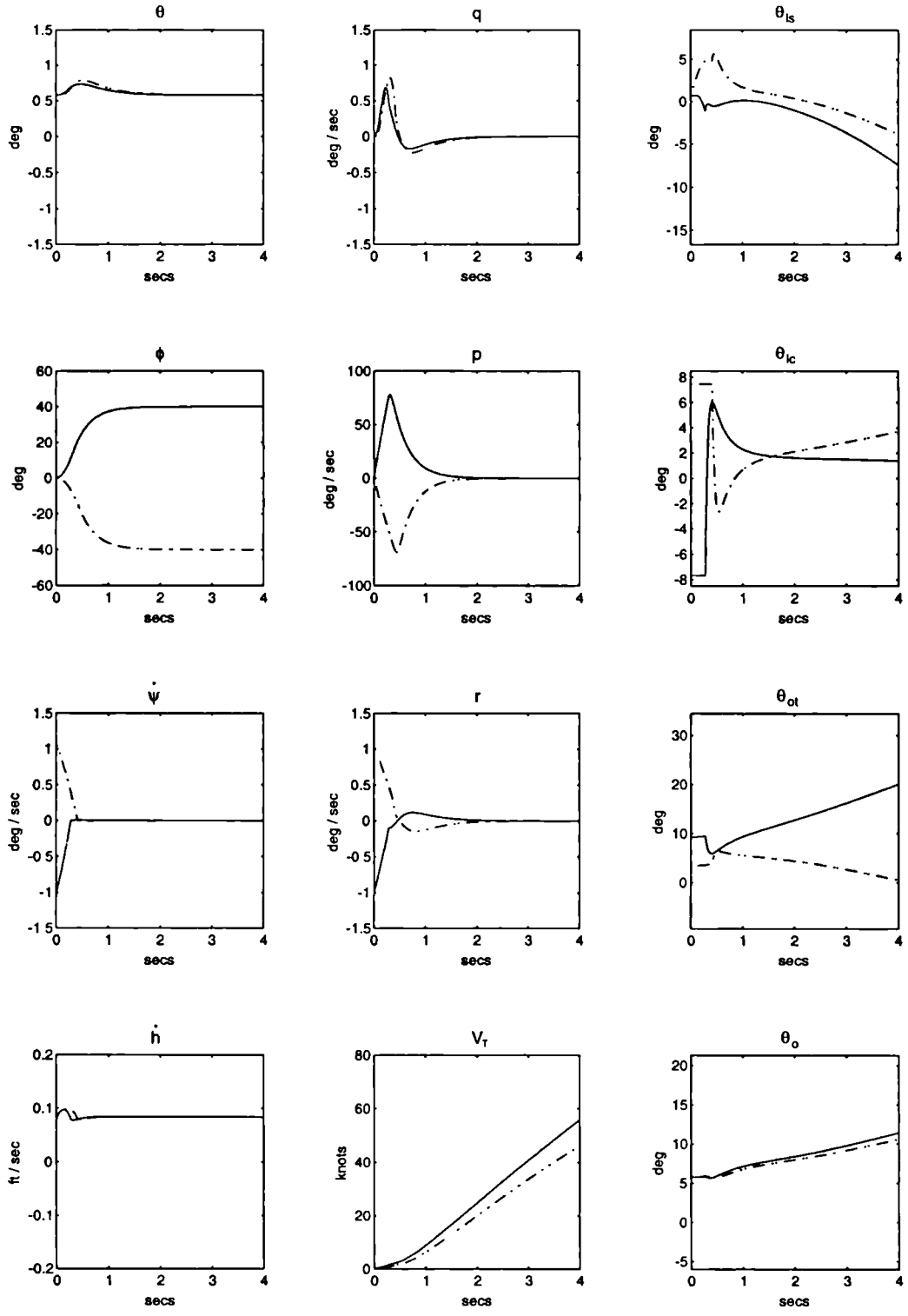

Figure 6.7: Sliding Mode Controller: ±40 degrees Demand in Bank Angle

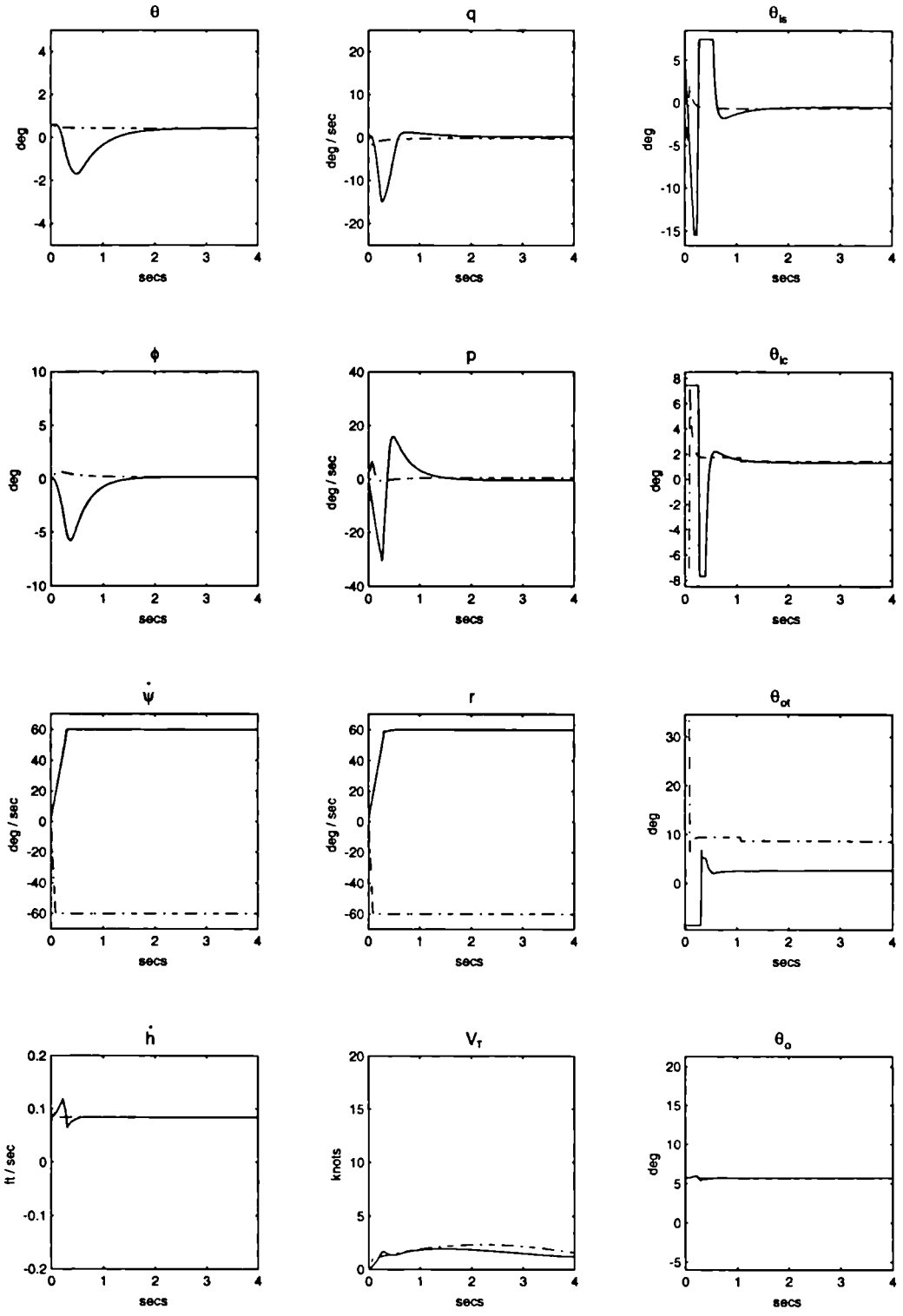

Figure 6.8: Sliding Mode Controller: ±60 degrees/sec Demand in Heading Rate

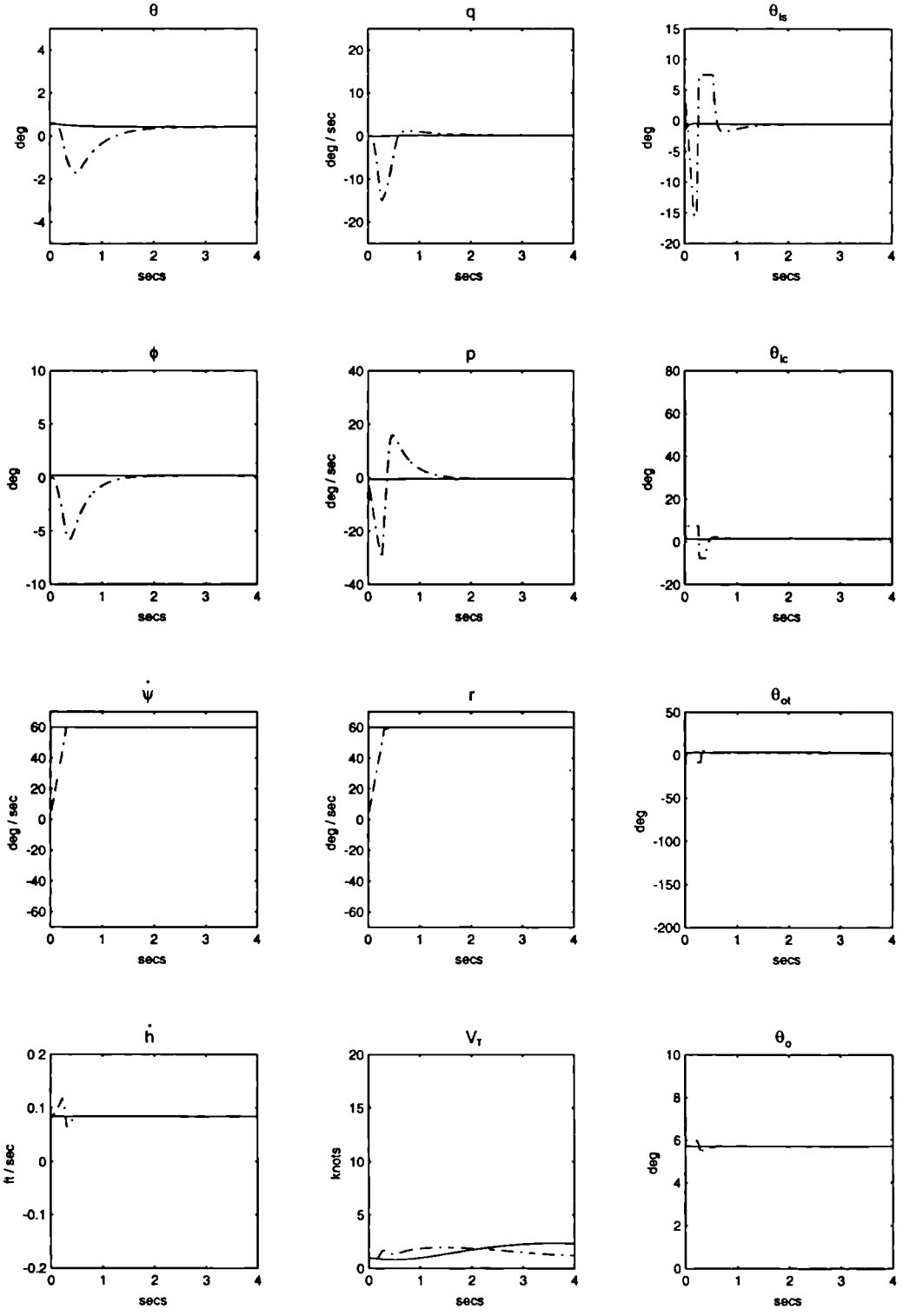

Figure 6.9: Sliding Mode Controller: ±60 degrees/sec Demand in Heading Rate

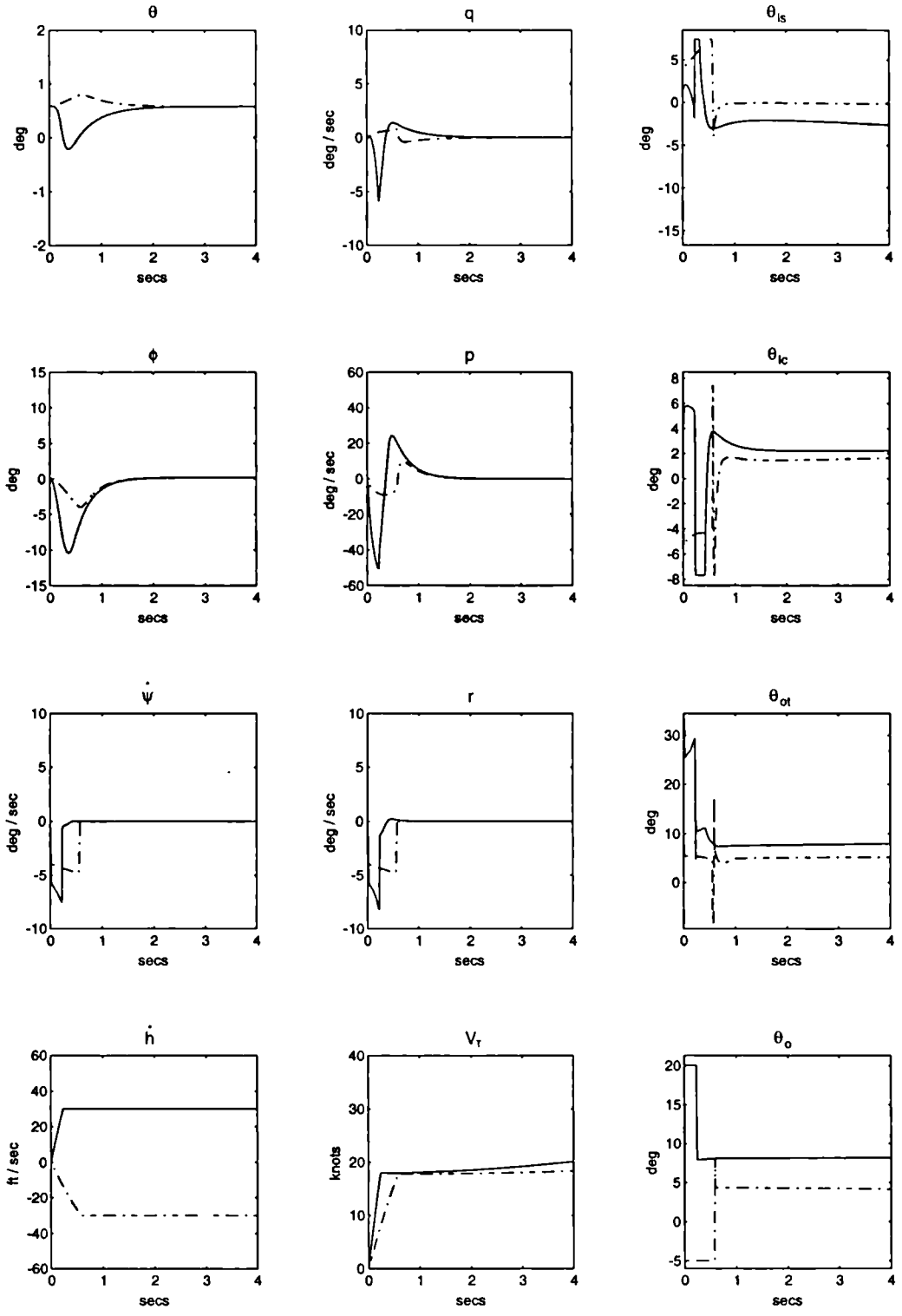

Figure 6.10: Sliding Mode Controller: ±30 ft/sec Demand in Altitude Rate

Lyapunov Based Control Law

Figures 6.11 to 6.14 show the performance of the Lyapunov control law to the same manœuvres executed in Figures 6.6 to 6.10 using the Sliding mode controller. In all cases very little difference exits between the responses produced using one robust control law rather than the other. However in all cases the transient coupling is reduced when the Lyapunov control law is applied. No conclusion regarding the superiority of one law over the other can be drawn since these small discrepancies are most certainly attributable to the differences in the tuning of parameters of each control law to provide a reasonable trade-off between tracking accuracy and robustness.

A final illustration of the performance of the robust control laws over the nominal control law is given in Figure 6.15 which shows the errors in pitch angle, roll angle, heading rate and altitude rate over four seconds following a +40 degrees demand in roll angle. As expected the nominal controller used with the nominal system provides decoupled responses. Coupling appears as uncertainty is introduced into the system and the nominal control provides insufficient compensation under these circumstances. The Sliding mode control law however eradicates most of this coupling reducing these effects to small transients that decay very quickly and at most takes about 2 seconds. These results are further improved using the Lyapunov control law where even the coupled transients are almost eliminated. It should be stressed again that the better performance achieved by the Lyapunov controller is related to the best selection of the tuning parameters that has been achieved to date.

Before concluding this section it should be noted that the step inputs applied to the system in producing the time responses shown, all followed the classical definition of a step, that is, an instantaneous change from one magnitude to another. However as pointed out in ADS 33-C [1], the step may be defined as a rapid change from one constant value to another with the input being made as rapidly as possible without exciting undesirable structural or rotor modes or approaching any aircraft safety limits, i.e. a ramp. This represents a less hostile input than that considered here and should certainly lead to even less coupled transient responses.

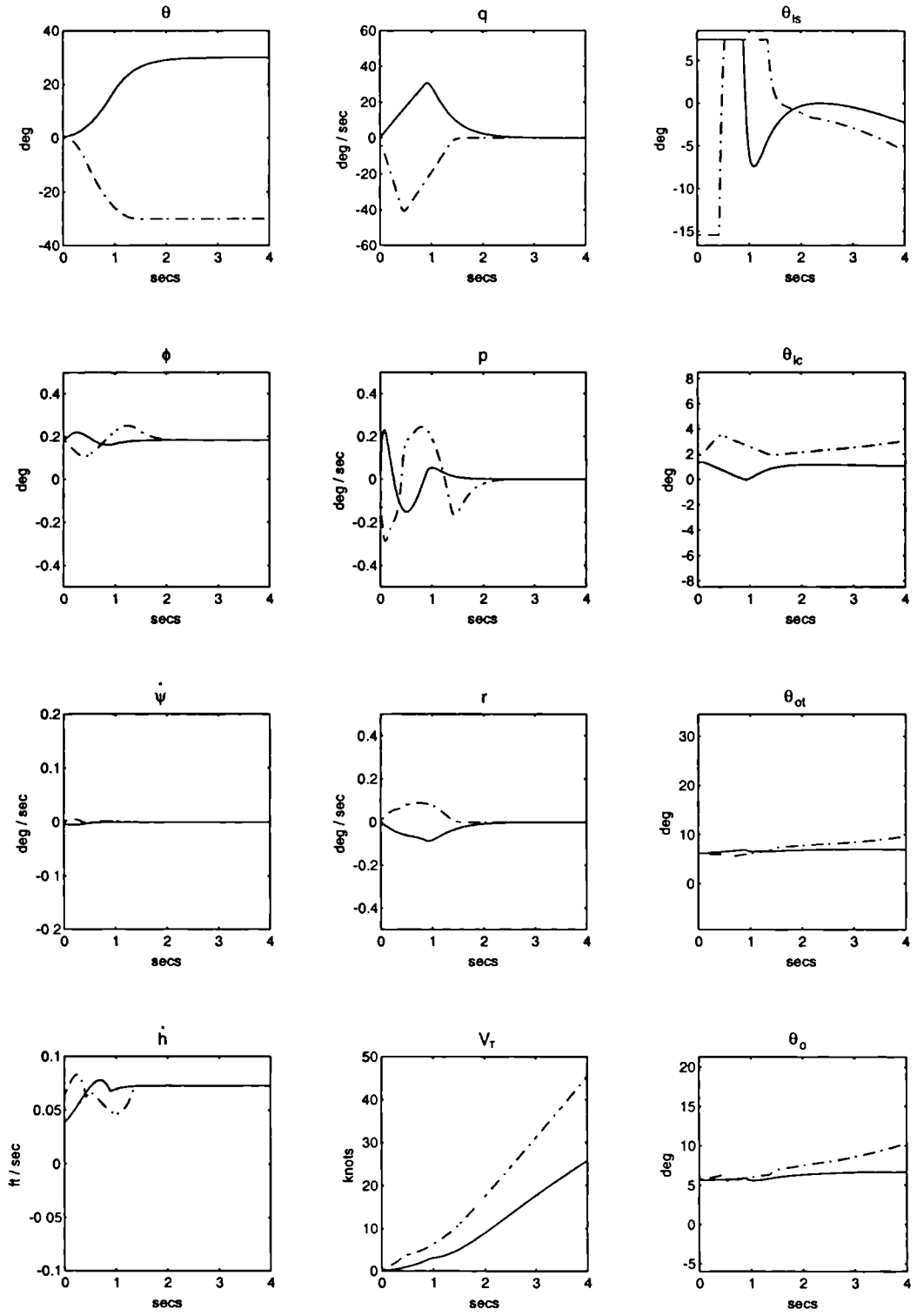

Figure 6.11: Lyapunov Controller: ±30 degrees Demand in Pitch Angle

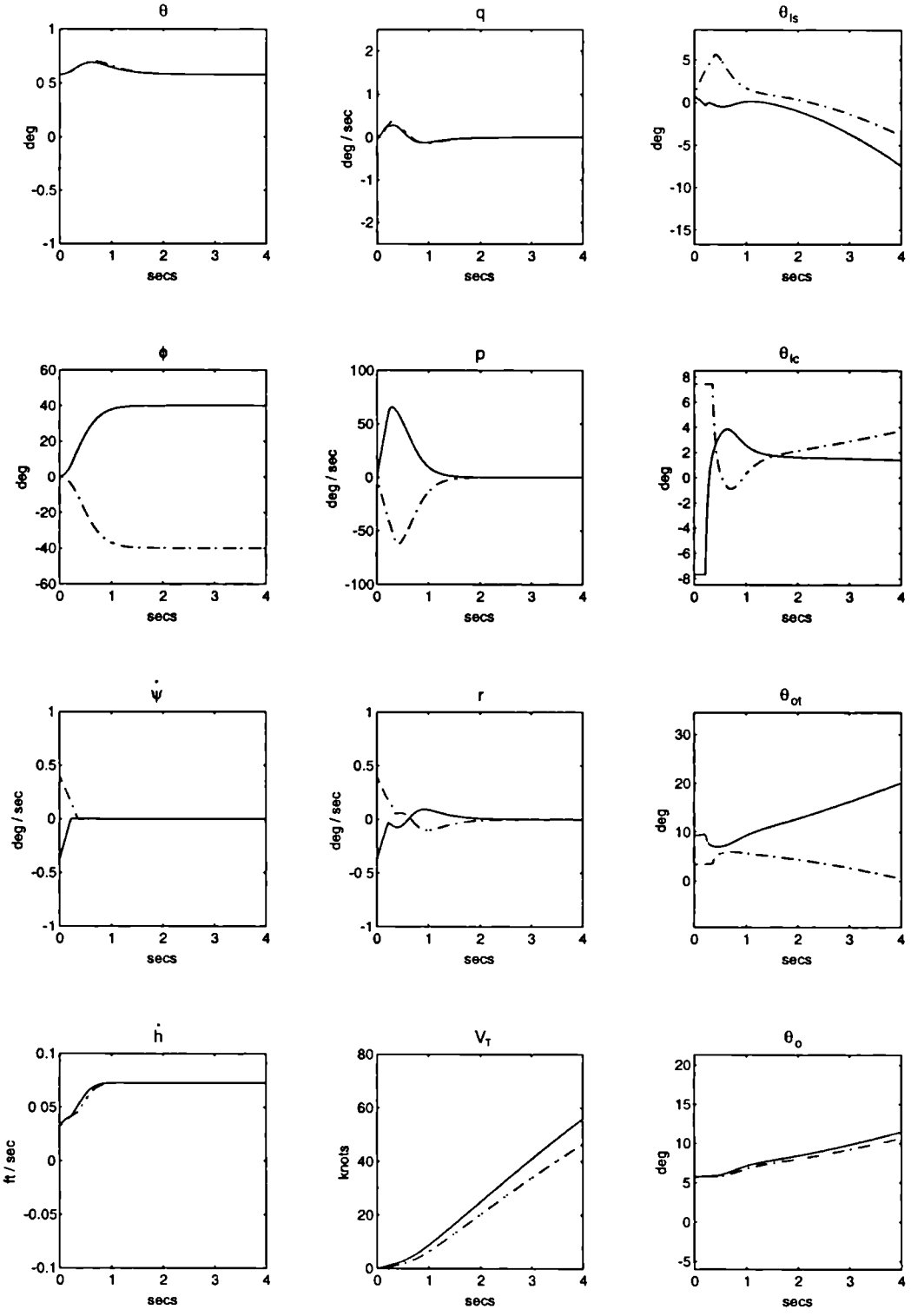

Figure 6.12: Lyapunov Controller: ±40 degrees Demand in Bank Angle

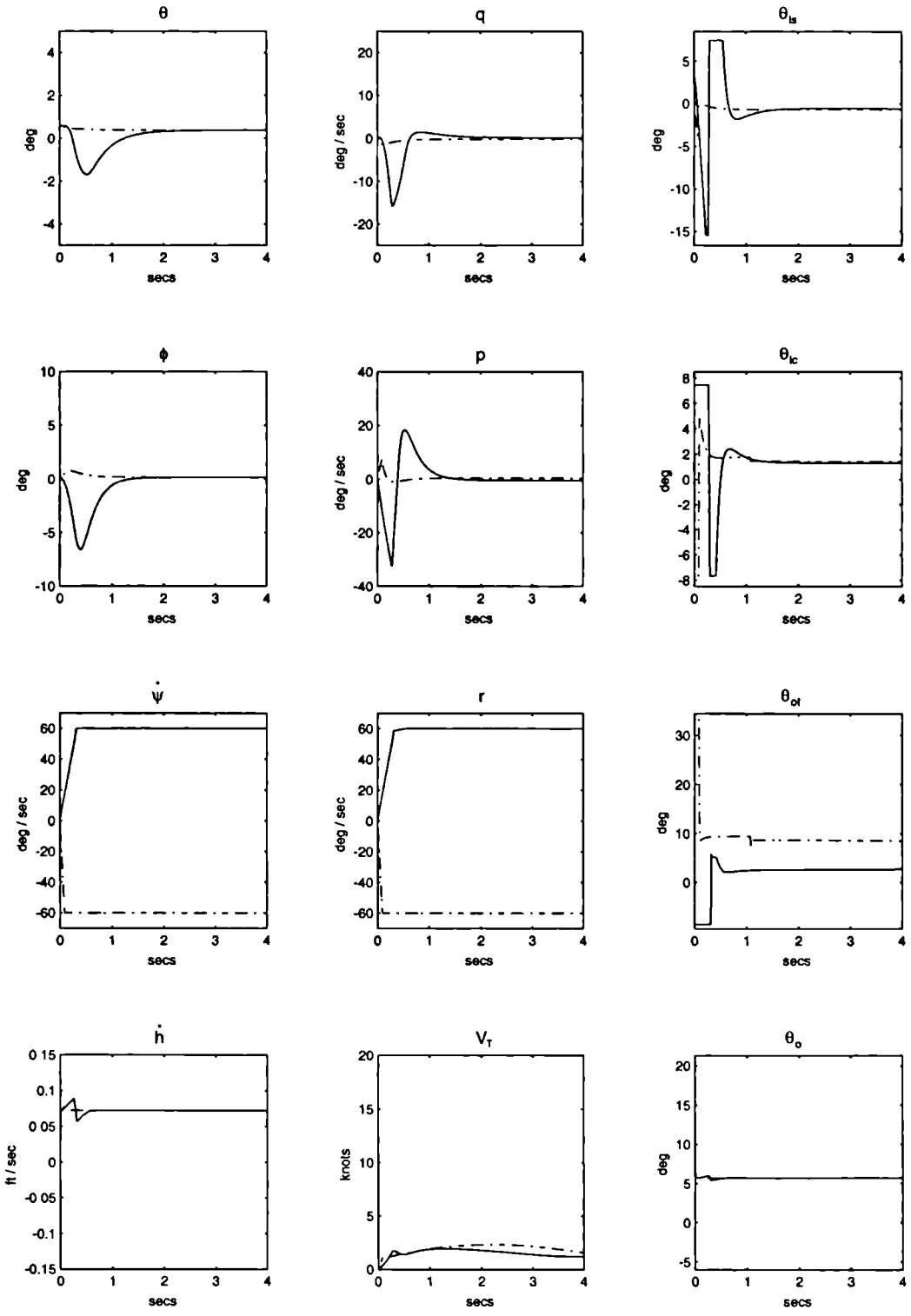

Figure 6.13: Lyapunov Controller: ±60 degrees/sec Demand in Heading Rate

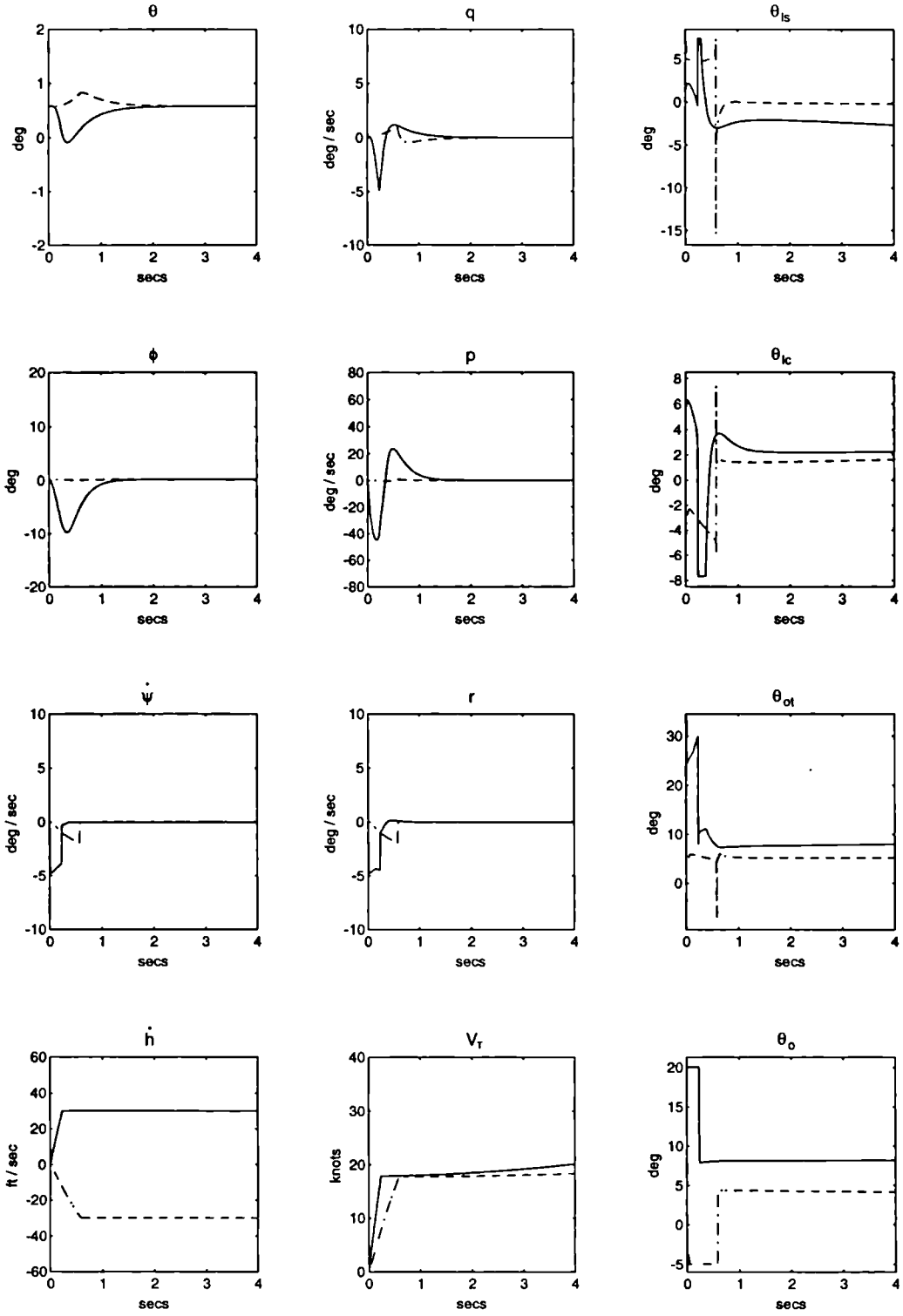

Figure 6.14: Lyapunov Controller: ±30 ft/sec Demand in Altitude Rate

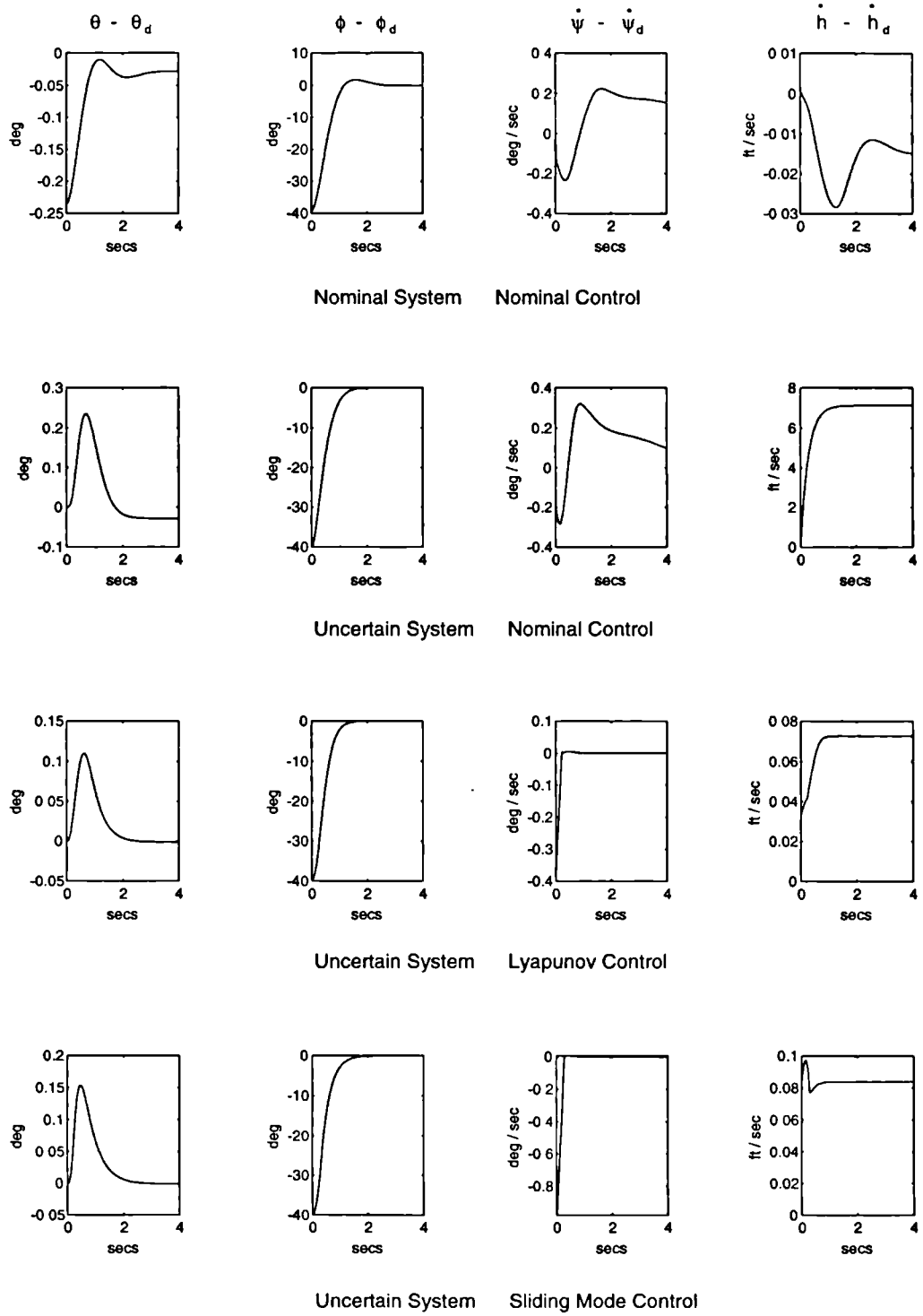

Figure 6.15: Comparison of Controllers: 40 degrees Demand in Bank angle

6.3 Handling Qualities Requirements

In addition to the above computer simulated results to step demand manœuvres, the control laws' performance was further investigated with regard to compliance with the handling qualities requirements of ADS 33-C [1]. These specifications are intended to ensure that no limitations on flight safety or on the capability to perform intended missions will result from deficiencies in flying qualities.

The acceptability of flying qualities is quantified in terms of *Levels* that are defined in the Cooper-Harper scale shown in Figure 6.17 overleaf. From this diagram it is clear that achievement of Level 1 flying qualities is most desirable for ease of pilot workload, ride comfort and safety. The complete specifications to be given shortly actually define the minimum responses to certain inputs for the attainment of a Level 1 rating. Computer simulation again allows for the evaluation of the system's performance against the Low speed and Hover specifications documented in [1].

Certain dynamic response characteristics that are important in each axis are next specified in order to show compliance with the relevant specifications. Not all of the Low speed and Hover requirements are applicable, however, and where they are not, comments will be made as to why this is so. To demonstrate that the response characteristics required for the Attitude Command Attitude Hold (ACAH) and the Rate Command (RC) systems are met, it is necessary to quote from the relevant sections of the design standard [1].

One technical detail is that some of the handling quality specifications are given in terms of the cockpit control inputs and some in terms of direct actuator inputs. The relationship between the two is illustrated in Figure 6.16

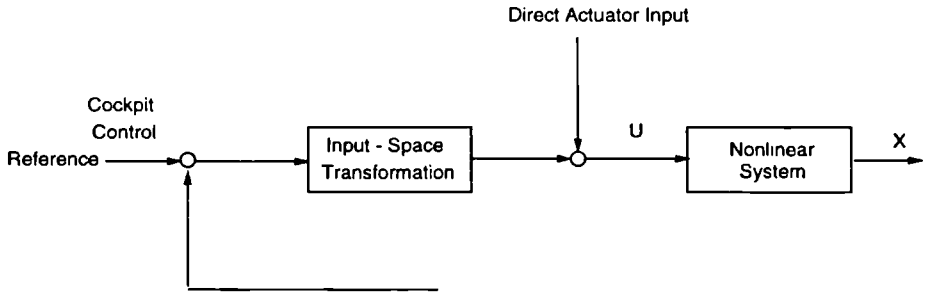

Figure 6.16: Cockpit control

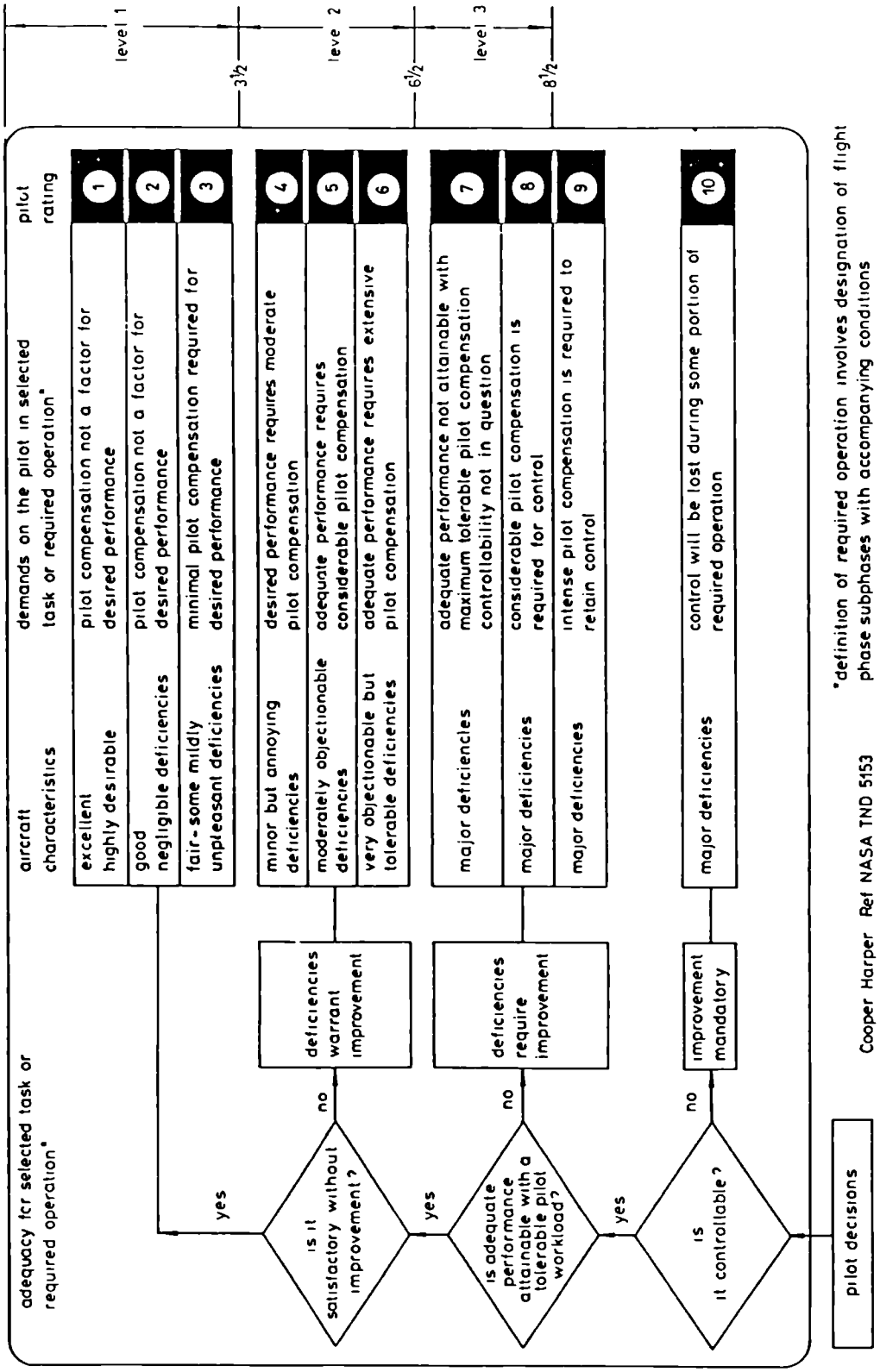

Figure 6.17: Cooper-Harper Scale From Yue et al [1990]

Attitude Hold

For Level 1 handling qualities the attitude (θ or ϕ) should return to within ± 10 % of the peak excursion (θ_{peak} or ϕ_{peak}) in less than 10 seconds following a pulse input as shown in Figure 6.18.

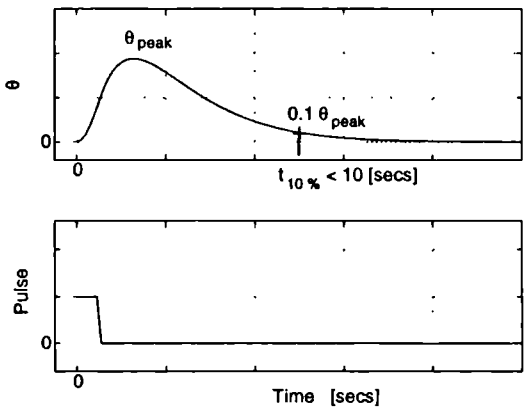

Figure 6.18: Response to Pulse

The peak attitude excursions should vary from the barely perceptible to at least 10 degrees. The attitude should also remain within the specified 10 % for at least 30 seconds. The pulse input should be inserted directly into the control actuator. Figures 6.19 to 6.20 below show that for both robust control laws and for both pitch attitude and roll attitude hold, Level 1 handling qualities are easily achieved.

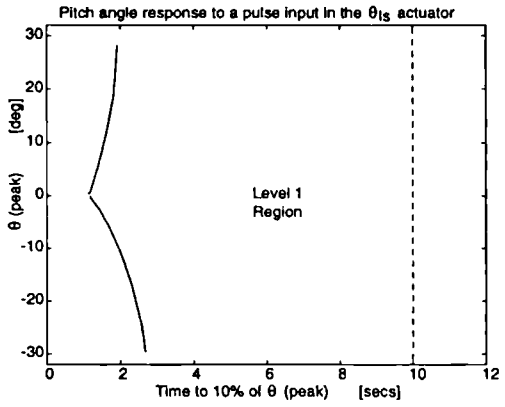

Figure 6.19: Lyapunov control

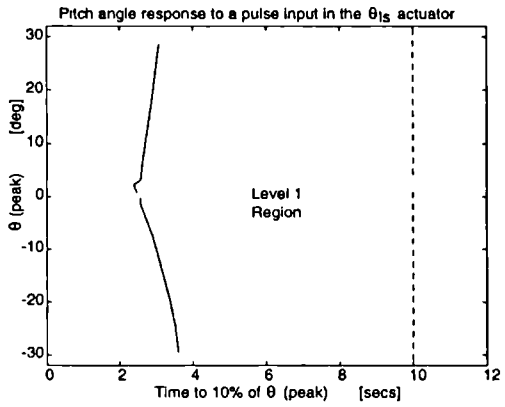

Sliding mode control

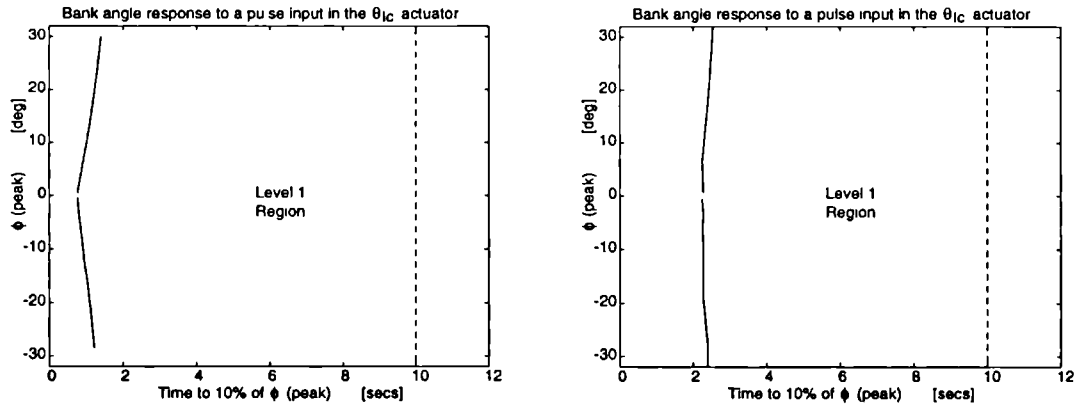

Figure 6.20: Lyapunov control Sliding mode control

Attitude Command

A step cockpit pitch (roll) controller force input, should produce a proportional pitch (roll) attitude change within 6 seconds. The attitude should remain essentially constant between 6 and 12 seconds following the step input. A separate trim control must be supplied to allow the pilot to null the cockpit controller forces at any achievable steady attitude.

From the time responses of Figures 6.6, 6.7, 6.11 and 6.12 it is clear that the first part of the specification is satisfied with the steady state values reached in less than 2 seconds. In the absence of a separate trim control (which was not included in the initial research objective) the attitude for large amplitude demands between 6 and 12 seconds does not remain constant. This is because the inability to null the controller forces causes them to rise continuously until actuator saturation occurs, at which point the controllers' performance degrades. Of course this is why a separate trim controller is essential if unnecessary continuous control effort is to be avoided. However for smaller amplitude demands such as -15 degrees demand pitch angle, the specification is easily met as shown in the Figure 6.21.

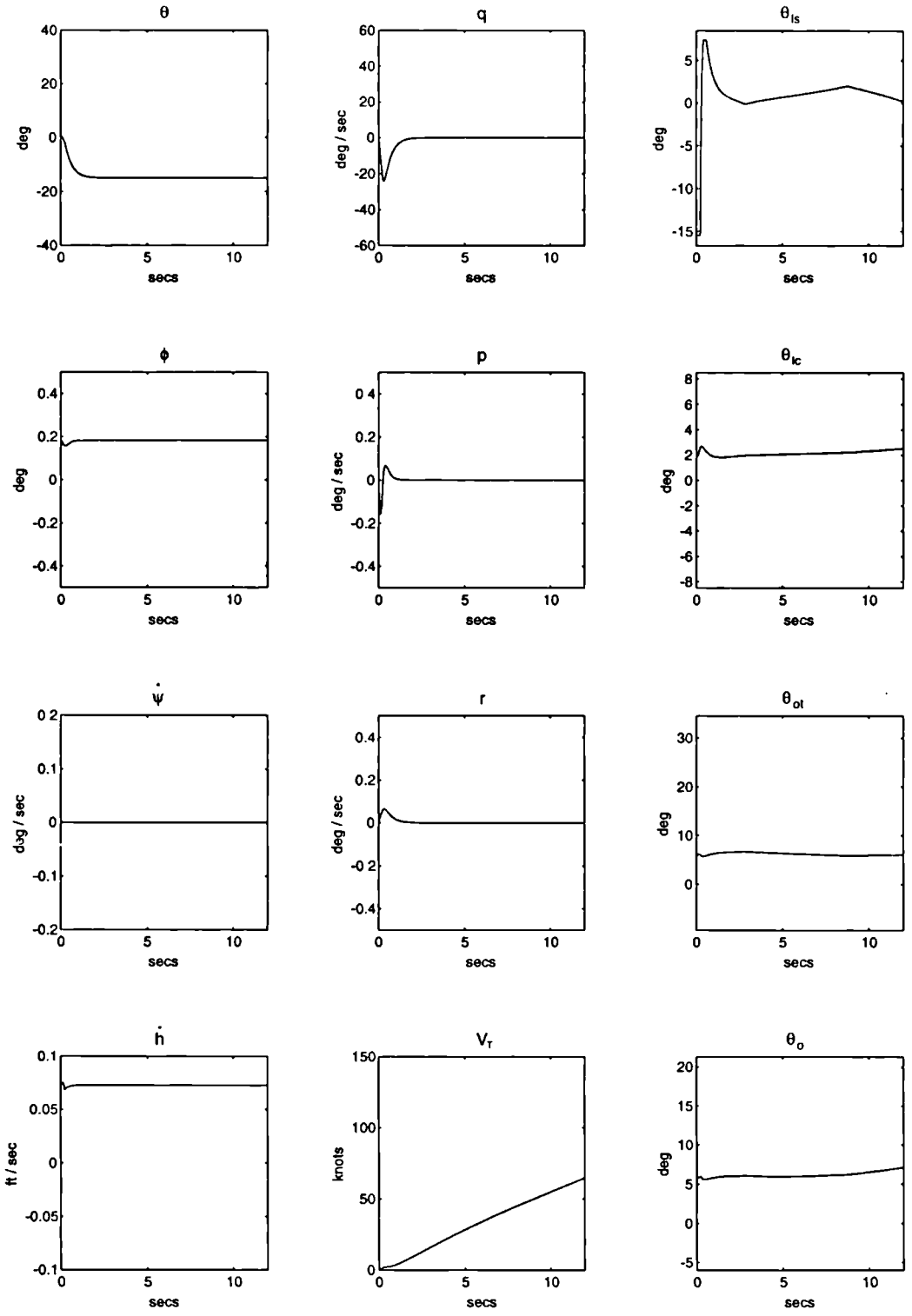

Figure 6.21: Lyapunov Controller: −15 degrees Demand in Pitch Angle

Heading Rate

The rate response should satisfy certain bandwidth requirements mentioned later. No requirement on the specific shape of the response to control inputs is specified except that the initial and the final cockpit control forces required to change from one steady heading to another shall not be of opposite sign.

Garrard and Low [47] found that the transfer function $\frac{r}{r_d} = \frac{4}{s+4}$ satisfies the Level 1 bandwidth requirements for yaw response. From this transfer function the time taken to reach 60 percent of the steady state value of r is 0.25 seconds. Figure 6.22 shows the responses to ±50, ±30, ±10 degrees/sec demands in heading rate. From this figure the time constants for both control laws are close to 0.25, this indicating that at least the Level 1 rise time requirements are met.

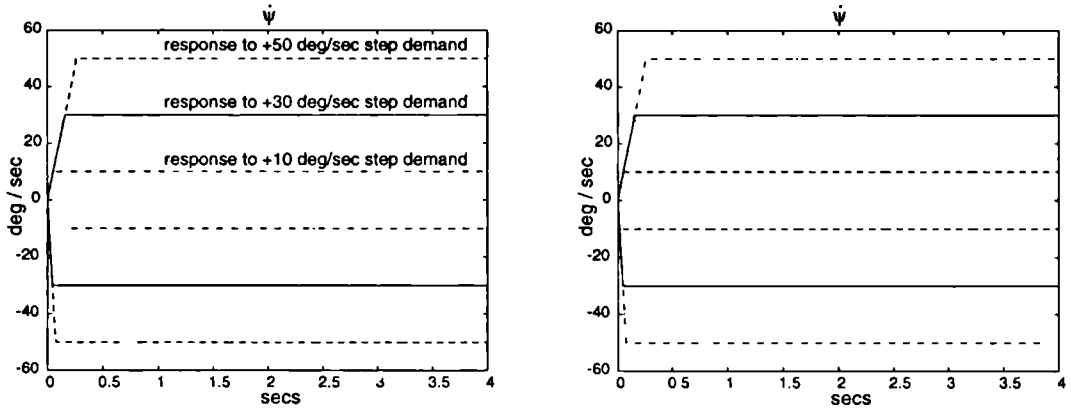

Figure 6.22: Lyapunov control Sliding mode control

Altitude Rate Command

For a rotorcraft in trim, a constant deflection of the vertical axis controller provides a constant steady state vertical velocity. It should also be possible for the pilot to null the cockpit controller force at any achievable vertical rate.

As above, Garrard and Low found that the transfer function $\frac{w}{w_d} = \frac{4}{s+4}$ satisfies the Level 1 bandwidth requirements. Figure 6.23 shows the responses to ±30, ±20, ±10 ft/sec demands in altitude rate. Again by inspection of this figure one can see that the

Level 1 rise time requirements for vertical rate are met.

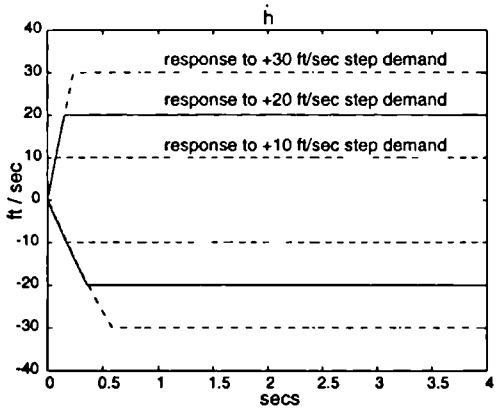

Figure 6.23: Lyapunov control

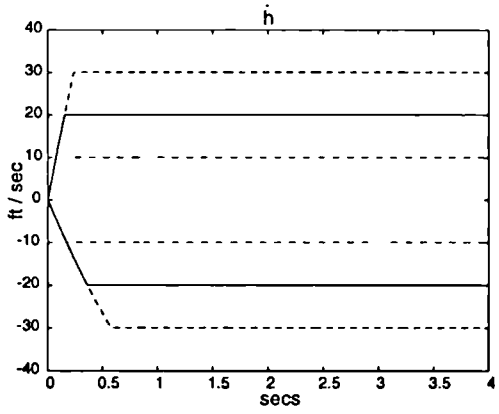

Sliding mode control

Moderate Amplitude Pitch (Roll) Attitude Changes

The variation of the ratio of the peak pitch (roll) rate to peak change in pitch (roll) attitude, $\frac{q_{peak}}{\Delta\theta_{peak}}$ ($\frac{p_{peak}}{\Delta\phi_{peak}}$) with minimum change in pitch (roll) attitude $\Delta\theta_{(min)}$ ($\Delta\phi_{(min)}$), as defined in Figure 6.24, should exceed the limits specified in Figures 6.25 and 6.26 below.

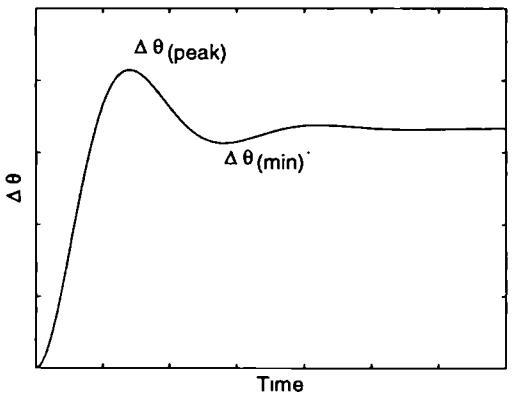

Figure 6.24: Change in Attitude

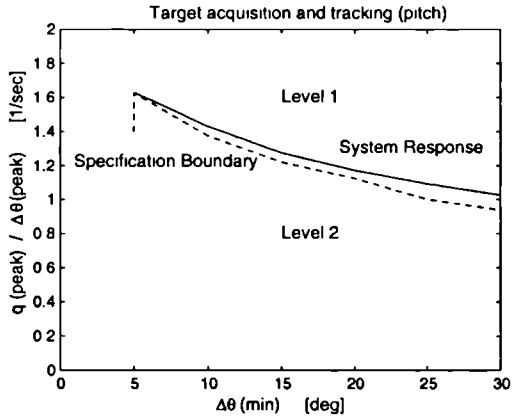

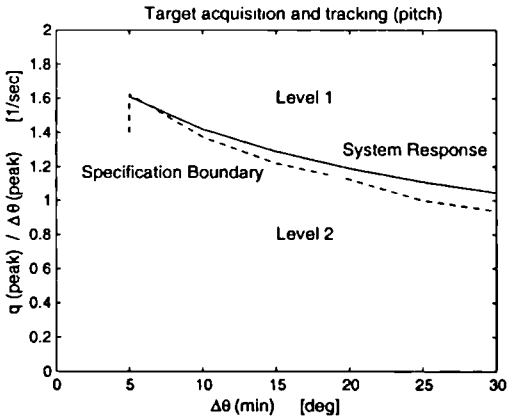

Figure 6.25: Lyapunov control Sliding mode control

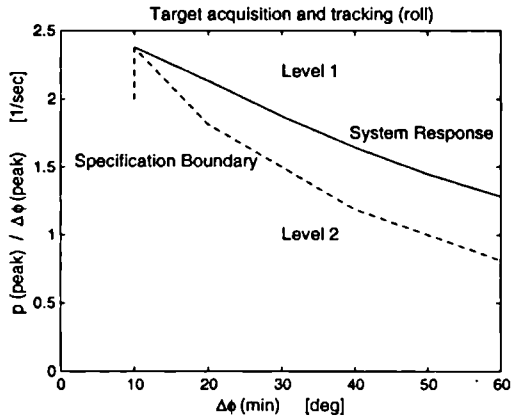

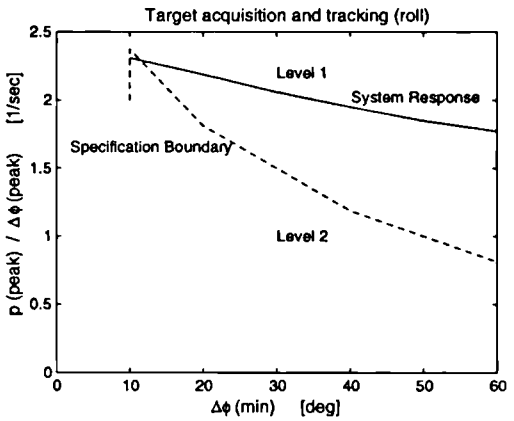

Figure 6.26: Lyapunov control Sliding mode control

Under both control laws, the pitch axis specification is easily satisfied. However, at very low roll angle demands the Level 1 boundary is traversed. This arises due to the necessity of constraining the speed of response of bank angle in order to suppress the transient coupling that occurs when a demand in heading rate is made.

Note that the limits shown are those for the most challenging mission tasks, i.e. Target acquisition and Tracking. For other less challenging mission tasks the Level 1 boundary is considerably lower and therefore for the control laws presented they provide no difficulty.

Large Amplitude Pitch (Roll) Attitude Changes

The minimum achievable attitude change from trim should not be less than ± 30 degrees in θ and ± 60 degrees in ϕ for Level 1 requirements under aggressive manœuvring. These attitudes must be achieved in each axis while limiting (limits not given in ADS 33 C) excursions in the other axes with appropriate control inputs. Other less stringent mission task elements require lower minimum achievable angles for Level 1.

The time responses, Figures 6.6 and 6.7, verify the capability of the control systems in enabling large amplitude demands to be achieved with a minimum of coupling in the other axes.

Moderate Amplitude Heading Changes

The ratio of peak yaw rate to peak change in heading $\frac{r_{peak}}{\Delta \psi_{peak}}$ as a function of the minimum heading change $\Delta\psi_{(min)}$, should exceed the limits specified in Figure 6.27 below.

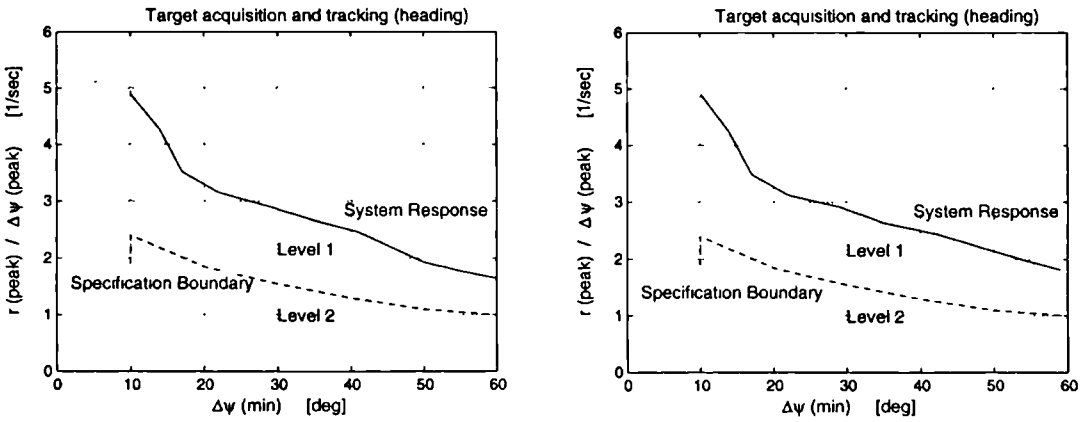

Figure 6.27: Lyapunov control Sliding mode control

This requirement was easily satisfied for both control laws.

Large Amplitude Heading Changes

The achievable yaw rate shall be no less than ±60 degrees/sec for Level 1 under the aggressive manœuvring mission tasks. Again the time responses in Figure 6.8 indicate that this is not a problem.

Interaxis Coupling

The general requirement states that control inputs to achieve a response in one axis shall not result in objectionable responses in one or more of the other axes. This requirement is formalized below where specific limits on interaxis coupling are given.

Pitch to Roll and Roll to Pitch Coupling during Aggressive Manœuvring

The ratio of the peak off-axis response to desired response $\frac{\theta_{pk}}{\phi}$ ($\frac{\phi_{pk}}{\theta}$) following an abrupt lateral (longitudinal) cyclic step input shall not exceed ±0.25 for level 1 handling qualities for at least 4 seconds after the input is initiated.

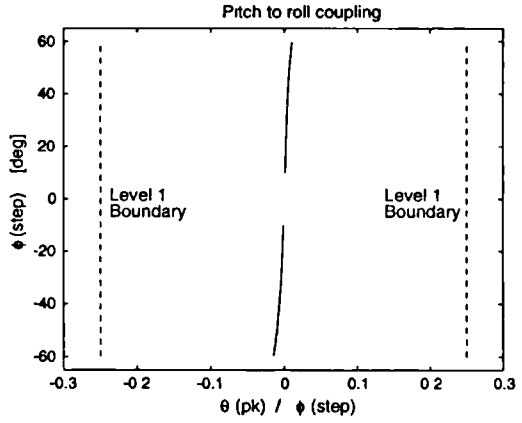

Figure 6.28: Lyapunov control

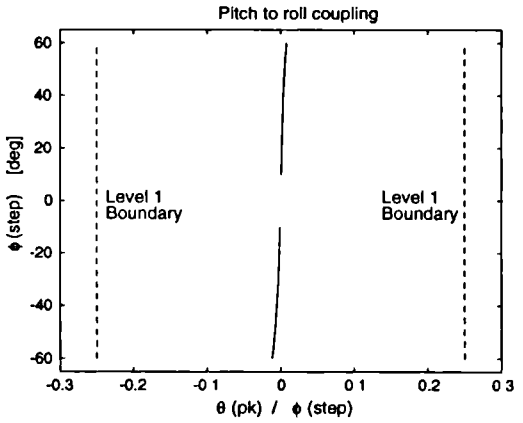

Sliding mode control

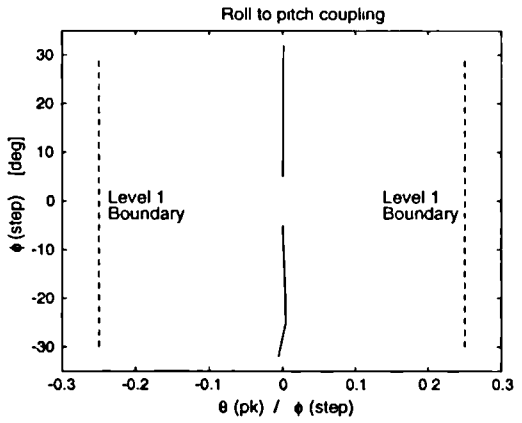

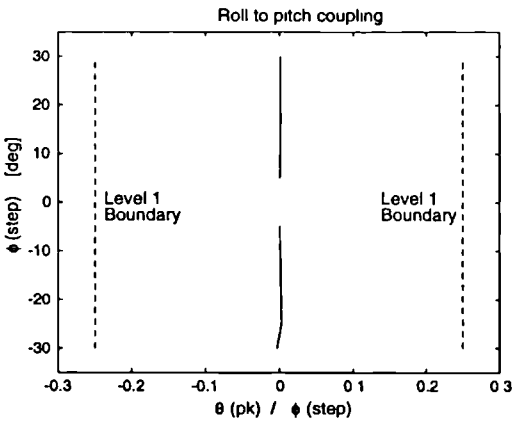

Figure 6.29: Lyapunov control Sliding mode control

In Figures 6.28 and 6.29, θ_{max} (ϕ_{max}) is the maximum attitude achieved over 4 seconds; as shown the coupling between the longitudinal and the lateral axes has virtually been eliminated by both control laws.

Yaw due to Collective

Finally, the yaw rate response to abrupt collective inputs with the directional controller free shall not exceed the boundaries specified in Figure 6.30 below. Additionally there shall be no objectionable yaw oscillations following step or ramp collective changes in the positive and negative directions. Oscillations involving yaw rates greater than 5 deg/sec shall be deemed objectionable.

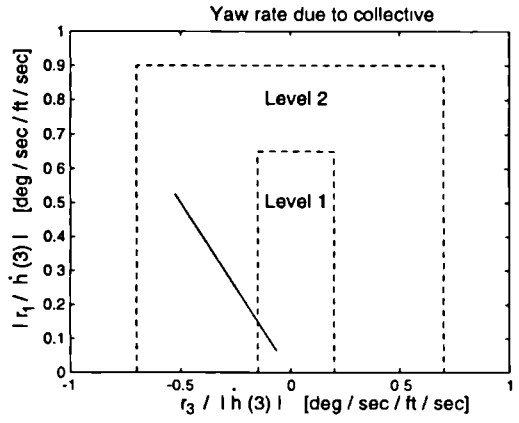

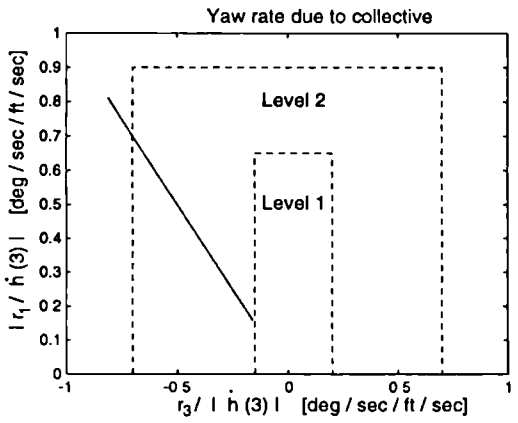

Figure 6.30: Lyapunov control Sliding mode control

The results indicate that the Level 1 handling qualities requirements have *not* been satisfied for most collective step changes. Only at quite large collective inputs does the helicopter response enter the Level 1 region. To see why this is so consider as shown in Figure 6.31 the typical response that occurs following a step demand in altitude rate.

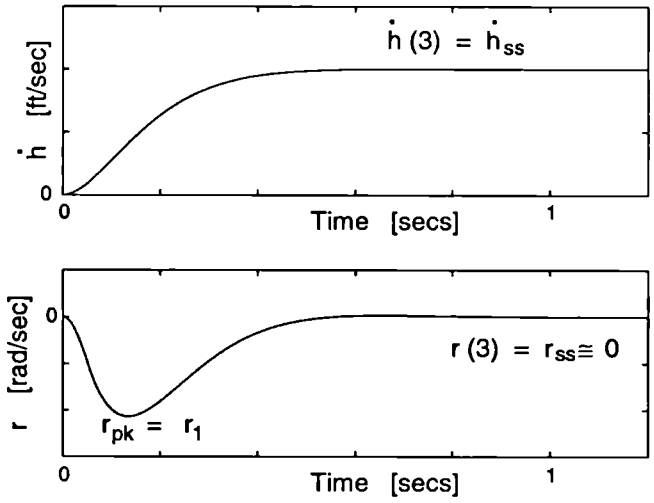

Figure 6.31: Typical Response

The parameters given in ADS 33-C are as follows:

r_1	=	The first peak in r before three seconds
$r(3)$	=	r at three seconds
r_3	=	$r_1 - r(3)$ if $r_1 < 0$
$\dot{h}(3)$	=	$\dot{h}$ at three seconds

For the typical response achieved in this study as shown in Figure 6.31

$$r_1 = r_{pk}, \qquad r(3) = 0, \qquad r_3 = r_{pk}, \qquad \dot{h}(3) = \dot{h}_d$$

Also in this study $r_1 = r_{pk}$ is small and varies very little with changes in $\dot{h}$. Therefore as $\dot{h}_d = \dot{h}(3) \rightarrow \infty$ then $\frac{r_1}{\dot{h}(3)} \rightarrow 0$, it therefore becomes clear that the Level 1 zone is entered for large collective demands.

The requirement is, however, fairly questionable since, as shown next, the presence of a non zero steady state yaw rate enables the helicopter to satisfy the Level 1 require-

ments. If it is assumed for the moment that $r(3) \neq 0$ and that r has some steady state value close to $r_1 = r_{pk}$ then $r_3 = r_1 - r(3) \simeq 0$ as shown in Figure 6.32 below.

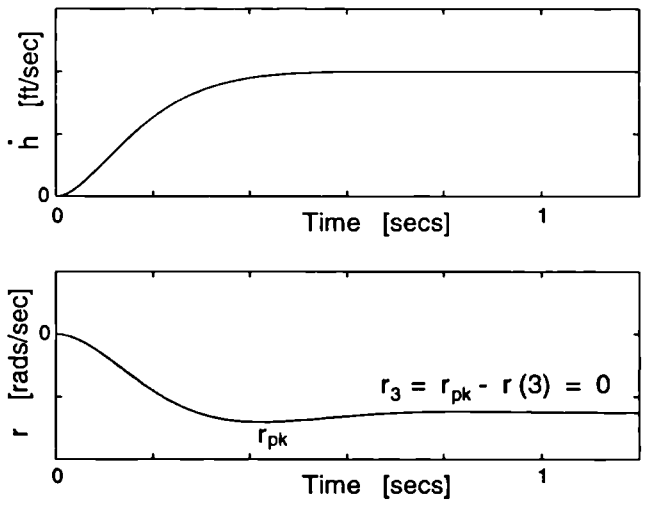

Figure 6.32: Possible Response

For this case, a persistent steady state error in r, the response then leads to satisfaction of the level 1 handling qualities as shown in Figure 6.33

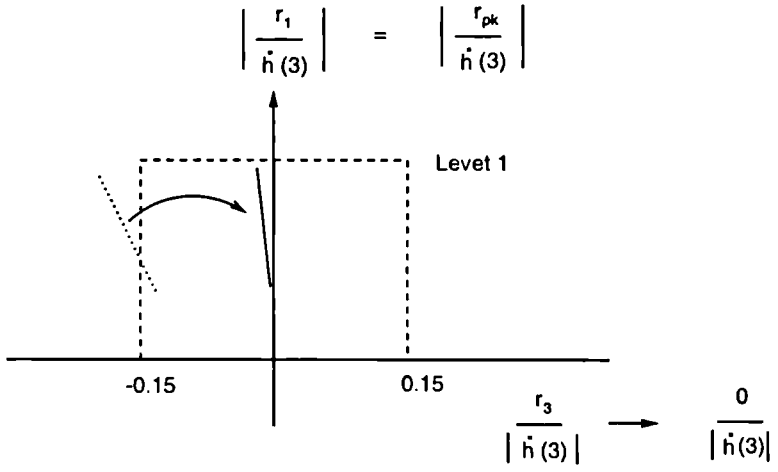

Figure 6.33: Yaw to Collective Coupling if $r_{pk} \approx r_{ss}$

Since a steady state error in yaw rate can always be found such that the requirement is met, then the requirement is not well-defined. For this reason, the failure of

the control laws to yield Level 1 performance in this single regard is deemed of little consequence.

6.4 Other Manœuvres

The response of the helicopter with Lyapunov controller to a bob-up manœuvre, i.e. a change from one altitude to another and then back down to the original altitude, is presented in Figure 6.34. These changes are effected by appropriate demands to altitude rate and causes the helicopter to rise quickly to a new altitude and maintain it for a certain period of time before descending back to the starting height. The response shows that throughout the manœuvre the other variables $\theta, \phi, \dot{\psi}$ remain virtually decoupled. The only problem is the large deviations in forward and lateral displacements arising from constraining θ and ϕ at zero and not at appropriate attitudes to minimise such drifts. This is where a pilot enters the loop and alters speed and displacement through changes in the decoupled pitch and roll attitudes.

The response of the helicopter with Lyapunov controller to a quick-step manœuvre, i.e. an acceleration to a new velocity followed by a deceleration back to the original velocity, is presented in Figure 6.35. This is effected by issuing appropriate demands to pitch angle which in turn causes the helicopter to accelerate quickly from hover to a certain forward speed, and then maintain it for about 5 seconds before decelerating back down to hover - or so it should. Notice that while the forward speed u correctly changes with corresponding pitch angle demands, the overall airspeed begins to drift after about 15 seconds. This is due to the small perturbations in ϕ causing the weakly damped lateral velocity v to meander. This is normally avoided by having a trimming controller or having the pilot enter the loop as in the bob-up manœuvre to minimise the deviations of v.

Figure 6.36 shows the gust response of the uncertain system with the Sliding mode controller. Following a positive 30 degrees demand in bank angle a 5 m/s (approx. 10 knots) gust, modelled as a step input in forward velocity u, is encountered one second after the demand. Decoupling of θ and $\dot{\psi}$ still occurs and ϕ tracks the demand almost unaffected. The presence of the gust which is clearly visible in the u response, affects the altitude rate causing a somewhat minor change in the achievable steady state response.

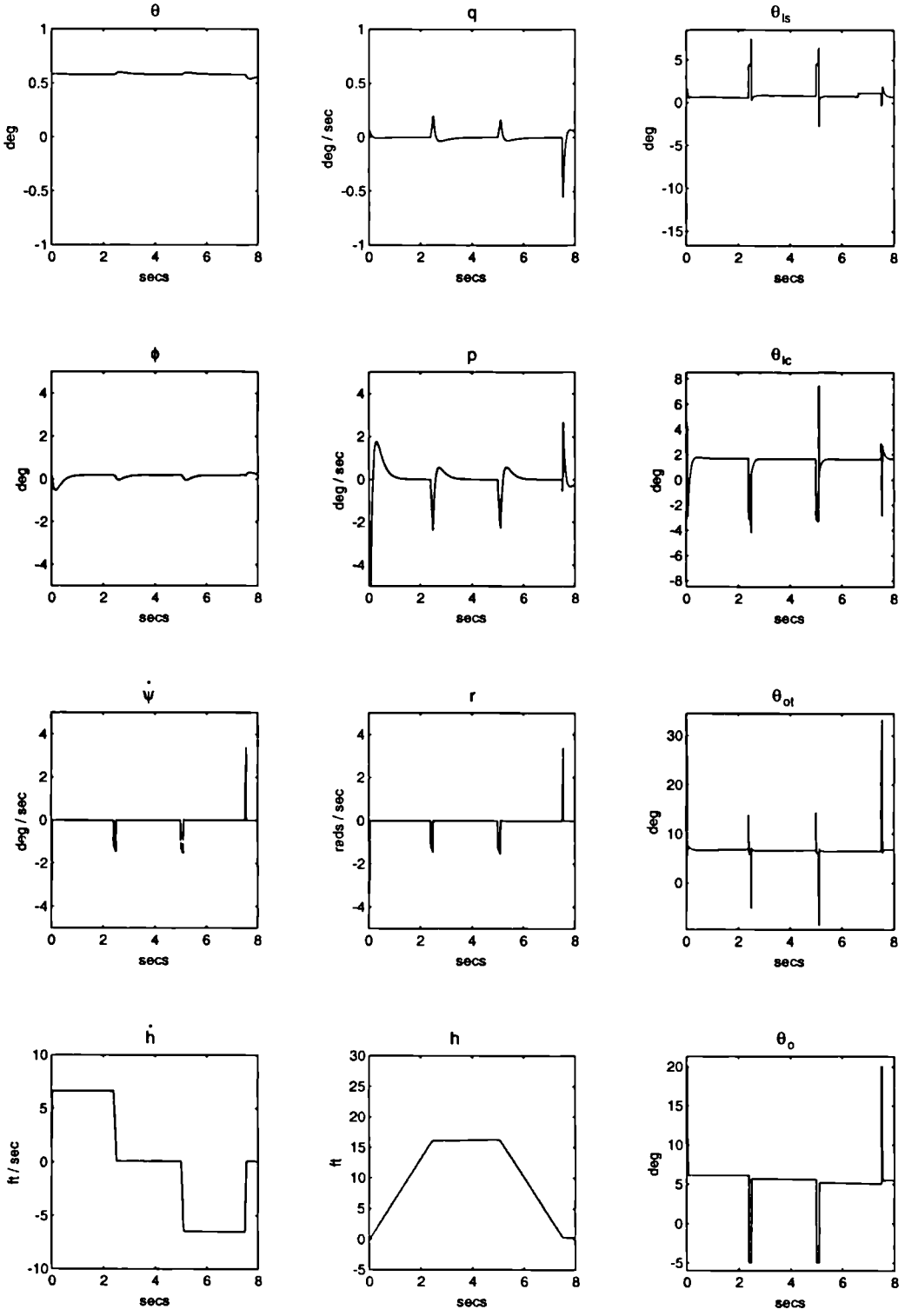

Figure 6.34: Lyapunov Controller: Bob-up Manœuvre

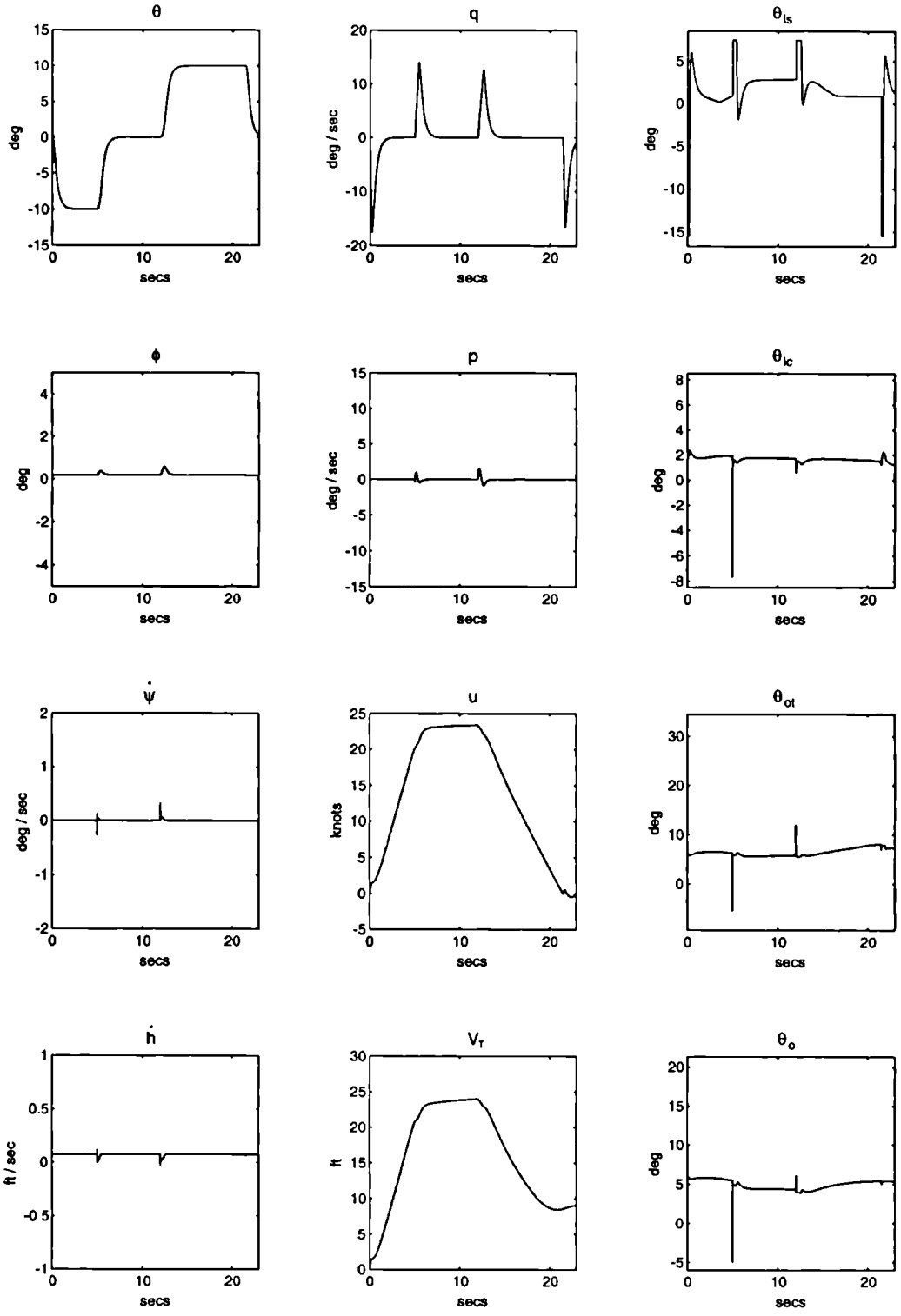

Figure 6.35: Lyapunov Controller: Quick-Step Manœuvre

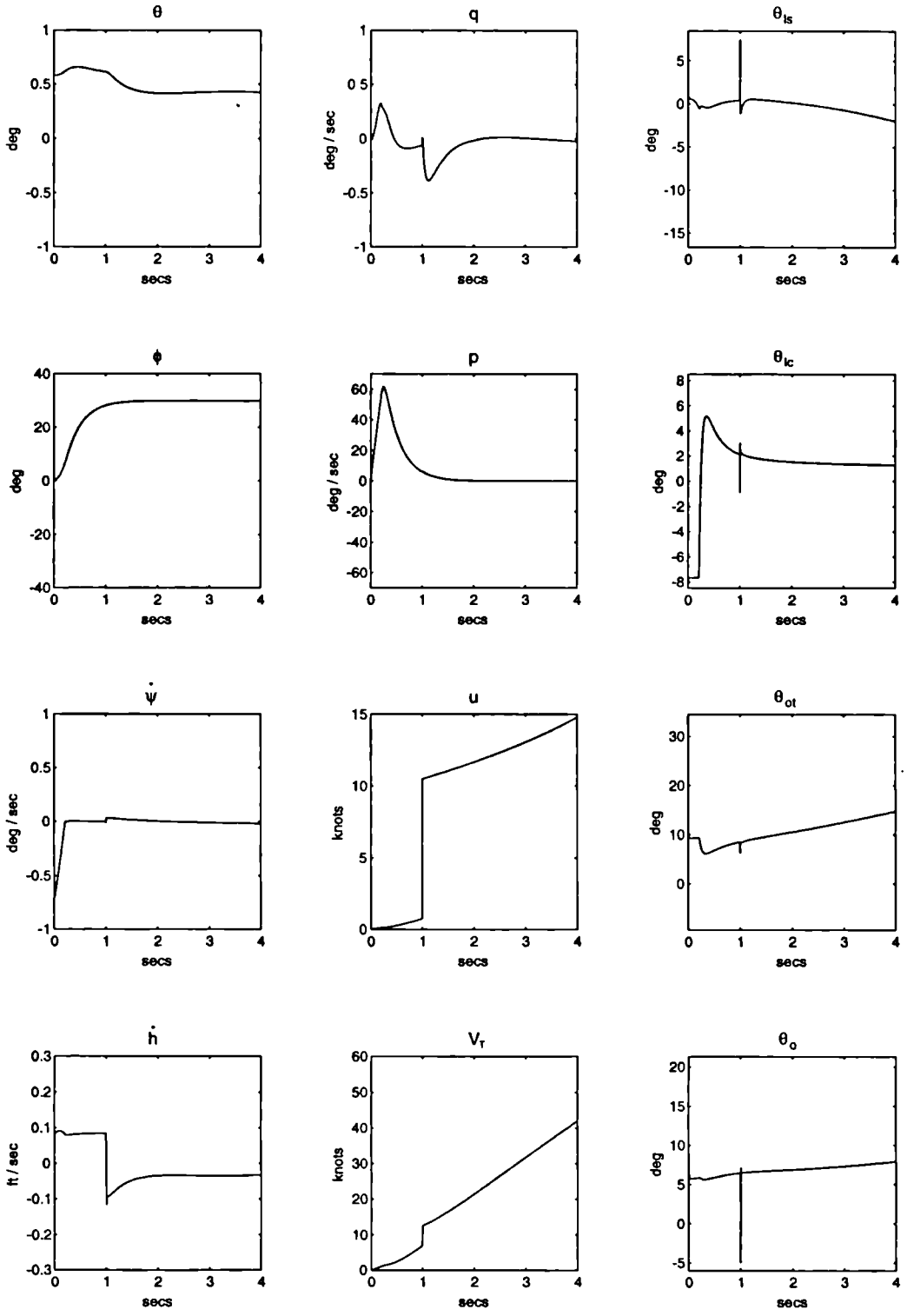

Figure 6.36: Sliding Mode Controller: Gust Response

6.5 Decoupling Matrix

As mentioned before, the Input-Output Linearization control law depends on the decoupling matrix, $E(x, \bar{\Theta})$, being nonsingular. Showing that $E(x, \Theta)^{-1}$ exists for all x and all Θ is quite difficult since $E(x, \bar{\Theta})$ as shown in Appendix B is an almost fully populated 4×4 matrix whose entries are complex nonlinear expressions. Indeed it appears to be beyond the current capabilities of *Mathematica* to do this. It is however possible to show through simulation that, during the following general manœuvres, (though any others may be tried):

- Pitching through ± 25 degrees
- Rolling through ± 40 degrees
- Yawing through rates of ± 50 degrees/sec
- Vertical Translation through ± 30 ft/sec

the determinant of the decoupling matrix is non zero. Even though the simulation was only run for four seconds it is clear that no singularities should arise in the near future. The figures shown were derived using a model with uncertainty and with a Lyapunov controller present. The determinant of the decoupling matrix using the other controllers is not shown since it is very similar.

Figure 6.37 shows the variation of the determinant, *Det*, of the decoupling matrix with changing demands in pitch angle over a period of four seconds. At large demands, about ± 30 degrees, the variation in *Det* is quite prominent, this is consistent with the significant actuator activity including saturation that is observable in Figure 6.11 for such demands. For smaller demands the changes in *Det* are quite small and again this is consistent with only low actuator activity for these demands.

The variations seen in Figure 6.38 can be similarly explained to those above. In Figure 6.13 greater control activity and control saturations occur for large positive demands in $\dot{\psi}$ than for similar amplitude negative demands, this phenomena is again apparent in Figure 6.39. Due to the scale in Figure 6.40 *Det* appears to have a minimum near to zero, however this is not actually so the minimum value is of the order of 1×10^5.

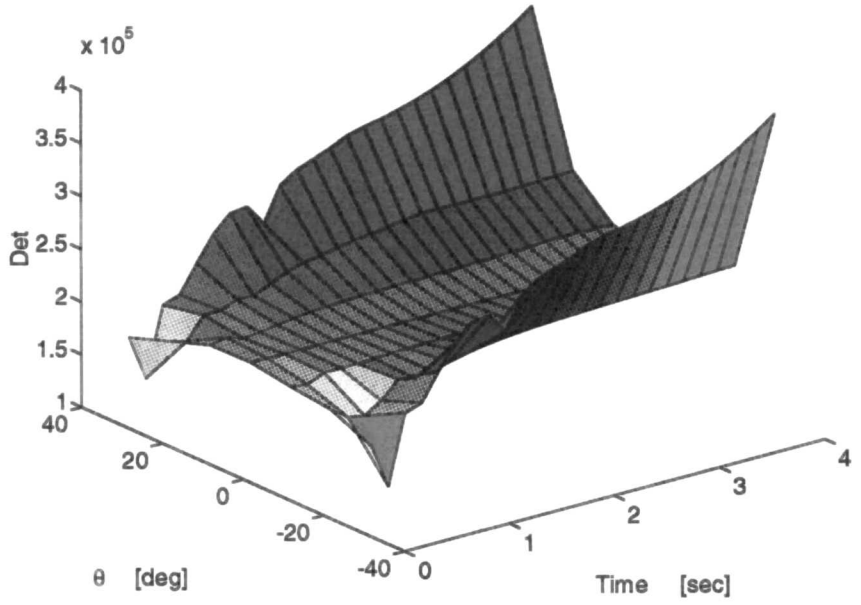

Figure 6.37: Lyapunov Controller: Determinant of Decoupling Matrix during Pitch Angle Demand Manœuvres

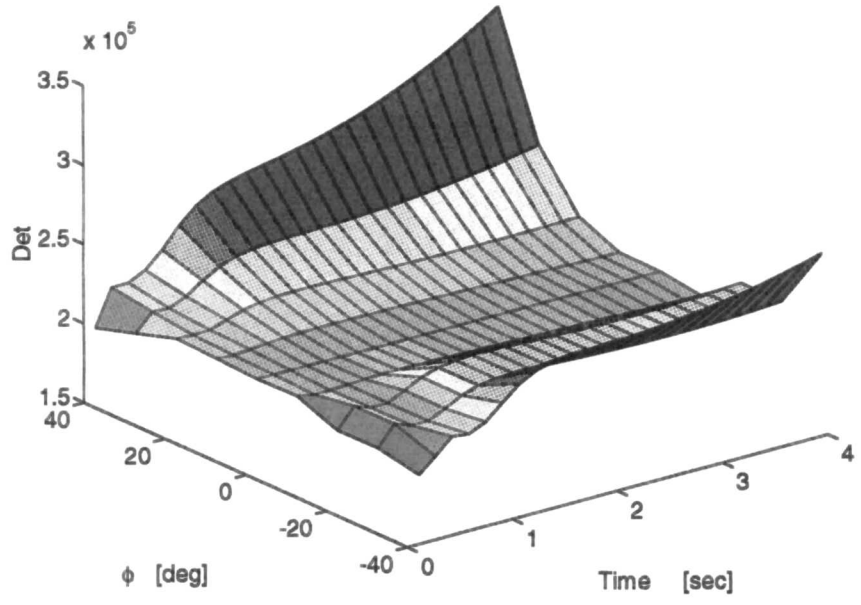

Figure 6.38: Lyapunov Controller: Determinant of Decoupling Matrix during Roll Angle Demand Manœuvres

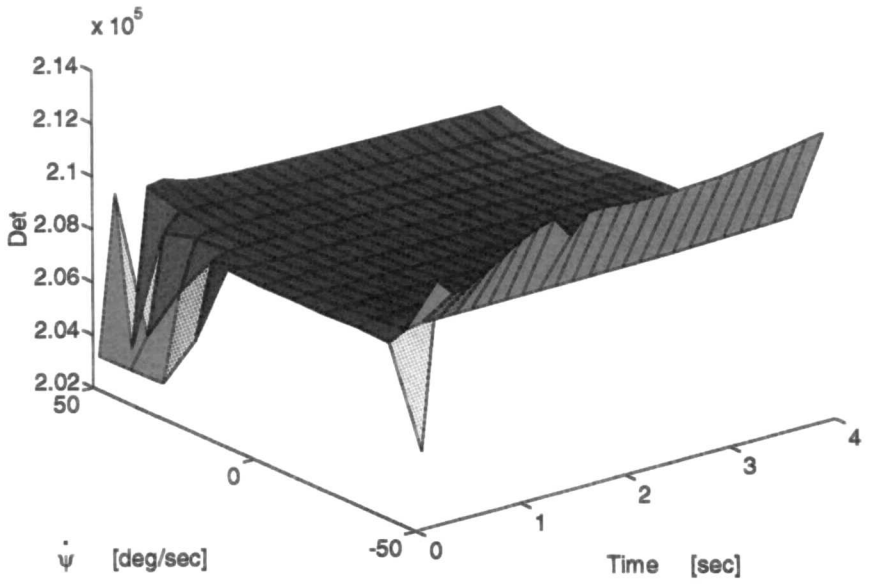

Figure 6.39: Lyapunov Controller: Determinant of Decoupling Matrix during Heading Rate Demand Manœuvres

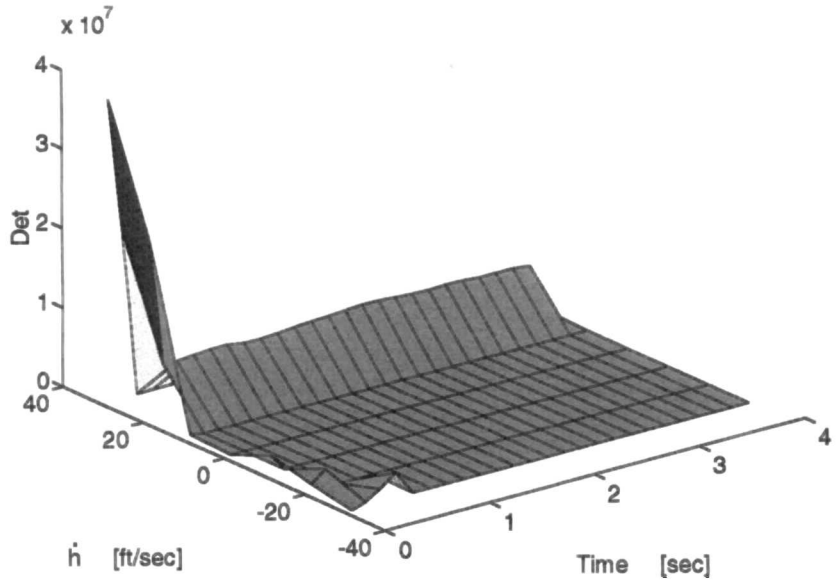

Figure 6.40: Lyapunov Controller: Determinant of Decoupling Matrix during Altitude Rate Demand Manœuvres

6.6 Summary

This presentation of results shows that the design objective to construct robust nonlinear hover and low speed controllers has been achieved. Furthermore the satisfaction of Level 1 handling qualities has also been demonstrated for both the Lyapunov and the Sliding mode control laws. The presence of limits on the available control power while causing a certain coupled transient response does not contribute to any unacceptable closed loop behaviour. In addition to the usual time responses intended to illustrate the decoupled behaviour of the closed loop system, manœuvres such as the *quick step* have been demonstrated thus further illustrating the functionality of the designs. Due to the current difficulty in showing analytically that the Decoupling matrix is indeed non-singular for all flight conditions, 3-D plots have been presented to illustrate the variation of the determinant of the matrix with time under various flight conditions. The plots clearly show that under the conditions considered the determinant is unlikely to become zero.

Chapter 7

Conclusions

The design of robust nonlinear control laws for helicopter systems has been demonstrated. The basic designs which employ methods from nonlinear geometric control theory are augmented by Lyapunov based and Sliding mode control techniques in order to enhance the robust stability properties of the closed loop systems.

By first implementing the full nonlinear model derived by Padfield [55] into the *Simulink* environment it was then possible to assess the performance of the controllers by means of computer simulation. The results illustrate good stable tracking, robustness to uncertainties and satisfaction of many Low Speed and Hover flying quality requirements documented in the Military Rotorcraft Handling Qualities Specification [1].

The controllers presented here are intended for use over the full flight envelope since the designs are based on the full nonlinear dynamics rather than linearized models. As a result, unlike linear designs, these control laws obviate the need for gain scheduling and the associated difficulties and deficiencies outlined in Chapter 1.

From a comparison of the performance of the Lyapunov controller with that of the Sliding mode design only small differences were evident, lending credence to the suggestion that the disparity generally arises as a result of differences in tuning parameters of each control law. The tuning of these parameters, which is required to achieve an adequate trade-off between tracking performance and robustness to uncertainties, still remains rather ad hoc. The availability of optimal tuning schemes to achieve desired performance characteristics may, however, eliminate the discrepancies altogether.

Even for systems exhibiting non-minimum phase properties, in this case instability of the internal dynamics associated with forward velocity u and lateral velocity v, it

is possible to utilize attributes of the physical system to overcome such instability problems. For the helicopter it is well known that the longitudinal and the lateral velocities are indirectly controlled by appropriate changes in the vehicle's attitude since the angular velocities evolve much faster than the translational ones.

The certain avoidance of additional complexity associated with finding the Input-Output relationship of a non-affine system was demonstrated by using an iterative scheme and exploiting a knowledge of the dynamic behaviour of the system.

To summarize, it has been demonstrated that nonlinear control laws which are valid over the entire flight envelope can be designed for a helicopter. These control laws which are based on the Differential Geometric Control theory of Input-Output Linearization have eliminated the gain scheduling requirement which is quite often an obstacle to achieving optimal performance using linear designs. Due to the nonlinear control terms in the helicopter model a straightforward application of the standard Input-Output Linearization techniques was not permitted, however the introduction of a new iterative scheme presented in Chapter 5 enabled the standard procedure to be applied and so avoided additional complexity involved in using a more general type of analysis. The closed loop robustness properties of the system has been enhanced by augmenting the Input-Output Linearization control laws in one of two ways; either employing a Sliding mode control technique or a Lyapunov-based control scheme. Both robust controllers perform well and simulation studies presented in this chapter confirm this. Furthermore compliance with the Pilot Handling Qualities Requirements of ADS 33-C was demonstrated with the Level 1 specifications achieved in almost all cases. The internal dynamics was addressed and it was shown in Chapter 5 that the modes associated with the internal dynamics can be indirectly controlled either by the pilot acting as a secondary outer loop or automatically by using feedback of the internal states. The issues surrounding an analytical proof of the invertability of the Decoupling matrix have not been resolved but 3-D plots of the evolution of the determinant of this matrix with time during certain flight conditions go some way towards a practical demonstration of the range of validity of the control laws, that is validity while the determinant remains non-zero.

7.1 Recommendations for Further Development

Several areas for further development are now apparent in order to build on the success of the current findings.

The first area to address is that of inclusion of a more comprehensive rotor dynamics model into the overall system description. This can be done either directly, i.e. having the rotor model present during the Input-Output Linearization procedure or indirectly by using this model to refine the uncertainty model for use with the robust control laws.

The addition of actuator saturation limits in the closed loop system has served the useful purpose of providing an initial glimpse at the effects of actuator systems on control law performance. Implementation of a comprehensive nonlinear actuator description, Stirling [72], is warranted since controller performance is generally known to degrade when limits, time lags, backlash and other nonlinearities associated with actuator systems are encountered.

As well as modelling the actuator, implementation of the *Conditioning Technique* of Hanus et al [27] to preserve (as much as possible) the control law integrity when encountering amplitude and rate saturation, may be required. This technique has been used successfully in H_∞ control law designs such as Hyde and Glover [33] and there is every reason to believe that it could also prove useful here.

An alternative approach to dealing with saturation once it has occured is to take its effects into account at the control law design stage. To do this the following avenue of investigation may be of use. Essentially the idea is to include the actuators with

limits into the overall system model before undertaking Input-Output Linearization. Consider the system given by:

$$\dot{x} = f(x) + G(x, u) \tag{7.1}$$

where $x \in \Re^n$ is the system state and $u \in \Re^m$ is the input to the system. In fact the presence of the actuation system shown schematically in Figure 7.1 creates a more realistic model:

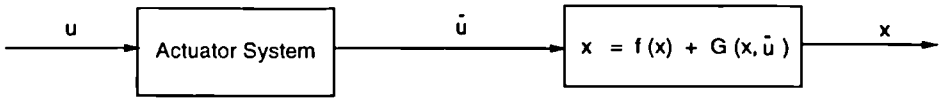

Figure 7.1: Effect of Actuator Dynamcis

In the usual case, i.e. not explicitly considering the actuator, the input u is designed to provide the state x with some desired properties, but u is not fully realizable due to the actuator dynamics. As a result the overall system properties tend to be somewhat *less* than desirable. The alternative is to insert the dynamics of the actuator into the system model by considering smooth approximations to the actuator limits such as the following authority limiting function in Figure 7.2:

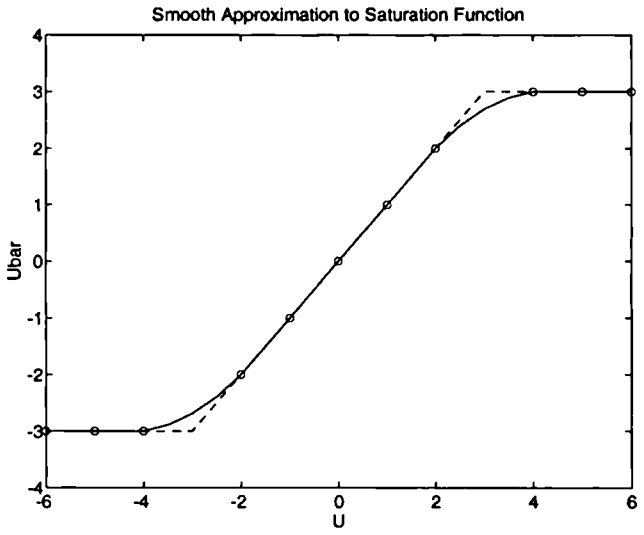

Figure 7.2: Approximate Authority Limiting Function

For this dual system, the control u may be designed since the original system is now aware of the corresponding value u that will actually affect it. Although this outline is very rudimentary and further thought maybe necessary, it is nevertheless believed to be worth investigating.

Even though full envelope controllers were designed here, these control laws generally sought to satisfy the low speed and hover requirements of [1] and as such their performance under high speed conditions may not satisfy the Level 1 specifications. This issue may be resolved with the addition of outer loop modes as suggested by

Postlethwaite et al. [57]. One such mode enabling *coordinated turns*, an important high speed quality, to be accomplished, may be achieved by augmenting heading rate demand as a function of bank angle at high speeds.

Another outer loop mode, implemented by Postlethwaite et al, provides a possible candidate for the additional trimming controller which is mandatory for (ACAH) designs. A trim-map may be used to offset the inner loop controller with the appropriate trim attitude. Further as noted in the reference the latter mode can be used continuously which in the cases presented in this thesis should help to eliminate the drifts in airspeed obtained during some of the manœuvres shown in Chapter 6.

The nonlinear control laws were designed here for continuous-time smooth systems; the possible digital implementation of these control laws may not, however, be straightforward. Arapostathis et al [2] found that sampling does affect linear equivalence and Feedback Linearization. More specifically they found that if a continuous system is linearizable by state coordinate changes then the discrete representation of the system is also linearizable by the same coordinate changes. On the other hand if the continuous system is linearizable by state coordinate changes and feedback then the sampled system will not necessarily be linearizable by state coordinate changes and feedback. This is because in the digital case the control input is necessarily a constant between sampling times. Clearly the issue regarding digital implementation of the Input-Output Linearization control laws requires investigation since coordinate changes and feedback are fundamental to such control laws.

In addition to Feedback Linearization considerations it is known, Utkin [77] and Fossard [19], that discontinuous controls smoothed by means of a boundary layer are sensitive to delays and that this smoothing causes the reappearance of the control chattering phenomenon. Although both the Lyapunov and the Sliding mode control laws will be affected by sampling, the resulting chattering may be eliminated by increasing the width of the boundary layer. Unfortunately, a subsequent degradation of the control law performance ensues with an increase in the magnitude of the tracking errors. The extent to which sampling will affect these controls needs quantifying.

The problem of determining analytically when (or if ever) the decoupling matrix is singular should be examined further. Perhaps a more in-depth knowledge of each component of the dynamic equations as well as their relative contributions under various

conditions will provide insight into making the problem more tractable.

Finally, the compromise that exists between robustness and tracking accuracy was investigated by Chang [8] and it was found that the introduction of a first order plus integral sliding condition eliminated this trade-off. One might incorporate this result into the helicopter Sliding mode control law derived in Chapter 5 in order to ascertain whether any further improvement to the results of Chapter 6 is possible. In addition, Singh [68] improved the tracking performance of his Lyapunov-based control law by means of integral feedback of the tracking errors. It would also be of interest to implement this idea.

Bibliography

[1] Anonymous. *Handling Qualities Requirements for Military Rotorcraft: Aeronautical Design Standard.* Technical Report ADS-33C, U.S. Army AVSCOM, 1989.

[2] A. Arapostathis, B. Jakubczyk, H. G. Lee, S. I. Marcus, and E. D. Sontag. *The effect of sampling on linear equivalence and feedback linearization.* Systems and Control Letters, 13:373–381, 1989.

[3] B. R. Barmish and G. Leitmann. *On the ultimate boundedness control of uncertain systems in the absence of matching assumptions.* IEEE Transactions on Automatic Control, AC-27(1):153–158, 1982.

[4] S. Battilotti. *A sufficient condition for nonlinear noninteracting control with stability via dynamic state feedback.* IEEE Transactions on Automatic Control, AC-36(9):1033–1045, 1992.

[5] S. Battilotti. *A sufficient condition for nonlinear noninteracting control with stability via dynamic state feedback: block-partitioned outputs.* International Journal of Control, 55(5):1141–1160, 1992.

[6] S. Behtash. *Robust output tracking for nonlinear systems.* International Journal of Control, 51(6):1381–1407, 1990.

[7] R. W. Brockett. *Feedback invariants for nonlinear systems.* In Proceedings of the IFAC Congress, Helsinki, pages 1115–1120, 1978.

[8] L. W. Chang. *A mimo sliding control with first order plus integral sliding condition.* Automatica, 27(5):853–858, 1991.

[9] B. Charlet, J. Levine, and R. Marino. *Dynamic feedback linearization with application to aircraft control.* In Proceedings of the 27th IEEE Conference on Decision and Control, pages 701–705, 1988.

[10] J. S. Chen and Y. H. Chen. *Robust control of nonlinear uncertain systems: A feedback linearization approach.* In Proceedings of the 30th IEEE Conference on Decision and Control, pages 2515 2520, 1991.

[11] Y. H. Chen. *Design of robust controllers for uncertain dynamical systems.* IEEE Transactions on Automatic Control, AC-33(5):487–491, 1988.

[12] Y. H. Chen and G. Leitmann. *Robustness of uncertain systems in the absence of matching assumptions.* International Journal of Control, 45(5):1527–1542, 1987.

[13] I. Cochin. *Analysis and Design of the Gyroscope for Inertial Guidance.* John Wiley and Sons , 1963.

[14] M. J. Corless and G. Leitmann. *Continuous state feedback guaranteeing uniform ultimate boundedness for uncertain dynamic systems.* IEEE Transactions on Automatic Control, AC-26(5):1139–1144, 1981.

[15] R. A. DeCarlo, H. Z. Stanislaw, and G. P. Matthews. *Variable structure control of nonlinear multivariable systems: A tutorial.* In Proceedings of the IEEE, volume 76, number 3, pages 212–232, 1988.

[16] H. Elmali and N. Olgac. *Robust output tracking control of nonlinear mimo systems via sliding mode technique.* Automatica, 28(1):145–*, 1992.

[17] B. Etkin. *Dynamics of atmospheric flight.* John Wiley and Sons, 1972.

[18] B. R. Fernández and J. R. Hedrick. *Control of multivariable nonlinear systems by the sliding mode method.* International Journal of Control, 46:1019–1040, 1987.

[19] A. J. Fossard. *Helicopter control law based on sliding mode with model following.* International Journal of Control, 57:1221–1235, 1993.

[20] L. C. Fu and T. L. Liao. *Globally stable robust tracking of nonlinear systems using variable structure control and with an application to a robotic manipulator* . IEEE Transactions on Automatic Control, AC-35(12):1345–1350, 1990.

[21] W. L. Garrard, E. Low, and S. Prouty. *Design of attitude and rate command systems for helicopters using eigenstructure assignment.* AIAA Journal of Guidance, Control and Dynamics, 12(6):783–791, 1989.

[22] S. Gopalswamy and J. K. Hedrick. *Control of high performance aircraft with unacceptable zerodynamics.* In Proceedings of the American Control Conference, pages 1834 1838, 1992.

[23] S. Gopalswamy and J. R. Hedrick. *Tracking nonlinear non-minimum phase systems using sliding control.* International Journal of Control, 57:1141 1158, 1993.

[24] S. Gutman. *Uncertain dynamical systems - A Lyapunov min-max approach.* IEEE Transactions on Automatic Control, AC-24(3):437 443, 1979.

[25] I. J. Ha and E. G. Gilbert. *Robust tracking in nonlinear systems.* IEEE Transactions on Automatic Control, AC-32(9):763–771, 1987.

[26] W. Hahn. *Stability of Motion.* Springer-Verlag, 1967.

[27] R. Hanus, M. Kinnaert, and J.L. Henrotte. *Conditioning technique, a general anti-windup and bumpless transfer method.* Automatica, 23(6):729–739, 1987.

[28] J. Hauser, S. Sastry, and G. Meyer. *Nonlinear control design for slightly non-minimum phase systems: Application to V/STOL aircraft.* Automatica, 28(4):665–679, 1992.

[29] M. W. Heighes, P. K . A Menon, and D. P. Schrage. *Synthesis of a helicopter full-authority controller.* AIAA Journal of Guidance, Control and Dynamics, 15(1):222–227, 1992.

[30] L. R. Hunt, R. Su, and G. Meyer. *Design for multi-input systems.* In Brockett, Millman and Sussman, editor, Differential Geometric Control Conference, volume 27, pages 268 298. Birkhauser, Boston, 1983.

[31] L. R. Hunt, R. Su, and G. Meyer. *Global transformations of nonlinear systems.* IEEE Transactions on Automatic Control, AC-28:24–31, 1983.

[32] L. R. Hunt and M. S. Verma. *Linear dynamics hidden by input-output linearization.* International Journal of Control, 53(3):731 740, 1991.

[33] R. A. Hyde and K. Glover. *Taking H_∞ control into flight.* In Proceedings of the 32nd IEEE Conference on Decision and Control, pages 1458 1463, 1993.

[34] A. Isidori. *Nonlinear Control Systems.* Springer Verlag, 2 edition, 1989.

[35] A. Isidori and C. I. Byrnes. *Output regulation of nonlinear systems.* IEEE Transactions on Automatic Control, AC-35(2):131 140, 1990.

[36] A. Isidori and J. W. Grizzle. *Fixed modes and nonlinear noninteracting control with stability.* IEEE Transactions on Automatic Control, AC-33(10):907–914, 1983.

[37] B. Jakubczyk and W. Respondek. *On linearization of control systems.* In the Science, Mathematics, Astronomy and Physics series of the Bulletin de l' Academie Polanaise des Sciences, 28(9-10):517–522, 1980.

[38] K. Khorasani. *Robust stabilization of nonlinear systems with unmodelled dynamics.* International Journal of Control, 50(3):827–844, 1989.

[39] C. Kravaris and S. Palanki. *A Lyapunov approach for robust nonlinear state feedback synthesis.* IEEE Transactions on Automatic Control, AC-33(12):1188 1191, 1988.

[40] A. J. Krener. *On the equivalence of control systems and the linearization of nonlinear systems.* SIAM Journal of Control, 11(4):670–676, 1973.

[41] M. Lambert, editor. *Jane's All The World's Aircraft - 84-th Year of Issue.* Janes Information Group Ltd., 1993-1994.

[42] S. H. Lane and R. F. Stengel. *Flight control design using nonlinear inverse dynamics.* Automatica, 24(4):471–483, 1988.

[43] G. Leitmann. *On the efficacy of nonlinear control in uncertain linear systems.* Journal of Dynamics Systems, Measurement and Control, 102:95 102, 1981.

[44] T. L. Liao, L. C. Fu, and C. F. Hsu. *Adaptive robust tracking of nonlinear systems with an application to a robotic manipulator.* Systems and Control Letters, 15:339–348, 1990.

[45] T. L. Liao, L. C. Fu, and C. F. Hsu. *Output tracking control of nonlinear systems with mismatched uncertainties.* Systems and Control Letters, 18:39 47, 1992.

[46] E. Licéaga and R. Bradley. *A geometric flight control system for helicopters.* In Royal Aeronautical Society Conference on Helicopter Handling Qualities and Control, pages 16.1–16.15, 1988.

[47] E. Low and W. Garrard. *Design of flight control systems to meet rotorcraft handling qualities specifications.* AIAA Journal of Guidance, Control and Dynamics, 16(1):69–78, 1993.

[48] J. M. Maciejowski. *Multivariable Feedback Design.* Addison Wesley, 1989.

[49] M. A. Manness and D. J. Murray-Smith. *Aspects of multivariable flight control law design for helicopters using eigenstructure assignment.* Journal of the Americal Helicopter Society, 37(3):18–32, 1992.

[50] P. K. Menon, M. E. Badgett, R. A. Walker, and E. L.Duke. *Nonlinear flight test trajectory controllers for aircraft.* AIAA Journal of Guidance, Control and Dynamics, 10(1):67–72, 1987.

[51] G. R. Meyer, R. Su, and L. R. Hunt. *Design of a helicopter autopilot by means of linearizing transformations.* Agard CP-321, pages 4:1–4:11, 1983.

[52] G. R. Meyer, R. Su, and L. R. Hunt. *Application of nonlinear transformations to automatic flight control.* Automatica, 20(1):103–107, 1984.

[53] G. Mullen. *Private Communication.* Westland Helicopters Limited (UK), 1991.

[54] H. Nijmeijer and A. J. van der Shaft. *Nonlinear Dynamical Control Systems.* Springer-Verlag, 1990.

[55] G. D. Padfield. *A theoretical model of helicopter flight mechanics for application to piloted simulation.* Tech Report TR 81048, RAE Farnborough, 1981.

[56] N. Pantalos. *Full linearization and sampled-data control schemes applied to helicopter flight control.* In IFAC Workshop: Evaluation of Adaptive Control Strategies, USSR, pages 233 240, 1989.

[57] I. Postlethwaite and S. Skogestad. *Advanced control of high performance helicopters: A case study.* In Robust multivariable control tutorial, pages 269 337. American Control Conference 1993, 1993.

[58] I. Postlethwaite and D. Walker. *Advanced control of high performance rotorcraft.* In Proceedings of the IMA conference on aerospace vehicle dynamics and control: Cranfield Institue of Technology, pages 161–179, 1992.

[59] R. W. Prouty. *Helicopter Performance, Stability and Control* . Robert E. Krieger Publishing Company - Florida, 1990.

[60] J. J. Romano and S. N. Singh. *I-O map inversion, zero dynamics and flight control.* IEEE Transactions on Aerospace and Electronic Systems, 26(6):1022 1028, 1990.

[61] W. J. Rugh. *Analytical Framework for gain scheduling.* IEEE Control Systems Magazine, pages 79 84, Jan 1991.

[62] G. H. Saunders. *Dynamics of Helicopter Flight.* John Wiley & Sons, Inc., 1975.

[63] J. Seddon. *Basic Helicopter Aerodynamics.* BSP Professional Books, 1990.

[64] J. S. Shamma. *Analysis and Design of Gain scheduled Control Systems.* PhD thesis, Massachusetts Institute of Technology, 1988.

[65] J. S. Shamma and M. Athans. *Gain scheduling: Potential hazards and possible remedies.* IEEE Control Systems Magazine, pages 101–107, June 1992.

[66] S. N. Singh. *Control of nearly singular decoupling systems and large aircraft manoeuvres.* IEEE Transactions on Aerospace and Electronic Systems, 24(6):775–784, 1988.

[67] S. N. Singh. *Asymptotically decoupled discontinuous control of systems and nonlinear aircraft manœuvre.* IEEE Transactions on Aerospace and Electronic Systems, 25(3):380–390, 1989.

[68] S. N. Singh. *Decoupled ultimate boundedness control of systems and large aircraft manoeuvre.* IEEE Transactions on Aerospace and Electronic Systems, 25(5):677–688, 1989.

[69] J. E. Slotine and W. Li. *Applied Nonlinear Control.* Prentice-Hall International, 1991.

[70] G. A. Smith and G. Meyer. *Aircraft automatic flight control system with model inversion.* AIAA Journal of Guidance, Control and Dynamics, 10(3):269 275, 1987.

[71] P. R. Smith. *Application of eigenstructure assignment to the control of powered lift combat aircraft.* Tech Memo FS 1009, RAE Bedford, Feb. 1991.

[72] R. Stirling. *Analysis Methods for Mathematical Modelling of Primary Flight Control Actuation Systems Standard Reference Document.* Tech Report SDL-103-TR-1, Stirling Dynamics Limited (UK), 1992.

[73] R. Su. *On the linear equivalents of nonlinear systems.* Systems and Control Letters, 2:48–52, 1982.

[74] R. Su, G. Meyer, and L. R. Hunt. *Robustness in nonlinear control.* In Brockett, Millman and Sussman, editor, Differential Geometric Control Conference, volume 27, pages 316–337. Birkhauser, Boston, 1983.

[75] M. D. Takahashi. *Synthesis and evaluation of an H_2 control law for a hovering helicopter.* AIAA Journal of Guidance, Control and Dynamics, 16(3):579 584, 1993.

[76] V. I. Utkin. *Variable structure systems with sliding mode: a survey.* IEEE Transactions on Automatic Control, AC-22(2):212–222, 1977.

[77] V. I. Utkin. *Sliding mode control in discrete-time and difference systems.* In A. S. I. Zinober, editor, Lecture notes in control and information sciences 193 - Variable Structure and Lyapunov Control, pages 87–107. Springer-Verlag, 1994.

[78] K. G. Wagner. *Nonlinear noninteraction with stability by dynamic feedback.* SIAM Journal of Control and Optimization, 29(3):609–622, 1991.

[79] D. Walker, I. Postlethwaite, J. Howitt, and N. Foster. *Rotorcraft flying qualities improvement using advanced control.* In Proceedings of American Helicopter Society/ Nasa Conference, San Francisco, pages 141–155, 1993.

[80] A. Yue and I. Postlethwaite. *H_∞ - optimal design for helicopter control.* In Proceedings of the American Control Conference, volume 2, pages 1679–1684, 1988.

[81] A. Yue and I. Postlethwaite. *Improvement of helicopter handling qualities using H_∞ - optimisation.* Proceedings of the IEE - pt. D, 137(3):115–129, 1990.

[82] A. S. I. Zinober, editor. *Deterministic Control of Uncertain Systems.* Peregrinus Ltd. , 1990.

[83] A. S. I. Zinober, editor. *Lecture notes in control and information sciences 193 - Variable Structure and Lyapunov Control.* Springer-Verlag , 1994.

Appendix A

Inertia Coefficients

$$
\begin{aligned}
I_1 &= \frac{I_{zz}\,(I_{yy} - I_{zz}) - (I_{xz})^2}{I_{xx}\,I_{zz} - (I_{xz})^2} \\
I_2 &= \frac{I_{xx} - I_{yy} + I_{zz}}{\frac{I_{xz}\,I_{zz}}{I_{xz}} - I_{xz}} \\
I_3 &= \frac{I_{xx}\,I_{xz}}{I_{xx}\,I_{xz} - (I_{xz})^2} \\
I_4 &= \frac{(I_{xz})^2}{I_{xx}\,I_{xz} - (I_{xz})^2} \\
I_5 &= \frac{I_{zz} - I_{xx}}{I_{yy}} \\
I_6 &= \frac{I_{xz}}{I_{yy}} \\
I_7 &= \frac{1}{I_{yy}} \\
I_8 &= \frac{(I_{xx})^2 - I_{xx}\,I_{yy} + (I_{xz})^2}{I_{xx}\,I_{zz} - (I_{xz})^2} \\
I_9 &= \frac{I_{yy} - I_{zz} - I_{zz}}{\frac{I_{xz}\,I_{zz}}{I_{xz}} - I_{xz}} \\
I_{10} &= \frac{\frac{(I_{xz})^2}{I_{zz}}}{I_{xx}\,I_{xz} - (I_{xz})^2} \\
I_{11} &= \frac{\frac{I_{xz}\,I_{xx}}{I_{zz}}}{I_{xx}\,I_{xz} - (I_{xz})^2}
\end{aligned}
$$

Appendix B

Equations of Motion

$$\dot{\mathbf{x}} = f(\mathbf{x}) + G(\mathbf{x}, \bar{\mathbf{u}})\,\mathbf{u}$$

where

$$\begin{aligned}
\mathbf{x} &= [\,u\,v\,w\,p\,q\,r\,\theta\,\phi\,]^T \\
\mathbf{u} &= [\,\theta_o\,\theta_{lc}\,\theta_{ls}\,\theta_{ot}\,]^T
\end{aligned}$$

$$\begin{aligned}
f_u &= vr - wq - g\sin\theta + \frac{X_f(\mathbf{x})}{m} + \frac{X_{r_0}(\mathbf{x})}{m} \\
f_v &= wp - ur + g\cos\theta\sin\phi + \frac{Y_f(\mathbf{x})}{m} + \frac{Y_{fn}(\mathbf{x})}{m} + \frac{Y_{r_0}(\mathbf{x})}{m} + \frac{Y_{t_0}(\mathbf{x})}{m} \\
f_w &= uq - vp + g\cos\theta\cos\phi + \frac{Z_f(\mathbf{x})}{m} + \frac{Z_{tp}(\mathbf{x})}{m} + \frac{Z_{r_0}(\mathbf{x})}{m} \\
f_p &= I_1\,q\,r + I_2\,p\,q + I_3\,\{L_{fn}(\mathbf{x}) + L_{r_0}(\mathbf{x}) + L_{t_0}(\mathbf{x})\} + \\
&\quad I_4\,\{N_f(\mathbf{x}) + N_{fn}(\mathbf{x}) + N_{r_0}(\mathbf{x}) + N_{t_0}(\mathbf{x})\} \\
f_q &= I_5\,r\,p + I_6\,(r^2 - p^2) + I_7\,\{M_f(\mathbf{x}) + M_{tp}(\mathbf{x}) + M_{r_0}(\mathbf{x})\} \\
f_r &= I_8\,p\,q + I_9\,q\,r + I_{10}\,\{L_{fn}(\mathbf{x}) + L_{r_0}(\mathbf{x}) + L_{t_0}(\mathbf{x})\} + \\
&\quad I_{11}\,\{N_f(\mathbf{x}) + N_{fn}(\mathbf{x}) + N_{r_0}(\mathbf{x}) + N_{t_0}(\mathbf{x})\} \\
f_\theta &= q\cos\phi - r\sin\phi \\
f_\phi &= p + [q\sin\phi + r\cos\phi]\tan\theta
\end{aligned}$$

Reducing $f(\mathbf{x})$ to its the rigid body and aerodynamic components yields, the following:

$$f_{rb}(\mathbf{x}) = \begin{Bmatrix}
vr - wq - g\sin\theta \\
wp - ur + g\cos\theta\sin\phi \\
uq - vp + g\cos\theta\cos\phi \\
I_1\,q\,r + I_2\,p\,q \\
I_5\,r\,p + I_6\,(r^2 - p^2) \\
I_8\,p\,q + I_9\,q\,r \\
q\cos\phi - r\sin\phi \\
p + [q\sin\phi + r\cos\phi]\tan\theta
\end{Bmatrix}$$

$$f_{aer}(\mathbf{x}) =$$

$$\left\{\begin{array}{c} \frac{X_f(\mathbf{x})}{m} + \frac{X_{r_0}(\mathbf{x})}{m} \\ \frac{Y_f(\mathbf{x})}{m} + \frac{Y_{fn}(\mathbf{x})}{m} + \frac{Y_{r_0}(\mathbf{x})}{m} + \frac{Y_{t_0}(\mathbf{x})}{m} \\ \frac{Z_f(\mathbf{x})}{m} + \frac{Z_{tp}(\mathbf{x})}{m} + \frac{Z_{r_0}(\mathbf{x})}{m} \\ I_3\{L_{fn}(\mathbf{x}) + L_{r_0}(\mathbf{x}) + L_{t_0}(\mathbf{x})\} + I_4\{N_f(\mathbf{x}) + N_{fn}(\mathbf{x}) + N_{r_0}(\mathbf{x}) + N_{t_0}(\mathbf{x})\} \\ I_7\{M_f(\mathbf{x}) + M_{tp}(\mathbf{x}) + M_{r_0}(\mathbf{x})\} \\ I_{10}\{L_{fn}(\mathbf{x}) + L_{r_0}(\mathbf{x}) + L_{t_0}(\mathbf{x})\} + I_{11}\{N_f(\mathbf{x}) + N_{fn}(\mathbf{x}) + N_{r_0}(\mathbf{x}) + N_{t_0}(\mathbf{x})\} \\ 0 \\ 0 \end{array}\right\}$$

Also

$$G(\mathbf{x}, \bar{\mathbf{u}}) = \begin{bmatrix} G_{11} & G_{12} & G_{13} & 0 \\ G_{21} & G_{22} & G_{23} & G_{24} \\ G_{31} & G_{32} & G_{33} & 0 \\ G_{41} & G_{42} & G_{43} & G_{44} \\ G_{51} & G_{52} & G_{53} & 0 \\ G_{61} & G_{62} & G_{63} & G_{64} \\ 0 & 0 & 0 & 0 \\ 0 & 0 & 0 & 0 \end{bmatrix}$$

where

$$\begin{aligned}
G_{11} &= \frac{X_{r_1}(\mathbf{x})}{m} + \frac{X_{r_6}(\mathbf{x})\,\bar{\theta}_o}{m} \\
G_{12} &= \frac{X_{r_3}(\mathbf{x})}{m} + \frac{X_{r_5}(\mathbf{x})\,\bar{\theta}_o}{m} + \frac{X_{r_7}(\mathbf{x})\,\bar{\theta}_{ls}}{m} + \frac{X_{r_9}(\mathbf{x})\,\bar{\theta}_{lc}}{m} \\
G_{13} &= \frac{X_{r_2}(\mathbf{x})}{m} + \frac{X_{r_4}(\mathbf{x})\,\bar{\theta}_o}{m} + \frac{X_{r_8}(\mathbf{x})\,\bar{\theta}_{ls}}{m} \\
G_{21} &= \frac{Y_{r_1}(\mathbf{x})}{m} + \frac{Y_{r_6}(\mathbf{x})\,\theta_o}{m} \\
G_{22} &= \frac{Y_{r_3}(\mathbf{x})}{m} + \frac{Y_{r_5}(\mathbf{x})\,\theta_o}{m} + \frac{Y_{r_7}(\mathbf{x})\,\theta_{ls}}{m} + \frac{Y_{r_9}(\mathbf{x})\,\bar{\theta}_{lc}}{m} \\
G_{23} &= \frac{Y_{r_2}(\mathbf{x})}{m} + \frac{Y_{r_4}(\mathbf{x})\,\theta_o}{m} + \frac{Y_{r_8}(\mathbf{x})\,\bar{\theta}_{ls}}{m} \\
G_{24} &= \frac{Y_{t_1}(\mathbf{x})}{m} \\
G_{31} &= \frac{Z_{r_1}(\mathbf{x})}{m} \\
G_{32} &= \frac{Z_{r_3}(\mathbf{x})}{m} \\
G_{33} &= \frac{Z_{r_2}(\mathbf{x})}{m} \\
G_{41} &= [I_3\,L_{r_1}(\mathbf{x}) + I_4\,N_{r_1}(\mathbf{x})] + [I_3\,L_{r_6}(\mathbf{x}) + I_4\,N_{r_6}(\mathbf{x})]\,\theta_o \\
G_{42} &= [I_3\,L_{r_3}(\mathbf{x}) + I_4\,N_{r_3}(\mathbf{x})] + [I_3\,L_{r_5}(\mathbf{x}) + I_4\,N_{r_5}(\mathbf{x})]\,\bar{\theta}_o + \\
&\quad [I_3\,L_{r_7}(\mathbf{x}) + I_4\,N_{r_7}(\mathbf{x})]\,\theta_{ls} + [I_3\,L_{r_9}(\mathbf{x}) + I_4\,N_{r_9}(\mathbf{x})]\,\bar{\theta}_{lc}
\end{aligned}$$

$$
\begin{aligned}
G_{43} &= [I_3\, L_{r_2}(\mathbf{x}) + I_4\, N_{r_2}(\mathbf{x})] + [I_3\, L_{r_4}(\mathbf{x}) + I_4\, N_{r_4}(\mathbf{x})]\, \theta_o + \\
&\quad [I_3\, L_{r_8}(\mathbf{x}) + I_4\, N_{r_8}(\mathbf{x})]\, \bar{\theta}_{ls} \\
G_{44} &= [I_3\, L_{t_1}(\mathbf{x}) + I_4\, N_{t_1}(\mathbf{x})] \\
G_{51} &= I_7\, M_{r_1}(\mathbf{x}) + I_7\, M_{r_6}(\mathbf{x})\, \theta_o \\
G_{52} &= I_7\, M_{r_3}(\mathbf{x}) + I_7\, M_{r_5}(\mathbf{x})\, \bar{\theta}_o + I_7\, M_{r_7}(\mathbf{x})\, \bar{\theta}_{ls} + I_7\, M_{r_9}(\mathbf{x})\, \bar{\theta}_{lc} \\
G_{53} &= I_7\, M_{r_2}(\mathbf{x}) + I_7\, M_{r_4}(\mathbf{x})\, \theta_o + I_7\, M_{r_8}(\mathbf{x})\, \bar{\theta}_{ls} \\
G_{61} &= [I_{10}\, L_{r_1}(\mathbf{x}) + I_{11}\, N_{r_1}(\mathbf{x})] + [I_{10}\, L_{r_6}(\mathbf{x}) + I_{11}\, N_{r_6}(\mathbf{x})]\, \theta_o \\
G_{62} &= [I_{10}\, L_{r_3}(\mathbf{x}) + I_{11}\, N_{r_3}(\mathbf{x})] + [I_{10}\, L_{r_5}(\mathbf{x}) + I_{11}\, N_{r_5}(\mathbf{x})]\, \bar{\theta}_o + \\
&\quad [I_{10}\, L_{r_7}(\mathbf{x}) + I_{11}\, N_{r_7}(\mathbf{x})]\, \bar{\theta}_{ls} + [I_{10}\, L_{r_9}(\mathbf{x}) + I_{11}\, N_{r_9}(\mathbf{x})]\, \bar{\theta}_{lc} \\
G_{63} &= [I_{10}\, L_{r_2}(\mathbf{x}) + I_{11}\, N_{r_2}(\mathbf{x})] + [I_{10}\, L_{r_4}(\mathbf{x}) + I_{11}\, N_{r_4}(\mathbf{x})]\, \bar{\theta}_o + \\
&\quad [I_{10}\, L_{r_8}(\mathbf{x}) + I_{11}\, N_{r_8}(\mathbf{x})]\, \bar{\theta}_{ls} \\
G_{64} &= [I_{10}\, L_{t_1}(\mathbf{x}) + I_{11}\, N_{t_1}(\mathbf{x})]
\end{aligned}
$$

State Space Transformation - Jacobian Matrix

The Jacobian Matrix $\frac{\partial \Phi(\mathbf{x})}{\partial \mathbf{x}}$ is as follows:

$$
\begin{bmatrix}
0 & 0 & 0 & 0 & 0 & 0 \\
0 & 0 & 0 & 0 & \cos\phi & -\sin\phi \\
0 & 0 & 0 & 0 & 0 & 0 \\
0 & 0 & 0 & 1 & \sin\phi\tan\theta & \cos\phi\tan\theta \\
0 & 0 & 0 & 0 & \sec\theta\sin\phi & \cos\phi\sec\theta \\
\sin\theta & -(\cos\theta\sin\phi) & -(\cos\phi\cos\theta) & 0 & 0 & 0 \\
1 & 0 & 0 & 0 & 0 & 0 \\
0 & 1 & 0 & 0 & 0 & 0
\end{bmatrix}
$$

$$
\begin{bmatrix}
1 & 0 \\
0 & -(r\cos\phi) - q\sin\phi \\
0 & 1 \\
\sec^2\theta\,(r\cos\phi + q\sin\phi) & (q\cos\phi - r\sin\phi)\tan\theta \\
\sec\theta\,(r\cos\phi + q\sin\phi)\tan\theta & \sec\theta\,(q\cos\phi - r\sin\phi) \\
u\cos\theta + (w\cos\phi + v\sin\phi)\sin\theta & \cos\theta\,(-(v\cos\phi) + w\sin\phi) \\
0 & 0 \\
0 & 0
\end{bmatrix}
$$

Input Space Transformation - Terms

The vector

$$L_f^r h(\mathbf{x}) = \begin{bmatrix} L_f^{r_1} h_1(\mathbf{x}) \\ L_f^{r_2} h_2(\mathbf{x}) \\ L_f^{r_3} h_3(\mathbf{x}) \\ L_f^{r_4} h_4(\mathbf{x}) \end{bmatrix}$$

where:

$$\begin{aligned} L_f^{r_1} h_1(\mathbf{x}) &= \{I_7 (M_f + M_{r_0} + M_{t_p}) + I_5 p r + I_6 (-p^2 + r^2)\} \cos\phi - \{I_{10} (L_{fn} + \\ &\quad L_{r_0} + L_{t_0}) + I_{11} (N_f + N_{fn} + N_{r_0} + N_{t_o}) + I_8 p q + I_9 q r\} \sin\phi + \\ &\quad \{-(r \cos\phi) - q \sin\phi\} \{p + r \cos\phi \tan\theta + q \sin\phi \tan\theta\} \end{aligned}$$

$$\begin{aligned} L_f^{r_2} h_2(\mathbf{x}) &= I_3 (L_{fn} + L_{r_0} + L_{t_0}) + I_4 (N_f + N_{fn} + N_{r_0} + N_{t_o}) + I_2 p q + I_1 q r + \\ &\quad \{q \cos\phi - r \sin\phi\} \{r \cos\phi \sec^2\theta + q \sec^2\theta \sin\phi\} + \\ &\quad \{I_{10} (L_{fn} + L_{r_0} + L_{t_0}) + I_{11} (N_f + N_{fn} + N_{r_0} + N_{t_o}) + I_8 p q + \\ &\quad I_9 q r\} \cos\phi \tan\theta + \{I_7 (M_f + M_{r_0} + M_{t_p}) + I_5 p r + I_6 (-p^2 + \\ &\quad r^2)\} \sin\phi \tan\theta + \{p + r \cos\phi \tan\theta + q \sin\phi \tan\theta\} \\ &\quad \{q \cos\phi \tan\theta - r \sin\phi \tan\theta\} \end{aligned}$$

$$\begin{aligned} L_f^{r_3} h_3(\mathbf{x}) &= \{I_{10} (L_{fn} + L_{r_0} + L_{t_0}) + I_{11} (N_f + N_{fn} + N_{r_0} + N_{t_o}) + I_8 p q + \\ &\quad I_9 q r\} \cos\phi \sec\theta + \{I_7 (M_f + M_{r_0} + M_{t_p}) + I_5 p r + I_6 (-p^2 + \\ &\quad r^2)\} \sec\theta \sin\phi + \sec\theta \{r \cos\phi + q \sin\phi\} \{q \cos\phi - \\ &\quad r \sin\phi\} \tan\theta + \sec\theta \{q \cos\phi - r \sin\phi\} \{p + \\ &\quad r \cos\phi \tan\theta + q \sin\phi \tan\theta\} \end{aligned}$$

$$\begin{aligned} L_f^{r_4} h_4(\mathbf{x}) &= -\cos\phi \cos\theta \{q u - p v + \frac{Z_f + Z_{r_0} + Z_{t_p}}{m} + g \cos\phi \cos\theta\} - \\ &\quad \cos\theta \sin\phi \{-(r u) + p w + \frac{Y_f + Y_{fn} + Y_{r_0} + Y_{t_0}}{m} + \\ &\quad g \cos\theta \sin\phi\} + \sin\theta \{r v - q w + \frac{X_f + X_{r_0}}{m} - g \sin\theta\} + \\ &\quad \{q \cos\phi - r \sin\phi\} \{u \cos\theta + w \cos\phi \sin\theta + \\ &\quad v \sin\phi \sin\theta\} + \{-(v \cos\phi \cos\theta) + w \cos\theta \sin\phi\} \{p + \\ &\quad r \cos\phi \tan\theta + q \sin\phi \tan\theta\} \end{aligned}$$

While the decoupling matrix E is:

$$E = \begin{bmatrix} E_1 & E_2 & E_3 & E_4 \end{bmatrix}$$

where

$$E_1 = \begin{bmatrix} G_{51}\cos\phi - G_{61}\sin\phi \\ G_{41} + G_{61}\cos\phi\tan\theta + G_{51}\sin\phi\tan\theta \\ \sec\theta\,(G_{61}\cos\phi + G_{51}\sin\phi) \\ -(G_{31}\cos\phi\cos\theta) - G_{21}\cos\theta\sin\phi + G_{11}\sin\theta \end{bmatrix}$$

$$E_2 = \begin{bmatrix} G_{52}\cos\phi - G_{62}\sin\phi \\ G_{42} + G_{62}\cos\phi\tan\theta + G_{52}\sin\phi\tan\theta \\ \sec\theta\,(G_{62}\cos\phi + G_{52}\sin\phi) \\ -(G_{32}\cos\phi\cos\theta) - G_{22}\cos\theta\sin\phi + G_{12}\sin\theta \end{bmatrix}$$

$$E_3 = \begin{bmatrix} G_{53}\cos\phi - G_{63}\sin\phi \\ G_{43} + G_{63}\cos\phi\tan\theta + G_{53}\sin\phi\tan\theta \\ \sec\theta\,(G_{63}\cos\phi + G_{53}\sin\phi) \\ -(G_{33}\cos\phi\cos\theta) - G_{23}\cos\theta\sin\phi + G_{13}\sin\theta \end{bmatrix}$$

$$E_4 = \begin{bmatrix} -(G_{64}\sin\phi) \\ G_{44} + G_{64}\cos\phi\tan\theta \\ G_{64}\cos\phi\sec\theta \\ -(G_{24}\cos\theta\sin\phi) \end{bmatrix}$$